NASA-TM-86270 19850006488

NASA Technical Memorandum 86270

Static Internal Performance of Single-Expansion-Ramp Nozzles With Various Combinations of Internal Geometric Parameters

Richard J. Re and Laurence D. Leavitt

DECEMBER 1984

NASA

NASA Technical Memorandum 86270

Static Internal Performance of Single-Expansion-Ramp Nozzles With Various Combinations of Internal Geometric Parameters

Richard J. Re and Laurence D. Leavitt
Langley Research Center
Hampton, Virginia

National Aeronautics
and Space Administration

Scientific and Technical
Information Branch

1984

Introduction

Many studies have been made of the integration of nonaxisymmetric nozzles into fighter airplane configurations (refs. 1–7). Some of these studies, primarily those introducing nonaxisymmetric nozzles into the airplane design process at an early stage, indicate that nonaxisymmetric nozzles can provide comparable or better level-flight performance than axisymmetric nozzles. In addition, nonaxisymmetric nozzle designs are generally more amenable to the incorporation of thrust vectoring to provide forces and moments for additional capabilities in airplane maneuver and control (ref. 8). A prerequisite for the evolution of practical nozzles for production airplanes is the establishment of an internal performance data base documenting the effects of nozzle internal geometry changes so that efficient nozzles can be selected.

The three principal types of nonaxisymmetric nozzles on which experimental internal performance data are available are the two-dimensional convergent-divergent nozzles (refs. 9–13), the single-expansion-ramp nozzle (refs. 11, 12, 14, and 15), and the wedge nozzle (refs. 12 and 16–19). The single-expansion-ramp nozzle (SERN) is a configuration originally developed with a hood-type jet deflector stowed in the expansion ramp to be deployed to provide high vector angles (up to 110°) for vertical take-off and landing (VTOL) operations (refs. 20–25). Most experimental investigations conducted on the SERN have concentrated on the uninstalled and installed performance of a specific nozzle design at various nozzle power settings during cruise and vectored-thrust operating modes. Limited data on the effects of systematic changes in nozzle internal geometry on performance are available. The effects of nozzle sidewall geometry on SERN internal performance are shown in reference 10 (unvectored thrust) and reference 14 (vectored thrust). Some static internal performance data showing the effects of nozzle expansion ratio, lower flap length, lower flap angle, and thrust vectoring are presented in reference 14.

The present paper contains static internal performance for 43 SERN configurations having various combinations of 5 internal geometric parameters. These five parameters are expansion-ramp length, expansion-ramp initial angle, expansion-ramp chordal angle, lower flap length, and lower flap angle. The various combinations of internal geometries produced nozzles with internal expansion ratios ranging from 1.05 to 1.50 and external expansion ratios ranging from 1.15 to 2.39. All the nozzles had the same throat area and aspect ratio (ratio of throat width to throat height). This investigation was conducted in the static-test facility of the Langley 16-Foot Transonic Tunnel at nozzle pressure ratios from 2 to 10.

Symbols and Abbreviations

All forces (with the exception of resultant gross thrust) and angles are referred to the model centerline (body axis). A detailed discussion of the data-reduction and calibration procedures as well as definitions of forces, angles, and propulsion relationships used herein can be found in reference 11.

A_e — nozzle exit area, cm^2

A_t — nozzle geometric throat area, cm^2

$(A_e/A_t)_e$ — external expansion ratio for ideally expanded flow (A_e is the vertical displacement between end of nozzle ramp and lower flap times the nozzle width)

$(A_e/A_t)_i$ — internal expansion ratio (A_e is measured in the vertical plane at end of nozzle lower flap)

F — measured thrust along body axis, N (see fig. 3)

F_i — ideal isentropic gross thrust, $w_p\sqrt{RT_{t,j}\left(\frac{2\gamma}{\gamma-1}\right)\left[1-\left(\frac{p_\infty}{p_{t,j}}\right)^{\frac{\gamma-1}{\gamma}}\right]}$, N

F_r — resultant gross thrust, $\sqrt{F^2+N^2}$, N

$h_{t,n}$ — nominal nozzle throat height, 2.54 cm

l_r — axial length of expansion portion of upper flap, cm (see fig. 3)

l_v — axial length of variable portion of lower flap, cm (see fig. 3)

M — measured pitching moment (about point on model centerline at station 74.65), N-m (see fig. 3)

N — measured normal force, N (see fig. 3)

NPR — nozzle pressure ratio, $p_{t,j}/p_\infty$

p — local static pressure, Pa

$p_{t,j}$ — jet total pressure, Pa

p_∞ — ambient pressure, Pa

R — gas constant, 287.3 J/kg-K

Sta. — model station, cm

$T_{t,j}$ — jet total temperature, K

w_i — ideal mass-flow rate, kg/sec

w_p — measured mass-flow rate, kg/sec

x — axial distance measured from nozzle connect station (positive downstream), cm

y vertical distance measured from horizontal model centerline (positive upward), cm

β lower flap angle, deg (see fig. 3)

γ ratio of specific heats, 1.3997 for air

Δ incremental value

δ_j resultant thrust-vector angle, $\tan^{-1}\frac{N}{F}$, deg (see fig. 3)

θ expansion-ramp chordal angle, deg (see fig. 3)

ρ initial angle of expansion ramp, deg (see fig. 3)

Nozzle component designations (see table I and fig. 3):

A,B,C,D,E, F,G,H,I,J, K,L,M,N,O upper flap (first character in configuration designation)

P,Q,R,S,T, U,V,W,X lower flap (second character in configuration designation)

1,2,3,4,5,6,7 sidewall (third character in configuration designation)

Apparatus and Methods

Static-Test Facility

This investigation was conducted in the static-test facility of the Langley 16-Foot Transonic Tunnel. All tests were conducted with the jet exhausting to atmosphere. This facility utilizes the same clean, dry-air supply as that used in the 16-Foot Transonic Tunnel and a similar air-control system, including valving, filters, and a heat exchanger (to operate the jet flow at constant stagnation temperature).

Single-Engine Propulsion-Simulation System

A sketch of the single-engine air-powered nacelle model on which various nozzles were mounted is presented in figure 1(a) with a typical nozzle configuration attached. The body shell forward of station 52.07 was removed for this investigation.

An external high-pressure air system provided a continuous flow of clean, dry air at a controlled temperature of about 300 K. This high-pressure air was varied up to approximately 10 atm (1 atm = 101.3 kPa) and was brought through a dolly-mounted support strut by six tubes which connect to a high-pressure plenum chamber. As shown in figure 1(b), the air was then discharged perpendicularly into the model low-pressure plenum through eight multiple-hole sonic nozzles equally spaced around the high-pressure plenum. This method was designed to minimize any forces imposed by the transfer of axial momentum as the air is passed from the nonmetric high-pressure plenum to the metric (mounted to the force balance) low-pressure plenum. Two flexible metal bellows are used as seals and serve to compensate for axial forces caused by pressurization.

The air was then passed from the model low-pressure plenum (circular in cross section) through a transition section, a choke plate, and an instrumentation section which were common for all nonaxisymmetric nozzles investigated. The transition section provided a smooth flow path for the airflow from the round low-pressure plenum to the rectangular choke plate and instrumentation section. The instrumentation section had a flow-path width-height ratio of 1.437 and was identical in geometry to the nozzle airflow entrance. All nozzle configurations were attached to the instrumentation section at model station 104.47.

Nozzle Design

The single-expansion-ramp nozzle (SERN) is a nonaxisymmetric, variable-area, internal/external expansion exhaust system. A photograph showing a typical SERN installed on the single-engine propulsion-simulation system is shown in figure 2. Basic SERN nozzle components consist of (1) a two-dimensional upper flap in which a portion of the flap surface downstream of the throat serves as an expansion ramp and (2) a relatively short two-dimensional lower flap. In several of the more recent SERN nozzle designs, the upper flap (ramp) is either fixed or only capable of variable geometry downstream of the nozzle throat (by rotation of the entire external ramp surface, ref. 15, or by deflection of a downstream portion of the ramp, ref. 14). The lower flap may also be fixed, but generally is variable to provide both power setting (A_t) and expansion ratio (A_e/A_t) control. One notable exception is the Augmented Deflector Exhaust Nozzle (ADEN), in which nozzle throat area is controlled by the upper ramp convergent-divergent flap, and expansion ratio is controlled by rotating the lower divergent flap. The SERN nozzle configurations of the present investigation represented nominally unvectored dry-power nozzles. The lower flap was varied downstream of the nozzle geometric throat; hence, changing lower flap angle primarily affected nozzle expansion ratio, not nozzle power setting.

Figure 3 presents a sketch of a typical nozzle configuration. The nozzle geometric parameters varied for the upper and the lower flaps are illustrated in figure 3 and are listed in table I for each of the 43 nozzle configurations tested. Internal surface coordinates of the 15 upper and the 9 lower flaps are given in tables II and III, respectively; geometry of the 7 sets of nozzle sidewalls used to build up particular configurations is given in figure 4. All test nozzles had a nominally constant exhaust-flow path width of 10.16 cm. The nominal throat aspect ratio of each nozzle (ratio of width to height) was 4.0. Examination of the upper and lower flap coordinates in tables II and III shows that the geometric throat for the nozzles was not in a plane perpendicular to the centerline but was slightly skewed.

All upper flaps had the same radius of curvature (1.65 cm) at the nozzle throat. Both the convergent portion and the initial flat portion of the expansion ramp were tangent to the throat radius. The initial ramp angle (ρ) was varied to produce selected values of the difference $\rho - \theta$. (See table I.) This was done by adjusting the lengths of the two flat portions of the expansion ramp to obtain the necessary initial ramp angle. The terminal angle (angle of internal surface at flap trailing edge relative to nozzle centerline) of the expansion ramp for all the upper flaps was 2.5°. The lower flaps had a radius of curvature of 0.51 cm at the nozzle throat except for those that had negative flap angles (−6.49° and −10.00°). The lower flaps that had negative terminal angles were essentially flat at the throat because the throat radius, which was present for positive values of lower flap angle (fig. 3), disappeared as the lower flap was rotated upward.

Instrumentation

A three-component strain-gage balance was used to measure the forces and moments on the model downstream of station 52.07 cm. (See fig. 1.) Jet total pressure was measured at a fixed station in the instrumentation section (see fig. 1(a)) by means of a four-probe rake through the upper surface, a three-probe rake through the side, and a three-probe rake through the corner. A thermocouple, also located in the instrumentation section, was used to measure jet total temperature. Mass-flow of the high-pressure air supplied to the nozzle was determined by calibration of pressure and temperature measurements in the high-pressure plenum against the known performance of standard axisymmetric choke nozzles. Internal static-pressure orifices were located on centerlines of the nozzle upper and lower flaps. The static-pressure orifice locations for each flap are given in table IV.

Data Reduction

All data were recorded simultaneously on magnetic tape. Approximately 50 frames of data, taken at a rate of 10 frames per second, were used for each data point; average values were used in computations. With the exception of resultant gross thrust F_r, all force data in this report are referenced to the model centerline.

The basic performance parameters used for the presentation of results are F/F_i, F_r/F_i, δ_j, and w_p/w_i. The internal thrust ratio F/F_i is the ratio of actual nozzle thrust (along the body axis) to ideal nozzle thrust, where ideal nozzle thrust is based on measured mass-flow rate and total temperature and pressure conditions in the nozzle throat, as defined in the symbols. The balance axial-force measurement, from which actual nozzle thrust is subsequently obtained, is initially corrected for model weight tares and balance interactions. Although the bellows arrangement was designed to eliminate pressure and momentum interactions with the balance, small bellows tares on all balance components still exist. These tares result from a small pressure difference between the ends of the bellows when internal velocities are high and from small differences in the forward and aft bellows spring constants when the bellows are pressurized. As discussed in reference 11, these bellows tares were determined by running calibration nozzles with known performance over a range of expected normal forces and pitching moments. The balance data were then corrected in a manner similar to that discussed in reference 11 to obtain actual nozzle thrust, normal force, and pitching moment. The resultant gross thrust F_r, used in resultant thrust ratio F_r/F_i, and the resultant thrust vector angle δ_j are then determined from these corrected balance data. Resultant thrust ratio F_r/F_i is equal to internal thrust ratio F/F_i as long as the jet-exhaust flow remains unvectored ($\delta_j = 0°$). Significant differences between F_r/F_i occur when jet-exhaust flow is turned from the axial direction, and the magnitude of these differences is a function of resultant thrust vector angle δ_j. Nozzle discharge coefficient w_p/w_i is the ratio of measured mass-flow rate to ideal mass-flow rate, where ideal mass-flow rate is based on jet total pressure $p_{t,j}$, jet total temperature $T_{t,j}$, and measured nozzle throat area. Nozzle discharge coefficient is then a measure of the ability of a nozzle to pass mass flow and is reduced by boundary-layer thickness and nonuniform flow in the throat.

Results and Discussion

The exhaust-flow expansion process for single-expansion-ramp nozzles occurs both internally and externally. That is, internal expansion of the flow occurs from the throat up to the end of the lower flap, where it is contained by the internal surfaces of the nozzle, and is controlled by the internal expansion ratio $(A_e/A_t)_i$. External expansion, which occurs from the end of the lower flap, is bounded by the expansion ramp and the free (ambient/exhaust) boundary, and is controlled by the external expansion ratio $(A_e/A_t)_e$. Thus, thrust performance is influenced by internal and external expansion ratios which tend to result in two performance peaks. In addition, expansion of the flow over the surface of the external ramp produces a resultant thrust force that is not aligned with the horizontal centerline of the model and varies with nozzle pressure ratio. Therefore, when a single-expansion-ramp nozzle is integrated into an airplane configuration, the vertical force component on the ramp and its contribution as a pitching moment must be included as a trim or control consideration.

Static pressures (as a ratio to jet total pressure) measured on the centerlines of the upper and lower flap internal surfaces are presented in table V. Basic nozzle internal performance data for the 43 configurations tested are presented graphically in figure 5. The data consist of nozzle thrust ratio F/F_i, resultant thrust ratio F_r/F_i, discharge coefficient w_p/w_i, thrust vector angle δ_j, and pitching-moment ratio $M/F_i h_{t,n}$ are presented as a function of nozzle pressure ratio NPR. For compactness of graphical presentation, the data with ramp chordal angle θ as the variable have been combined for two configurations on each page (figs. 5(a) through 5(p)). For configurations with upper flaps A through H, only two values of a given variable were tested for a given set of four other geometric variables. For upper flaps I through O, three values of each geometric variable were investigated for a given set of four other variables, with configuration OT5 (fig. 5(q)) having the intermediate value of each of the five variables. The internal performance data for the configurations with upper flaps I through O are presented graphically in figures 5(q) through 5(u) for each of the five geometric variables. Table I, which contains a summary of the important geometric parameters of all 43 nozzle configurations, also indicates which part of figure 5 contains internal performance data and which part of table V contains static-pressure data.

Internal Static-Pressure Distributions

Typical internal static-pressure distributions for selected nozzle configuration comparisons are shown in figures 6 through 10. All pressure-distribution comparisons presented were obtained from combinations of upper flaps I through O and lower flaps T through X. Comparisons were made for values of NPR equal to 4.0 and 10.0.

The data of figures 6 through 10 exhibit characteristics typical of single-expansion-ramp nozzles (refs. 10 and 14) at underexpanded conditions (NPR greater than design NPR). When the ambient pressure (or back pressure) is less than the nozzle exit pressure, an adjustment in pressure must occur downstream of the exit plane. This adjustment takes the form of a series of expansion waves radiating from the exit of the lower flap and impinging on the upper ramp. If the external ramp is long enough, these expansion waves will reflect off the ramp and again off the jet free-boundary, forming compression waves which again intersect the ramp surface. (For example, see NPR $\approx$ 4 data of figs. 6 through 10.) These compression waves may coalesce into a shock wave that causes a sharp rise in pressure on the ramp. The pattern of alternate expansion and compression is repeated downstream, and decreases in ramp pressure result from another series of expansion waves. At overexpanded nozzle conditions (NPR less than design NPR), the ambient pressure is greater than the nozzle exit pressure, and the adjustment will take place upstream of the nozzle exit and start as a compression or a shock wave, depending upon the degree of overexpanded flow. Again, the alternating expansion/compression process takes place. The frequency of the occurrence of the expansion/compression cycle will increase with decreasing NPR. None of the data presented in figures 6 through 10 were at highly overexpanded conditions; hence, no evidence of an internal shock exists, but an examination of the pressure data shown in table V (especially of the higher-expansion-ratio data of configurations DQ3 and HQ4) will show these shocks at low nozzle pressure ratios.

Effect of ramp chordal angle. Typical effects of varying ramp angle θ on upper and lower flap centerline pressure distributions are presented in figure 6. As seen, pressures on the ramp tend to increase (except near the end of the ramp) as the ramp is rotated downward, especially for values of NPR that clearly exceed the design NPR (which ranges from 3.3 to 4.1, depending upon configuration). Since the ramp projects a large normal area, an increase in ramp pressures would be expected to result in an increase in normal force and, hence, an increase in pitching moment. At NPR = 4.0, an exhaust-flow shock appears to be standing on the ramp surface and tends to move downstream on the ramp as ramp angle decreases from 13.4° to 4.4°. In fact, this shock appears to induce some separation on the aft portion of the ramp, as evidenced by the manner in which the pressures reach a "plateau" (especially for θ = 13.4° and 8.9°). The shock apparently moves off the ramp as nozzle pressure ratio is increased from 4.0 to 10.0.

Examination of the lower flap pressure distributions indicates that ramp-angle changes had little or no effect on the lower flap static pressures. The above observations are typical of those found for similar nozzles with similar values of ramp angle and are discussed in reference 15. It is also interesting to note that the sonic line at the nozzle throat appears to be skewed, based on the fact that the critical pressure ratio ($p/p_{t,j} = 0.528$) occurs farther downstream on the lower flap than it does on the ramp. This was expected from examination of ramp and lower flap coordinates (as discussed in the section on nozzle design). Throat location is independent of ramp angle and nozzle pressure ratio for the comparison presented.

Effect of ramp length. Typical effects of varying ramp length on upper and lower flap centerline pressure distributions are presented in figure 7. Unfortunately, ramp shape changes somewhat as ramp length is increased. (Hence, changes in external expansion ratio occur.) As a result, only small segments of the ramp retain identical shape. All three configurations are identical up to $x/h_{t,n} = 4.75$. The midlength ramp and the long ramp have identical geometries up to $x/h_{t,n} = 5.75$. As can be seen, the static-pressure distributions indicate that there is no change in ramp pressures up to the location at which ramp-shape changes occur. As might be expected, changes in ramp length have no effect on lower flap centerline pressures. The expansion/compression process typical of single-expansion-ramp nozzles is clearly evident in figure 7, especially for NPR = 4.0. The nozzle expands the exhaust flow over the ramp until a shock is formed (sudden static pressure rise on the ramp), followed again by flow expansion. The shock is positioned farther aft on the ramp as ramp length and external expansion ratio increase at NPR = 4.0. The shock is probably downstream of the ramp at NPR = 10.0 on all but the shortest ramp length, where shock position is unaffected by increasing NPR from 4.0 to 10.0. This shock on configuration MT6 is believed to be a shock formed as supersonic exhaust flow is compressed in the curved segment of the ramp beginning just downstream of $x/h_{t,n} = 5.0$. (See table II(c).)

Effect of initial ramp angle. Typical effects of varying initial ramp angle ρ on upper and lower flap centerline pressure distributions are presented in figure 8. Increasing initial ramp divergence angle results in increased flow expansion and reduced static pressures on the forward portion of the ramp followed by a reversal of the trends at values of $x/h_{t,n} > 6.15$. These observations are independent of nozzle pressure ratio for values of NPR $\geq$ 4.0. At NPR = 4.0, a shock is formed on the aft portion of the ramp for all three configurations presented. The configuration with the steepest initial ramp angle results in the earliest formation of the shock on the ramp surface. As initial ramp angle decreases, the shock moves aft on the ramp. Initial ramp angle has no effect on lower flap centerline pressures throughout the range of NPR tested.

Effect of lower flap angle. Typical effects of varying lower flap angle β on upper and lower flap centerline pressure distributions are presented in figure 9. As seen, rotating the lower flap up (from $\beta = 10^\circ$ to $\beta = -10^\circ$) generally increased pressures on both the ramp (up to $x/h_{t,n} = 6.5$) and lower flap. The throat location on the lower flap obviously moves downstream as the lower flap is rotated up. Since the position of the throat on the ramp remains essentially unchanged, the throat becomes more inclined (upward) as the lower flap is rotated up. These results are similar to the results obtained in reference 15. It should be pointed out that variations in lower flap terminal angle do result in significant changes in nozzle internal expansion ratio (and hence in design nozzle pressure ratio) and make direct comparisons at specific values of NPR somewhat difficult. In fact, for three configurations of this comparison, the design NPR based on internal expansion ratio ranges from approximately 2.7 to 5.0 for lower flap angles of -10° and 10°, respectively. With the lower flap rotated up to -10°, the nozzle internal expansion ratio is reduced to 1.06, thereby reducing the value of NPR required for fully expanded flow to 2.7. Thus, configuration OX7 (with lower flap rotated up) is operating at underexpanded conditions at NPR = 4.0 and apparently has a shock (or compression region) in the nozzle upstream of the exit which remains unaffected by increased NPR. This particular configuration with a relatively low design NPR allows formation of two distinct expansion/compression cycles on the ramp.

Based on the pressure data in figure 9, it would be difficult to predict which configuration provided the largest normal-force component. Pressures increased both on the lower flap and the ramp as the lower flap terminal angle was rotated up, and the resultant forces tended to cancel each other.

Effect of lower flap length. Effects of varying lower flap length on upper and lower flap centerline pressure distributions are presented in figure 10. Lower flap length has little or no effect on ramp pressures up to $x/h_{t,n} = 5.0$. Once NPR is high enough to move the shock off the ramp (e.g., at NPR = 10.0), it becomes apparent that pressures on the ramp increase as lower flap length increases. Based on these pressures, an increase in positive normal force (and δ_j) would be expected as lower flap length increases. Lower flap length appears to affect location of the throat on the lower flap and thus causes some variation in the inclination of the throat plane. The throat location is independent of NPR over the range of NPR tested.

As is the case for lower flap angle, nozzle internal expansion ratio varies significantly as lower flap length is varied. The short lower flap (configuration OU7), which is operating at underexpanded conditions at NPR = 4.0, induces a region of compression (possibly a mild shock) relatively early on the ramp. The midlength and long lower flaps, operating at fully expanded and overexpanded flow conditions, respectively, induce shocks and flow separation on the ramp. These shocks occur farther downstream on the ramp than for the short lower flap configuration OU7. As mentioned previously, these shocks appear to move downstream of the ramp as NPR approaches 10.0.

Static Internal Performance

The static-internal-performance data of the 43 nozzle configurations tested are presented in figure 5. An index for the internal performance data is presented in table I along with a summary of the important geometric characteristics.

Variations in single-expansion-ramp nozzle geometry generally result in changes in nozzle internal and/or external expansion ratio, thereby shifting the pressure ratios for optimum performance. When such geometric variations are made, performance changes are expected but cannot be described as beneficial or detrimental, since the nozzles cannot be compared on equal terms at a given pressure ratio. In addition, ramp internal surface geometry varies in a manner unlikely to be the result of component actuation of a practical variable-geometry nozzle. For example, the lengths of the two flat portions of the expansion surface were varied to obtain the desired combinations of the three upper ramp variables selected as parameters requiring investigation. However, the lower flap geometry, for a given length, was flat, so that a change in lower flap angle (for a given upper flap) does represent a possible alternate setting for a variable-geometry nozzle. Therefore, the nozzles of this investigation should be considered separate designs except when lower flap angle (for a given lower flap length) is varied for a given upper flap. The establishment of empirical relations for the prediction of internal performance of nozzles having a large number of geometric parameters varied in a controlled manner is described in reference 26.

Examination of the expansion ratios (table I) for the 43 configurations indicates that the internal and external expansion ratios are nearly the same for two groups of nozzles having various combinations of geometric parameters. Performance comparisons for these two groups of nozzles are made in figure 11. For example, seven nozzles have an internal expansion ratio of approximately 1.20 with an external expansion ratio of approximately 1.68. Since these nozzles have essentially the same optimum design parameters (design NPR), their performance can be compared (fig. 11(a)). The wide spread in the thrust-ratio data and the resultant-thrust-ratio data at a given nozzle pressure ratio indicates that differences in nozzle geometry have significant effects. In the vicinity of and below the pressure ratio (3.8) for optimum internal expansion, configuration KT5 has the best thrust (F/F_i) performance. At nozzle pressure ratios above 4.5, configuration OT5 has the best thrust performance. Thrust vector angle and pitching-moment ratio vary greatly from configuration to configuration up to a nozzle pressure ratio of about 7.5. At and above this nozzle pressure ratio, which approximately equals the pressure ratio for optimum external expansion, the data for thrust vector angle (or pitching-moment ratio) appear to merge into a narrow band. Similar results are evident in figure 11(b) for five other nozzles having nearly common optimum design points.

If, as mentioned earlier, angular movement of the lower flap (with a given upper flap) is a possible mechanical capability of a practical variable-geometry nozzle, then there are 17 variable-geometry nozzles represented in this investigation. Angular rotation of the lower flap results in a change in both internal and external expansion ratios and is, therefore, a response appropriate to a change in ambient pressure, such as would result from a change in flight Mach number. Comparisons of the effect of lower flap deflection on thrust ratio and pitching-moment ratio are presented in figure 12. Upward rotation of the lower flap results in peak thrust ratio shifting to a lower pressure ratio and provides values of peak performance which are generally greater than or equal to the values of peak performance for those configurations with the lower flap rotated downward. Often, the performance of the configurations with upward rotated lower flaps is higher throughout the entire range of pressure ratio. The effects of lower flap angle on performance are greater for configurations with the long lower flap, since a given flap-angle change results in a greater change in internal and external expansion ratios.

All the nozzles have high levels of discharge coefficient ranging from 0.964 to 0.983. (See fig. 5.) The effects of nozzle geometry on discharge coefficient are small. Examination of the discharge-coefficient data in figure 5 indicates that lower flap angle is the only parameter of the five investigated that has a measurable effect. This can be illustrated by subtraction of the average value of discharge coefficient (at constant NPR) for configurations having a lower flap angle of 0° from the average values of discharge coefficient of each of the other lower flap angles. A plot of the variation of such an incremental discharge coefficient against lower flap angle is presented in figure 13 for a nozzle pressure ratio of 5.0. As can be seen, nozzle discharge coefficient tends to increase as the lower flap is rotated downward from $\beta = -10°$ to $\beta = 6°$. Continued downward rotation to angles above 6° provides no additional improvement.

Concluding Remarks

The effects of five geometric design parameters on the internal performance of single-expansion-ramp nozzles were investigated at nozzle pressure ratios up to 10 in the static-test facility of the Langley 16-Foot Transonic Tunnel. The geometric variables on the expansion-ramp surface of the upper flap consisted of ramp chordal angle, ramp length, and initial ramp angle. On the lower flap, the geometric variables consisted of flap angle and flap length.

For these configurations on which meaningful comparisons could be made (those with internal and external expansion ratios approximately the same), it was apparent that the geometric parameters investigated had a significant impact on thrust ratio and thrust vector angle. Upward rotation of the lower flap acted to reduce both internal and external expansion ratio and provided peak performance levels which were generally greater than or equal to those levels of peak performance for configurations in which the lower flap was rotated downward. Often the performance of the configurations with the upward rotated lower flap was higher throughout the entire range of nozzle pressure ratio tested.

Langley Research Center
National Aeronautics and Space Administration
Hampton, VA 23665
September 27, 1984

References

1. *F-15 2-D Nozzle System Integration Study. Volume I—Technical Report.* NASA CR-145295, 1978.
2. Stevens, H. L.: *F-15/Nonaxisymmetric Nozzle System Integration Study Support Program.* NASA CR-135252, 1978.
3. Bergman, D.; Mace J. L.; and Thayer, E. B.: Non-Axisymmetric Nozzle Concepts for an F-111 Test Bed. AIAA-77-841, July 1977.
4. Wasson, H. R.; Hall, G. R.; and Palcza, J. L.: Results of a Feasibility Study To Add Canards and ADEN Nozzle to the YF-17. AIAA-77-1227, Aug. 1977.
5. Goetz, G. F.; Petit, J. E.; and Sussman, M. B.: Non-Axisymmetric Nozzle Design and Evaluation for F-111 Flight Demonstration. AIAA-78-1025, July 1978.
6. Hiley, P. E.; Wallace, H. W.; and Booz, D. E.: Nonaxisymmetric Nozzles Installed in Advanced Fighter Aircraft. *J. Aircr.*, vol. 13, no. 12, Dec. 1976, pp. 1000–1006.
7. Hiley, P. E.; and Bowers, D. L.: Advanced Nozzle Integration for Supersonic Strike Fighter Application. AIAA-81-1441, July 1981.
8. Berrier, B. L.; and Re, R. J.: A Review of Thrust-Vectoring Schemes for Fighter Aircraft. AIAA-78-1023, July 1978.
9. Mason, Mary L.; Putnam, Lawrence E.; and Re, Richard J.: *The Effect of Throat Contouring on Two-Dimensional Converging-Diverging Nozzles at Static Conditions.* NASA TP-1704, 1980.
10. Berrier, Bobby L.; and Re, Richard J.: *Effects of Several Geometric Parameters on the Static Internal Performance of Three Nonaxisymmetric Nozzle Concepts.* NASA TP-1468, 1979.
11. Capone, Francis J.: *Static Performance of Five Twin-Engine Nonaxisymmetric Nozzles With Vectoring and Reversing Capability.* NASA TP-1224, 1978.
12. Willard, C. M.; Capone, F. J.; Konarski, M.; and Stevens, H. L.: Static Performance of Vectoring/Reversing Nonaxisymmetric Nozzles. AIAA-77-840, July 1977.
13. Re, Richard J.; and Leavitt, Laurence D.: *Static Internal Performance Including Thrust Vectoring and Reversing of Two-Dimensional Convergent-Divergent Nozzles.* NASA TP-2253, 1984.
14. Re, Richard J.; and Berrier, Bobby L.: *Static Internal Performance of Single Expansion-Ramp Nozzles With Thrust Vectoring and Reversing.* NASA TP-1962, 1982.
15. Berrier, Bobby L.; and Leavitt, Laurence D.: *Static Internal Performance of Single-Expansion-Ramp Nozzles With Thrust Vectoring Capability up to 60°.* NASA TP-2364, 1984.
16. Capone, Francis J.; and Berrier, Bobby L.: *Investigation of Axisymmetric and Nonaxisymmetric Nozzles Installed on a 0.10-Scale F-18 Prototype Airplane Model.* NASA TP-1638, 1980.
17. Capone, Francis J.; Hunt, Brian L.; and Poth, Greg E.: Subsonic/Supersonic Nonvectored Aeropropulsive Characteristics of Nonaxisymmetric Nozzles Installed on an F-18 Model. AIAA-81-1445, July 1981.
18. Maiden, Donald L.; and Petit, John E.: Investigation of Two-Dimensional Wedge Exhaust Nozzles for Advanced Aircraft. *J. Aircr.*, vol. 13, no. 10, Oct. 1976, pp. 809–816.
19. Capone, Francis J.; and Maiden, Donald L.: *Performance of Twin Two-Dimensional Wedge Nozzles Including Thrust Vectoring and Reversing Effects at Speeds up to Mach 2.20.* NASA TN D-8449, 1977.
20. Schnell, W. C.; and Grossman, R. L.: Vectoring Non-Axisymmetric Nozzle Jet Induced Effects on a V/STOL Fighter Model. AIAA-78-1080, July 1978.
21. Schnell, W. C.; Grossman, R. L.; and Hoff, G. E.: Comparison of Non-Axisymmetric and Axisymmetric Nozzles Installed on a V/STOL Fighter Model. Preprint 770983, Soc. Automot. Eng., Nov. 1977.
22. Lander, J. A.; and Palcza, J. Lawrence: Exhaust Nozzle Deflector Systems for V/STOL Fighter Aircraft. AIAA-74-1169, Oct. 1974.
23. Lander, J. A.; Nash, D. O.; and Palcza, J. Lawrence: Augmented Deflector Exhaust Nozzle (ADEN) Design for Future Fighters. AIAA-75-1318, Sept.-Oct. 1975.
24. Nash, D. O.; Wakeman, T. G.; and Palcza, J. L.: Structural and Cooling Aspects of the ADEN Nonaxisymmetric Exhaust Nozzle. *Trans. ASME, Ser. A: J. Eng. Power*, vol. 100, no. 2, Apr. 1978, pp. 308–316.
25. Miller, E. H.: Performance of a Forward Swept Wing Fighter Utilizing Thrust Vectoring. AIAA-83-2482, Oct. 1983.
26. Speir, Donald W.; and Blozy, Jack T.: Development of Exhaust Nozzle Internal Performance Prediction Techniques for Advanced Aircraft Applications. AIAA-81-1490, July 1981.

TABLE I.- NOZZLE AND FLAP GEOMETRIC PARAMETERS

Config.	θ, deg	$\rho - \theta$, deg	$l_r/h_{t,n}$	$l_v/h_{t,n}$	β, deg	$(A_e/A_t)_i$	$(A_e/A_t)_e$	Internal performance data	Static-pressure data
AP1	5.98	3.05	2.88	0.575	6.49	1.20	1.37	Figure 5(a)	Table V(a)
BP1	11.82	3.05	2.88	.575	6.49	1.21	1.64	5(a)	V(a)
CP1	5.98	6.95	2.88	.575	6.49	1.20	1.40	5(b)	V(b)
DP1	11.82	6.95	2.88	.575	6.49	1.24	1.64	5(b)	V(b)
EP2	5.98	3.05	6.12	.575	6.49	1.17	1.72	5(c)	V(c)
FP2	11.82	3.05	6.12	.575	6.49	1.21	2.32	5(c)	V(c)
GP2	5.98	6.95	6.12	.575	6.49	1.20	1.67	5(d)	V(d)
HP2	11.82	6.95	6.12	.575	6.49	1.21	2.32	5(d)	V(d)
AQ3	5.98	3.05	2.88	1.225	6.49	1.33	1.45	5(e)	V(e)
BQ3	11.82	3.05	2.88	1.225	6.49	1.41	1.72	5(e)	V(e)
CQ3	5.98	6.95	2.88	1.225	6.49	1.39	1.45	5(f)	V(f)
DQ3	11.82	6.95	2.88	1.225	6.49	1.50	1.72	5(f)	V(f)
EQ4	5.98	3.05	6.12	1.225	6.49	1.33	1.80	5(g)	V(g)
FQ4	11.82	3.05	6.12	1.225	6.49	1.41	2.40	5(g)	V(g)
GQ4	5.98	6.95	6.12	1.225	6.49	1.40	1.75	5(h)	V(h)
HQ4	11.82	6.95	6.12	1.225	6.49	1.50	2.39	5(h)	V(h)
AR1	5.98	3.05	2.88	.575	−6.49	1.06	1.20	5(i)	V(i)
BR1	11.82	3.05	2.88	.575	−6.49	1.08	1.47	5(i)	V(i)
CR1	5.98	6.95	2.88	.575	−6.49	1.06	1.15	5(j)	V(j)
DR1	11.82	6.95	2.88	.575	−6.49	1.10	1.47	5(j)	V(j)
ER2	5.98	3.05	6.12	.575	−6.49	1.05	1.55	5(k)	V(k)
FR2	11.98	3.05	6.12	.575	−6.49	1.07	2.18	5(k)	V(k)
GR2	5.98	6.95	6.12	.575	−6.49	1.08	1.50	5(l)	V(l)
HR2	11.82	6.95	6.12	.575	−6.49	1.10	2.18	5(l)	V(l)
AS3	5.98	3.05	2.88	1.225	−6.49	1.05	1.15	5(m)	V(m)
BS3	11.82	3.05	2.88	1.225	−6.49	1.15	1.42	5(m)	V(m)
CS3	5.98	6.95	2.88	1.225	−6.49	1.10	1.15	5(n)	V(n)
DS3	11.82	6.95	2.88	1.225	−6.49	1.21	1.42	5(n)	V(n)
ES2	5.98	3.05	6.12	1.225	−6.49	1.05	1.50	5(o)	V(o)
FS2	11.82	3.05	6.12	1.225	−6.49	1.14	2.10	5(o)	V(o)
GS2	5.98	6.95	6.12	1.225	−6.49	1.14	1.40	5(p)	V(p)
HS2	11.82	6.95	6.12	1.225	−6.49	1.20	2.12	5(p)	V(p)
IT5	4.40	5.00	4.50	.900	0.0	1.13	1.33	5(q)	V(q)
JT5	13.40	5.00	4.50	.900	0.0	1.23	2.08	5(q)	V(q)
KT5	8.90	2.00	4.50	.900	0.0	1.16	1.70	5(r)	V(r)
LT5	8.90	8.00	4.50	.900	0.0	1.20	1.67	5(r)	V(r)
MT6	8.90	5.00	2.00	.900	0.0	1.18	1.30	5(s)	V(s)
NT2	8.90	5.00	7.00	.900	0.0	1.19	2.05	5(s)	V(s)
OU7	8.90	5.00	4.50	.400	0.0	1.08	1.67	5(t)	V(t)
OV4	8.90	5.00	4.50	1.400	0.0	1.30	1.67	5(t)	V(t)
OW5	8.90	5.00	4.50	.900	10.00	1.35	1.82	5(u)	V(u)
OX7	8.90	5.00	4.50	.900	−10.00	1.06	1.87	5(u)	V(u)
OT5	8.90	5.00	4.50	.900	0.0	1.19	1.70	5(q)	V(v)

TABLE II.- NONDIMENSIONALIZED UPPER FLAP COORDINATES

(a) Upper flaps A through E

All upper flaps		Flap A		Flap B		Flap C		Flap D		Flap E	
$x/h_{t,n}$	$y/h_{t,n}$	$x/h_{t,n}$	$y/h_{t,n}$	$x/h_{t,n}$	$y/h_{t,n}$	$x/h_{t,n}$	$y/h_{t,n}$	$x/h_{t,n}$	$y/h_{t,n}$	$x/h_{t,n}$	$y/h_{t,n}$
0.000	1.389 *	4.242	.008 *	4.275	.014	4.251	.010	4.251	.010	4.242	.008 *
2.350	1.299 *	5.459	.202 *	4.307	.022 *	4.285	.016 *	4.275	.014	6.866	.425 *
2.405	1.294	5.515	.210	5.703	.392 *	4.700	.112 *	4.307	.022	6.936	.436
2.449	1.286	5.571	.218	5.769	.410	4.726	.118	4.327	.028	7.005	.446
2.504	1.272	5.627	.225	5.834	.426	4.753	.123	4.349	.035 *	7.075	.456
2.559	1.252	5.683	.231	5.900	.441	4.806	.134	5.402	.392 *	7.145	.465
2.603	1.232	5.740	.236	5.966	.456	4.858	.145	5.458	.411	7.214	.473
2.658	1.202	5.796	.241	6.032	.470	4.911	.154	5.514	.428	7.284	.481
2.702	1.173	5.852	.245	6.098	.483	4.964	.163	5.570	.443	7.354	.488
2.757	1.133	5.908	.249	6.164	.495	5.017	.172	5.626	.458	7.424	.495
2.801	1.096	5.964	.252	6.230	.506	5.070	.180	5.682	.471	7.493	.502
2.856	1.044	5.992	.253	6.296	.517	5.122	.187	5.738	.483	7.563	.508
2.900	.999 *	6.020	.255 *	6.361	.527	5.175	.194	5.793	.494	7.633	.513
3.600	.239 *	7.020	.298 *	6.427	.536	5.229	.200	5.849	.504	7.702	.519
3.654	.184			6.493	.545	5.281	.206	5.905	.513	7.772	.524
3.708	.139			6.559	.553	5.334	.211	5.961	.521	7.842	.528
3.751	.108			6.625	.560	5.386	.216	6.017	.528	7.912	.533
3.805	.076			6.691	.566	5.439	.221	6.073	.535	7.981	.537
3.859	.050			6.757	.572	5.492	.225	6.129	.541	8.051	.560
3.902	.034			6.822	.577	5.545	.229	6.185	.546	8.121	.544
3.956	.019			6.888	.582	5.598	.233	6.241	.551	8.190	.547
4.010	.009			6.954	.585	5.650	.236	6.296	.555	8.260	.550 *
4.054	.004			7.020	.589	5.703	.239	6.352	.559	10.260	.638 *
4.108	.001					5.756	.242	6.408	.561		
4.140	0.000					5.809	.245	6.464	.564		
4.152	.000					5.862	.247	6.520	.567 *		
4.202	.003					5.914	.250	7.020	.589 *		
						5.967	.252				
						5.994	.253				
						6.020	.255 *				
						7.020	.298 *				

*Straight line contour between two indicated ordinates.

TABLE II.- Continued

(b) Upper flaps F through J

All upper flaps		Flap F		Flap G		Flap H		Flap I		Flap J	
$x/h_{t,n}$	$y/h_{t,n}$	$x/h_{t,n}$	$y/h_{t,n}$	$x/h_{t,n}$	$y/h_{t,n}$	$x/h_{t,n}$	$y/h_{t,n}$	$x/h_{t,n}$	$y/h_{t,n}$	$x/h_{t,n}$	$y/h_{t,n}$
0.000	1.389 *	4.251	.010	4.251	.010	4.251	.010	4.231	.006	4.251	.010
2.350	1.299 *	4.275	.014	4.285	.016 *	4.275	.014	4.246	.009 *	4.275	.014
2.405	1.294	4.307	.022 *	5.700	.341 *	4.307	.022	5.080	.147 *	4.307	.022
2.449	1.286	7.405	.845 *	5.778	.358	4.327	.028	5.099	.150	4.327	.028
2.504	1.272	7.548	.882	5.586	.374	4.349	.035 *	5.118	.153	4.345	.033 *
2.559	1.252	7.691	.917	5.934	.389	6.733	.845 *	5.157	.159	6.357	.703 *
2.603	1.232	7.834	.950	6.012	.402	6.859	.886	5.195	.165	6.471	.759
2.658	1.202	7.976	.981	6.090	.414	6.985	.924	5.233	.170	6.585	.773
2.702	1.173	8.119	1.011	6.168	.425	7.112	.959	5.272	.165	6.700	.804
2.757	1.133	8.262	1.039	6.246	.435	7.238	.990	5.310	.179	6.814	.833
2.801	1.096	8.405	1.066	6.324	.445	7.364	1.019	5.349	.184	6.928	.860
2.856	1.044	8.547	1.090	6.402	.453	7.491	1.046	5.387	.188	7.042	.884
2.900	.999 *	8.690	1.113	6.480	.460	7.617	1.069	5.425	.192	7.156	.906
3.600	.239 *	8.833	1.135	6.558	.467	7.744	1.091	5.464	.195	7.270	.926
3.654	.184	8.975	1.155	6.636	.473	7.870	1.110	5.502	.199	7.384	.944
3.708	.139	9.118	1.173	6.714	.478	7.996	1.127	5.541	.202	7.499	.961
3.751	.108	9.261	1.190	6.792	.483	8.123	1.143	5.579	.205	7.613	.976
3.805	.076	9.404	1.205	6.870	.488	8.249	1.156	5.618	.208	7.727	.989
3.859	.050	9.546	1.219	6.948	.492	8.375	1.168	5.656	.211	7.841	1.001
3.902	.034	9.689	1.231	7.026	.496	8.502	1.179	5.694	.213	7.955	1.011
3.956	.019	9.832	1.242	7.104	.500	8.628	1.189	5.733	.215	8.069	1.021
4.010	.009	9.975	1.252	7.192	.503	8.755	1.197	5.771	.218	8.183	1.029
4.054	.004	10.117	1.260	7.260	.507 *	8.881	1.205	5.810	.220	8.298	1.036
4.108	.001	10.260	1.267	10.260	.638 *	9.007	1.211	5.848	.222	8.412	1.093
4.140	0.000					9.134	1.217	5.886	.224	8.526	1.049
4.152	.000					9.260	1.223 *	5.925	.226	8.640	1.054
4.202	.003					10.260	1.267 *	5.963	.227		
								6.002	.229		
								6.021	.230		
								6.040	.231 *		
								8.640	.344 *		

*Straight line contour between two indicated ordinates.

TABLE II.- Concluded

(c) Upper flaps K through O

All upper flaps		Flap K		Flap L		Flap M		Flap N		Flap O	
$x/h_{t,n}$	$y/h_{t,n}$	$x/h_{t,n}$	$y/h_{t,n}$	$x/h_{t,n}$	$y/h_{t,n}$	$x/h_{t,n}$	$y/h_{t,n}$	$x/h_{t,n}$	$y/h_{t,n}$	$x/h_{t,n}$	$y/h_{t,n}$
0.000	1.389 }*	4.251	.010	4.251	.010	4.251	.010	4.296	.019 }*	4.296	.019 }*
2.350	1.299 }*	4.263	.012 }*	4.275	.014	4.296	.019 }*	7.174	.731 }*	6.095	.464 }*
2.405	1.294	6.613	.464 }*	4.329	.028 }*	5.032	.203 }*	7.224	.743	6.126	.472
2.449	1.286	6.714	.483	5.765	.464 }*	5.046	.207	7.273	.755	6.157	.479
2.504	1.272	6.816	.502	5.824	.481	5.061	.210	7.372	.777	6.219	.493
2.559	1.252	6.917	.519	5.882	.497	5.089	.217	7.470	.798	6.281	.507
2.603	1.232	7.018	.536	5.941	.512	5.131	.225	7.569	.818	6.342	.519
2.658	1.202	7.120	.551	6.000	.525	5.174	.234	7.667	.836	6.404	.531
2.702	1.173	7.221	.566	6.059	.537	5.216	.241	7.766	.854	6.466	.542
2.757	1.133	7.322	.580	6.117	.548	5.259	.247	7.865	.870	6.528	.552
2.801	1.096	7.424	.594	6.176	.558	5.301	.253	7.963	.884	6.590	.562
2.856	1.044	7.525	.606	6.235	.566	5.344	.259	8.062	.898	6.651	.571
2.900	.999 }*	7.627	.618	6.294	.574	5.386	.263	8.161	.911	6.713	.579
3.600	.239 }*	7.728	.629	6.352	.581	5.429	.268	8.259	.923	6.775	.587
3.654	.184	7.829	.639	6.411	.588	5.471	.271	8.358	.934	6.837	.594
3.708	.139	7.931	.649	6.470	.593	5.514	.275	8.457	.945	6.899	.601
3.751	.108	8.032	.658	6.529	.599	5.556	.278	8.555	.954	6.960	.608
3.805	.076	8.133	.666	6.587	.603	5.598	.280	8.654	.963	7.022	.613
3.859	.050	8.235	.673	6.646	.607	5.641	.283	8.752	.971	7.084	.619
3.902	.034	8.336	.680	6.705	.611	5.683	.285	8.851	.978	7.146	.624
3.956	.019	8.437	.686	6.764	.614	5.712	.286	8.950	.985	7.208	.628
4.010	.009	8.539	.692	6.823	.617	5.726	.287	9.048	.992	7.269	.633
4.054	.004	8.640	.696	6.881	.620	5.740	.287 }*	9.147	.998	7.331	.637
4.108	.001			6.940	.622 }*	6.140	.305 }*	9.246	1.003	7.393	.640
4.140	0.000			8.640	.696 }*			9.344	1.008	7.455	.644
4.152	.000							9.443	1.013	7.516	.647
4.202	.003							9.541	1.018	7.578	.650
								9.591	1.020	7.609	.651
								9.640	1.022 }*	7.640	.653 }*
								11.140	1.088 }*	8.640	.696 }*

*Straight line contour between two indicated ordinates.

TABLE III. - NONDIMENSIONALIZED LOWER FLAP COORDINATES

All lower flaps		Flap P		Flap Q		Flap R		Flap S	
$x/h_{t,n}$	$y/h_{t,n}$	$x/h_{t,n}$	$y/h_{t,n}$	$x/h_{t,n}$	$y/h_{t,n}$	$x/h_{t,n}$	$y/h_{t,n}$	$x/h_{t,n}$	$y/h_{t,n}$
0.0	−1.390 }	4.030	−1.012	4.121	−1.001	4.030	−1.012	4.030	−1.012
3.000	−1.220 } *	4.057	−1.008	4.121	−1.001	4.057	−1.008	4.057	−1.008
3.045	−1.217	4.089	−1.004	4.143	−1.000	4.082	−1.005 }	4.082	−1.005 }
3.090	−1.214	4.121	−1.001	4.170	−.999	4.858	−.916 } *	5.508	−.842 } *
3.135	−1.211	4.143	−1.000	4.174	−1.000				
3.180	−1.207	4.170	−.999	4.180	−1.000				
3.225	−1.202	4.174	−1.000	4.188	−1.000				
3.270	−1.197	4.180	−1.000	4.193	−1.001 }				
3.315	−1.190	4.188	−1.000	5.395	−1.138 } *				
3.360	−1.182	4.193	−1.001 }						
3.405	−1.172	4.745	−1.063 } *						
3.450	−1.161 }								
3.900	−1.041 } *								
3.922	−1.035								
3.949	−1.029								
3.976	−1.023								
4.003	−1.017								

Flap T		Flap U		Flap V		Flap W		Flap X	
$x/h_{t,n}$	$y/h_{t,n}$	$x/h_{t,n}$	$y/h_{t,n}$	$x/h_{t,n}$	$y/h_{t,n}$	$x/h_{t,n}$	$y/h_{t,n}$	$x/h_{t,n}$	$y/h_{t,n}$
4.030	−1.012	4.030	−1.012	4.030	−1.012	4.030	−1.012	4.022	−1.014 }
4.057	−1.008	4.057	−1.008	4.057	−1.008	4.057	−1.008	5.244	−.798 } *
4.089	−1.004	4.089	−1.004	4.089	−1.004	4.089	−1.004		
4.121	−1.001	4.121	−1.001	4.121	−1.001	4.121	−1.001		
4.143	−1.000	4.143	−1.000	4.143	−1.000	4.143	−1.000		
4.170	−.999 }	4.170	−.999 }	4.170	−.999 }	4.170	−.999		
5.070	−.999 } *	4.570	−.999 } *	5.570	−.999 } *	4.180	−1.000		
						4.190	−1.001		
						4.197	−1.001		
						4.205	−1.002 }		
						5.070	−1.155 } *		

*Straight line contour between two indicated ordinates.

TABLE IV.- STATIC-PRESSURE ORIFICE LOCATIONS FOR UPPER AND LOWER FLAPS

(a) Upper flaps

Flap	$x/h_{t,n}$							
A	3.675	4.140	4.500	5.000	5.500	5.900	6.400	6.900
B	↓	↓	↓	↓	↓	↓	↓	↓
C	↓	↓	↓	↓	↓	↓	↓	↓
D	↓	↓	↓	↓	↓	↓	↓	↓
E	↓	↓	↓	5.500	6.500	7.600	8.700	10.000
F	↓	↓	↓	↓	↓	↓	↓	↓
G	↓	↓	↓	↓	↓	↓	↓	↓
H	↓	↓	↓	↓	↓	↓	↓	↓
I	↓	↓	↓	5.000	5.800	6.600	7.500	8.400
J	↓	↓	↓	↓	↓	↓	↓	↓
K	↓	↓	↓	↓	↓	↓	↓	↓
L	↓	↓	↓	↓	↓	↓	↓	↓
M	↓	↓	4.300	4.500	4.800	5.100	5.500	6.000
N	↓	↓	4.500	5.500	6.800	8.100	9.400	10.900
O	3.675	4.140	4.500	5.000	5.800	6.600	7.500	8.400

(b) Lower flaps

Flap	$x/h_{t,n}$				
P	3.925	4.170	4.330	4.490	4.640
Q	↓	4.170	4.500	4.840	5.280
R	↓	4.287	4.440	4.600	4.750
S	↓	4.287	4.650	5.000	5.400
T	↓	4.170	4.430	4.690	4.950
U	↓	↓	4.270	4.370	4.470
V	↓	↓	4.600	5.030	5.450
W	↓	↓	4.430	4.690	4.950
X	3.925	4.348	4.600	4.850	5.100

TABLE V.- RATIO OF INTERNAL STATIC PRESSURE TO JET TOTAL PRESSURE ON THE SURFACE OF THE UPPER AND LOWER FLAPS

(a) Configurations AP1 and BP1

Configuration AP1

NPR	Upper flap								Lower flap				
	$p/p_{t,j}$ for $x/h_{t,n}$ of -								$p/p_{t,j}$ for $x/h_{t,n}$ of -				
	3.675	4.140	4.500	5.000	5.500	5.900	6.400	6.900	3.925	4.170	4.330	4.490	4.640
2.003	.736	.371	.316	.417	.488	.597	.557	.501	.713	.384	.375	.369	.363
2.505	.736	.371	.315	.258	.367	.413	.496	.470	.712	.382	.371	.368	.354
3.010	.735	.371	.315	.257	.190	.331	.425	.454	.711	.380	.370	.367	.353
3.407	.736	.371	.314	.257	.189	.219	.205	.366	.712	.380	.369	.367	.353
4.010	.738	.371	.313	.257	.189	.218	.205	.150	.712	.379	.368	.367	.353
5.015	.740	.371	.313	.256	.188	.216	.205	.147	.712	.378	.367	.366	.352
6.021	.746	.371	.312	.256	.187	.214	.205	.147	.712	.378	.366	.366	.352
7.492	.757	.371	.312	.256	.186	.213	.205	.147	.712	.377	.366	.366	.352
8.605	.769	.371	.311	.256	.186	.212	.206	.147	.713	.377	.366	.366	.352
10.037	.775	.370	.311	.256	.186	.211	.206	.147	.715	.377	.366	.360	.352

Configuration BP1

NPR	Upper flap								Lower flap				
	$p/p_{t,j}$ for $x/h_{t,n}$ of -								$p/p_{t,j}$ for $x/h_{t,n}$ of -				
	3.675	4.140	4.500	5.000	5.500	5.900	6.400	6.900	3.925	4.170	4.330	4.490	4.640
2.009	.733	.364	.236	.399	.401	.467	.561	.551	.712	.379	.371	.364	.361
2.782	.735	.365	.235	.200	.314	.323	.341	.375	.710	.377	.366	.363	.349
2.504	.733	.305	.235	.201	.336	.347	.406	.458	.711	.378	.367	.363	.349
2.990	.734	.365	.235	.200	.299	.311	.321	.341	.710	.377	.366	.364	.349
3.414	.734	.365	.235	.200	.150	.264	.290	.299	.711	.377	.365	.364	.349
4.007	.734	.305	.235	.200	.146	.134	.168	.166	.711	.376	.365	.363	.349
5.012	.735	.365	.235	.200	.146	.134	.168	.166	.711	.376	.364	.363	.349
6.041	.736	.365	.235	.200	.145	.133	.168	.166	.712	.376	.364	.363	.350
7.537	.736	.305	.234	.200	.145	.132	.168	.166	.712	.376	.364	.364	.350
8.640	.736	.304	.234	.200	.145	.132	.168	.166	.712	.376	.365	.364	.351
10.048	.736	.303	.233	.200	.145	.132	.168	.166	.714	.376	.305	.364	.351

TABLE V.- Continued

(b) Configurations CP1 and DP1

Configuration CP1

NPR	Upper flap								Lower flap				
	$p/p_{t,j}$ for $x/h_{t,n}$ of -								$p/p_{t,j}$ for $x/h_{t,n}$ of -				
	3.675	4.140	4.500	5.000	5.500	5.900	6.400	6.900	3.925	4.170	4.330	4.490	4.640
2.012	.753	.350	.258	.420	.552	.582	.534	.485	.713	.380	.372	.366	.358
2.518	.753	.350	.257	.264	.416	.498	.493	.423	.712	.378	.369	.366	.347
3.017	.753	.351	.257	.263	.235	.382	.476	.411	.711	.377	.368	.365	.347
3.403	.753	.350	.257	.263	.235	.231	.368	.431	.711	.377	.367	.365	.347
4.007	.753	.350	.257	.263	.235	.230	.201	.173	.712	.376	.365	.364	.346
5.031	.753	.350	.257	.263	.235	.229	.202	.141	.712	.375	.364	.364	.346
6.057	.753	.350	.257	.263	.234	.229	.202	.141	.712	.374	.364	.364	.346
7.529	.753	.350	.256	.263	.234	.229	.202	.141	.712	.374	.364	.364	.347
8.623	.753	.350	.256	.263	.234	.228	.202	.141	.712	.373	.364	.364	.347
10.080	.753	.349	.256	.263	.234	.228	.202	.141	.714	.373	.365	.364	.348

Configuration DP1

NPR	Upper flap								Lower flap				
	$p/p_{t,j}$ for $x/h_{t,n}$ of -								$p/p_{t,j}$ for $x/h_{t,n}$ of -				
	3.675	4.140	4.500	5.000	5.500	5.900	6.400	6.900	3.925	4.170	4.330	4.490	4.640
1.986	.739	.353	.336	.380	.395	.460	.538	.540	.713	.379	.371	.364	.362
2.512	.739	.355	.194	.221	.331	.359	.439	.460	.712	.376	.368	.364	.348
3.027	.739	.356	.193	.180	.300	.310	.327	.348	.711	.375	.366	.363	.348
3.407	.739	.356	.194	.179	.247	.279	.313	.340	.711	.375	.366	.363	.348
4.007	.739	.356	.193	.179	.135	.170	.218	.183	.712	.375	.365	.363	.348
5.004	.739	.355	.193	.179	.135	.170	.217	.175	.712	.374	.364	.363	.348
6.013	.739	.355	.193	.179	.135	.169	.217	.175	.712	.373	.363	.363	.348
7.524	.739	.355	.193	.179	.135	.169	.217	.175	.712	.373	.363	.363	.349
8.586	.739	.355	.192	.179	.135	.169	.217	.175	.713	.372	.364	.363	.349
10.027	.739	.355	.192	.179	.134	.168	.217	.175	.714	.372	.364	.364	.349

TABLE V.- Continued

(c) Configurations EP2 and FP2

Configuration EP2

NPR	Upper flap								Lower flap				
	$p/p_{t,j}$ for $x/h_{t,n}$ of -								$p/p_{t,j}$ for $x/h_{t,n}$ of -				
	3.675	4.140	4.500	5.500	6.500	7.600	8.700	10.000	3.925	4.170	4.330	4.490	4.640
1.990	.712	.363	.316	.468	.537	.556	.512	.500	.711	.378	.371	.364	.359
2.529	.713	.363	.317	.288	.447	.465	.412	.422	.709	.377	.367	.365	.348
3.009	.713	.363	.316	.183	.330	.427	.380	.279	.709	.376	.366	.364	.348
3.410	.713	.363	.316	.183	.294	.381	.344	.256	.709	.376	.365	.365	.348
4.045	.714	.363	.316	.183	.157	.282	.336	.225	.710	.375	.364	.364	.348
5.002	.714	.363	.316	.183	.144	.211	.261	.258	.710	.375	.363	.364	.348
6.012	.714	.363	.316	.183	.144	.095	.193	.255	.710	.375	.363	.364	.348
7.500	.714	.364	.317	.183	.144	.095	.060	.172	.711	.374	.363	.365	.349
8.630	.715	.364	.317	.183	.144	.095	.060	.097	.711	.374	.363	.365	.349
10.013	.715	.364	.317	.183	.144	.095	.060	.080	.713	.375	.364	.365	.349

Configuration FP2

NPR	Upper flap								Lower flap				
	$p/p_{t,j}$ for $x/h_{t,n}$ of -								$p/p_{t,j}$ for $x/h_{t,n}$ of -				
	3.675	4.140	4.500	5.500	6.500	7.600	8.700	10.000	3.925	4.170	4.330	4.490	4.640
2.020	.734	.368	.234	.406	.535	.536	.545	.514	.711	.379	.370	.365	.355
2.518	.734	.369	.234	.312	.393	.463	.464	.438	.710	.378	.367	.365	.349
3.007	.734	.370	.234	.150	.284	.397	.399	.390	.710	.377	.366	.364	.349
3.391	.735	.370	.234	.149	.259	.315	.407	.301	.710	.377	.366	.365	.349
4.022	.735	.371	.234	.149	.226	.250	.315	.370	.710	.377	.364	.364	.349
5.005	.735	.371	.233	.149	.115	.203	.247	.284	.711	.376	.364	.364	.349
5.995	.736	.371	.232	.149	.114	.154	.180	.281	.711	.376	.363	.365	.349
7.495	.736	.371	.232	.150	.114	.072	.142	.201	.711	.377	.363	.365	.350
8.523	.735	.371	.232	.150	.114	.072	.057	.174	.712	.377	.364	.366	.350
8.536	.735	.371	.232	.150	.114	.072	.057	.172	.712	.377	.363	.366	.350
10.038	.736	.371	.232	.150	.113	.072	.057	.049	.713	.377	.364	.366	.350

TABLE V.- Continued

(d) Configurations GP2 and HP2

Configuration GP2

NPR	Upper flap $p/p_{t,j}$ for $x/h_{t,n}$ of -								Lower flap $p/p_{t,j}$ for $x/h_{t,n}$ of -				
	3.675	4.140	4.500	5.500	6.500	7.600	8.700	10.000	3.925	4.170	4.330	4.490	4.640
2.000	.737	.366	.260	.477	.594	.525	.506	.500	.712	.380	.370	.364	.359
2.532	.737	.367	.260	.358	.453	.461	.376	.378	.710	.379	.366	.364	.349
3.002	.737	.368	.260	.304	.351	.446	.303	.363	.710	.378	.365	.364	.349
3.407	.738	.368	.259	.159	.315	.364	.377	.293	.710	.378	.364	.363	.349
3.998	.738	.369	.259	.158	.217	.406	.273	.150	.710	.377	.363	.363	.349
5.037	.738	.369	.259	.158	.184	.245	.331	.205	.711	.376	.362	.363	.349
6.000	.738	.369	.258	.158	.184	.109	.200	.267	.711	.376	.361	.363	.349
7.537	.738	.370	.258	.158	.183	.109	.062	.183	.711	.377	.361	.364	.350
8.739	.738	.370	.257	.159	.183	.109	.062	.100	.712	.376	.362	.364	.350
8.585	.738	.370	.258	.159	.183	.109	.062	.101	.712	.376	.363	.364	.350
10.051	.738	.369	.257	.159	.184	.109	.062	.081	.713	.376	.363	.364	.350

Configuration HP2

NPR	Upper flap $p/p_{t,j}$ for $x/h_{t,n}$ of -								Lower flap $p/p_{t,j}$ for $x/h_{t,n}$ of -				
	3.675	4.140	4.500	5.500	6.500	7.600	8.700	10.000	3.925	4.170	4.330	4.490	4.640
1.981	.769	.355	.201	.439	.525	.577	.560	.510	.712	.379	.371	.362	.363
2.507	.769	.356	.200	.322	.367	.475	.489	.409	.710	.377	.367	.362	.348
3.005	.770	.357	.199	.287	.289	.370	.429	.346	.710	.376	.366	.362	.348
3.421	.770	.357	.199	.250	.258	.316	.396	.331	.710	.376	.365	.362	.348
3.990	.770	.358	.198	.123	.229	.251	.341	.327	.710	.376	.364	.362	.347
5.004	.770	.357	.198	.123	.177	.202	.318	.240	.710	.375	.363	.361	.347
6.019	.771	.357	.198	.123	.091	.193	.249	.235	.711	.375	.363	.362	.348
7.502	.771	.357	.197	.123	.090	.100	.218	.261	.711	.375	.363	.362	.348
8.742	.772	.357	.197	.123	.090	.101	.085	.248	.712	.375	.363	.362	.348
8.618	.772	.357	.197	.123	.090	.101	.090	.257	.712	.375	.363	.362	.348
10.085	.772	.357	.196	.123	.090	.101	.085	.066	.713	.375	.364	.362	.349

TABLE V.- Continued

(e) Configurations AQ3 and BQ3

Configuration AQ3

NPR	Upper flap								Lower flap				
	$p/p_{t,j}$ for $x/h_{t,n}$ of -								$p/p_{t,j}$ for $x/h_{t,n}$ of -				
	3.675	4.140	4.500	5.000	5.500	5.900	6.400	6.900	3.925	4.170	4.500	4.840	5.280
2.055	.762	.368	.314	.255	.395	.474	.560	.508	.711	.383	.367	.309	.460
2.517	.763	.369	.314	.255	.284	.356	.436	.444	.710	.381	.365	.309	.331
3.028	.763	.370	.314	.256	.183	.221	.370	.439	.710	.380	.365	.309	.223
3.396	.763	.370	.314	.255	.183	.220	.213	.267	.710	.379	.364	.309	.223
4.015	.764	.371	.314	.255	.183	.220	.213	.185	.710	.378	.363	.308	.223
5.028	.764	.371	.314	.255	.183	.218	.212	.184	.710	.377	.362	.308	.222
6.018	.764	.371	.314	.255	.182	.219	.211	.185	.709	.376	.362	.308	.222
7.512	.765	.371	.313	.255	.182	.218	.212	.185	.709	.376	.362	.307	.222
8.644	.765	.371	.313	.255	.182	.217	.212	.185	.710	.375	.362	.307	.222
10.006	.764	.371	.313	.255	.182	.217	.212	.185	.713	.375	.362	.307	.222

Configuration BQ3

NPR	Upper flap								Lower flap				
	$p/p_{t,j}$ for $x/h_{t,n}$ of -								$p/p_{t,j}$ for $x/h_{t,n}$ of -				
	3.675	4.140	4.500	5.000	5.500	5.900	6.400	6.900	3.925	4.170	4.500	4.840	5.280
2.023	.734	.366	.237	.383	.381	.426	.513	.538	.714	.384	.366	.308	.471
2.521	.734	.367	.237	.201	.329	.335	.348	.385	.711	.382	.364	.308	.330
3.008	.734	.368	.237	.201	.278	.294	.306	.325	.710	.381	.363	.307	.223
3.457	.735	.368	.237	.201	.144	.134	.201	.339	.710	.380	.362	.307	.223
4.112	.736	.368	.236	.200	.143	.134	.168	.183	.710	.379	.361	.307	.223
4.979	.735	.368	.236	.200	.143	.133	.168	.183	.709	.377	.360	.307	.222
6.071	.736	.369	.236	.201	.143	.132	.168	.183	.708	.376	.360	.307	.222
7.551	.736	.368	.236	.201	.143	.131	.168	.184	.708	.375	.360	.307	.222
8.613	.736	.368	.236	.201	.143	.131	.168	.184	.708	.375	.360	.307	.222
10.037	.736	.369	.235	.201	.143	.130	.168	.184	.709	.374	.360	.307	.222

TABLE V.- Continued

(f) Configurations CQ3 and DQ3

Configuration CQ3

NPR	Upper flap								Lower flap				
	$p/p_{t,j}$ for $x/h_{t,n}$ of -								$p/p_{t,j}$ for $x/h_{t,n}$ of -				
	3.675	4.140	4.500	5.000	5.500	5.900	6.400	6.900	3.925	4.170	4.500	4.840	5.280
1.994	.756	.352	.260	.276	.490	.595	.540	.495	.712	.382	.366	.310	.481
2.554	.755	.353	.260	.264	.232	.409	.497	.438	.710	.379	.365	.309	.324
3.018	.756	.353	.260	.264	.232	.233	.417	.446	.709	.378	.364	.308	.221
3.408	.756	.353	.260	.263	.232	.232	.212	.401	.710	.378	.363	.308	.221
3.983	.756	.353	.260	.263	.232	.231	.212	.185	.710	.377	.361	.308	.221
5.045	.756	.353	.260	.264	.232	.230	.212	.187	.710	.376	.360	.307	.220
6.002	.756	.353	.259	.264	.232	.230	.211	.187	.710	.376	.360	.308	.220
7.503	.756	.353	.259	.264	.232	.230	.210	.181	.710	.376	.360	.307	.220
8.626	.756	.353	.259	.264	.232	.229	.210	.182	.710	.376	.360	.307	.220
10.044	.756	.353	.259	.264	.231	.229	.210	.181	.712	.375	.360	.307	.219

Configuration DQ3

NPR	Upper flap								Lower flap				
	$p/p_{t,j}$ for $x/h_{t,n}$ of -								$p/p_{t,j}$ for $x/h_{t,n}$ of -				
	3.675	4.140	4.500	5.000	5.500	5.900	6.400	6.900	3.925	4.170	4.500	4.840	5.280
1.990	.738	.354	.258	.355	.378	.427	.501	.530	.711	.380	.365	.307	.475
2.542	.739	.355	.195	.180	.302	.332	.394	.451	.710	.378	.363	.307	.331
2.983	.739	.356	.195	.181	.274	.287	.318	.371	.709	.377	.363	.307	.221
3.386	.739	.357	.195	.180	.134	.280	.339	.361	.709	.376	.361	.306	.220
3.985	.739	.357	.195	.180	.134	.167	.218	.193	.710	.376	.360	.305	.220
5.036	.740	.357	.195	.180	.133	.166	.218	.193	.710	.375	.359	.305	.220
5.998	.740	.357	.195	.180	.133	.166	.218	.193	.710	.375	.359	.305	.219
7.447	.740	.356	.194	.180	.133	.165	.218	.193	.710	.374	.359	.305	.219
8.570	.740	.356	.194	.179	.133	.165	.218	.192	.710	.374	.359	.305	.219
10.023	.740	.356	.194	.179	.133	.165	.218	.193	.712	.374	.359	.305	.219

TABLE V.- Continued

(g) Configurations EQ4 and FQ4

Configuration EQ4

NPR	Upper flap $p/p_{t,j}$ for $x/h_{t,n}$ of -								Lower flap $p/p_{t,j}$ for $x/h_{t,n}$ of -				
	3.675	4.140	4.500	5.500	6.500	7.600	8.700	10.000	3.925	4.170	4.500	4.840	5.280
2.004	.713	.361	.317	.390	.554	.557	.510	.497	.711	.378	.366	.308	.466
2.516	.714	.362	.317	.181	.372	.493	.398	.406	.710	.378	.363	.308	.336
2.983	.714	.363	.318	.179	.313	.415	.408	.281	.710	.377	.363	.307	.223
3.445	.715	.363	.317	.179	.277	.352	.312	.284	.710	.376	.362	.307	.223
3.993	.715	.363	.317	.179	.149	.296	.391	.209	.710	.376	.361	.306	.223
4.969	.715	.363	.317	.179	.149	.136	.323	.347	.710	.376	.359	.306	.222
6.011	.715	.363	.317	.179	.149	.136	.097	.294	.710	.375	.358	.306	.222
7.523	.715	.363	.317	.179	.148	.135	.090	.080	.711	.375	.358	.306	.222
8.600	.715	.363	.317	.180	.148	.135	.090	.062	.711	.375	.358	.306	.222
10.023	.715	.363	.317	.180	.148	.135	.090	.050	.712	.375	.359	.306	.222

Configuration FQ4

NPR	Upper flap $p/p_{t,j}$ for $x/h_{t,n}$ of -								Lower flap $p/p_{t,j}$ for $x/h_{t,n}$ of -				
	3.675	4.140	4.500	5.500	6.500	7.600	8.700	10.000	3.925	4.170	4.500	4.840	5.280
1.994	.735	.370	.234	.360	.513	.550	.550	.520	.712	.379	.367	.310	.472
2.533	.736	.370	.233	.297	.333	.442	.471	.426	.711	.378	.364	.310	.320
2.988	.735	.371	.233	.148	.270	.370	.423	.372	.710	.377	.364	.309	.225
3.446	.736	.372	.233	.148	.245	.291	.392	.323	.710	.377	.363	.309	.224
3.995	.736	.372	.232	.148	.220	.246	.314	.376	.710	.377	.361	.308	.224
5.010	.736	.371	.233	.148	.116	.206	.237	.292	.710	.376	.360	.308	.223
6.037	.736	.371	.232	.148	.115	.092	.206	.266	.711	.376	.359	.308	.223
7.516	.737	.371	.232	.148	.115	.092	.088	.221	.710	.376	.359	.308	.223
8.604	.737	.371	.232	.148	.115	.092	.088	.069	.711	.376	.359	.308	.223
10.051	.737	.371	.232	.148	.114	.092	.089	.069	.712	.376	.360	.309	.223

TABLE V.- Continued

(h) Configurations GQ4 and HQ4

Configuration GQ4

NPR	Upper flap, $p/p_{t,j}$ for $x/h_{t,n}$ of -								Lower flap, $p/p_{t,j}$ for $x/h_{t,n}$ of -				
	3.675	4.140	4.500	5.500	6.500	7.600	8.700	10.000	3.925	4.170	4.500	4.840	5.280
1.999	.738	.365	.259	.402	.572	.536	.509	.501	.711	.378	.365	.308	.480
2.518	.739	.365	.259	.341	.386	.474	.415	.407	.710	.377	.364	.307	.336
2.995	.738	.366	.259	.215	.324	.433	.325	.362	.710	.377	.362	.306	.222
3.432	.739	.367	.258	.156	.311	.400	.302	.260	.710	.376	.361	.306	.221
4.004	.739	.367	.258	.156	.190	.421	.308	.155	.710	.376	.360	.306	.221
4.988	.739	.368	.258	.156	.189	.156	.389	.205	.710	.375	.358	.305	.220
6.003	.739	.368	.257	.156	.189	.156	.195	.260	.710	.375	.358	.305	.220
7.532	.740	.368	.257	.157	.189	.156	.092	.166	.711	.375	.358	.306	.220
8.575	.740	.368	.257	.157	.188	.156	.092	.076	.711	.375	.358	.306	.220
10.038	.739	.368	.257	.157	.189	.157	.092	.050	.712	.375	.358	.306	.220

Configuration HQ4

NPR	Upper flap, $p/p_{t,j}$ for $x/h_{t,n}$ of -								Lower flap, $p/p_{t,j}$ for $x/h_{t,n}$ of -				
	3.675	4.140	4.500	5.500	6.500	7.600	8.700	10.000	3.925	4.170	4.500	4.840	5.280
1.997	.769	.355	.201	.406	.441	.532	.578	.522	.710	.378	.364	.307	.474
2.506	.770	.356	.199	.326	.339	.399	.478	.434	.709	.377	.362	.307	.342
3.004	.770	.357	.198	.283	.280	.321	.401	.379	.708	.377	.362	.306	.222
3.407	.770	.357	.198	.239	.252	.293	.386	.345	.708	.376	.360	.306	.222
4.030	.771	.357	.198	.122	.222	.234	.330	.349	.709	.376	.359	.306	.221
4.966	.771	.357	.198	.122	.189	.207	.270	.244	.709	.375	.358	.305	.221
5.004	.771	.357	.197	.122	.188	.206	.269	.246	.709	.375	.358	.305	.221
5.982	.771	.357	.197	.122	.091	.192	.285	.309	.709	.375	.357	.305	.221
7.551	.772	.357	.197	.122	.091	.121	.127	.306	.709	.375	.357	.305	.220
8.628	.772	.357	.196	.122	.091	.121	.127	.164	.709	.375	.357	.305	.220
10.005	.772	.357	.196	.122	.090	.121	.127	.075	.711	.375	.358	.306	.220

TABLE V.- Continued

(i) Configurations AR1 and BR1

Configuration AR1

NPR	Upper flap, $p/p_{t,j}$ for $x/h_{t,n}$ of -								Lower flap, $p/p_{t,j}$ for $x/h_{t,n}$ of -				
	3.675	4.140	4.500	5.000	5.500	5.900	6.400	6.900	3.925	4.287	4.440	4.600	4.750
2.031	.771	.397	.380	.528	.589	.588	.515	.481	.736	.626	.573	.521	.455
2.525	.772	.398	.382	.432	.387	.541	.492	.367	.734	.625	.571	.520	.455
3.018	.772	.399	.382	.431	.348	.326	.385	.365	.733	.625	.570	.520	.454
3.433	.772	.400	.382	.430	.348	.304	.345	.292	.733	.625	.570	.520	.454
4.037	.772	.400	.381	.430	.348	.304	.203	.240	.732	.624	.569	.520	.454
5.056	.773	.400	.381	.430	.348	.304	.203	.135	.732	.625	.570	.520	.454
6.041	.773	.400	.380	.430	.348	.305	.203	.135	.732	.625	.571	.521	.455
7.492	.773	.400	.380	.431	.348	.306	.204	.135	.731	.626	.572	.521	.455
8.614	.774	.399	.380	.431	.349	.307	.204	.135	.732	.628	.573	.522	.456
10.050	.774	.399	.380	.431	.349	.308	.205	.136	.733	.629	.575	.523	.457

Configuration BR1

NPR	Upper flap, $p/p_{t,j}$ for $x/h_{t,n}$ of -								Lower flap, $p/p_{t,j}$ for $x/h_{t,n}$ of -				
	3.675	4.140	4.500	5.000	5.500	5.900	6.400	6.900	3.925	4.287	4.440	4.600	4.750
2.013	.744	.398	.287	.392	.586	.605	.604	.533	.737	.623	.574	.522	.456
2.505	.744	.398	.285	.325	.389	.525	.564	.497	.735	.622	.572	.521	.455
3.002	.744	.398	.285	.325	.287	.346	.483	.505	.734	.622	.570	.520	.455
3.427	.745	.398	.285	.324	.287	.234	.344	.433	.733	.622	.570	.520	.455
4.056	.745	.398	.284	.324	.287	.234	.200	.188	.733	.622	.570	.520	.455
5.034	.745	.398	.284	.324	.287	.234	.200	.165	.732	.622	.570	.520	.455
6.017	.745	.398	.283	.324	.287	.234	.201	.166	.731	.622	.571	.520	.455
7.517	.745	.397	.283	.324	.287	.235	.201	.166	.731	.624	.572	.521	.456
8.632	.745	.397	.282	.324	.287	.235	.202	.166	.731	.625	.573	.522	.456
10.054	.745	.396	.282	.324	.287	.236	.202	.166	.734	.627	.575	.523	.457

TABLE V.- Continued

(j) Configurations CR1 and DR1

Configuration CR1

NPR	Upper flap								Lower flap				
	$p/p_{t,j}$ for $x/h_{t,n}$ of -								$p/p_{t,j}$ for $x/h_{t,n}$ of -				
	3.675	4.140	4.500	5.000	5.500	5.900	6.400	6.900	3.925	4.287	4.440	4.600	4.750
2.040	.761	.377	.314	.611	.611	.542	.494	.477	.737	.622	.572	.518	.450
2.532	.761	.378	.313	.444	.593	.498	.396	.341	.735	.620	.570	.518	.449
2.998	.761	.378	.313	.438	.427	.544	.399	.285	.734	.620	.569	.518	.449
3.405	.762	.378	.313	.437	.427	.314	.454	.286	.733	.620	.569	.518	.449
4.018	.762	.378	.312	.437	.428	.313	.201	.325	.732	.619	.569	.518	.449
4.985	.762	.378	.312	.436	.428	.314	.201	.131	.732	.619	.569	.518	.450
6.055	.762	.377	.311	.437	.428	.314	.201	.131	.731	.620	.570	.519	.450
7.524	.761	.377	.311	.437	.429	.315	.201	.131	.730	.622	.571	.519	.450
8.619	.761	.377	.310	.436	.429	.316	.201	.132	.730	.623	.572	.519	.451
10.067	.761	.377	.310	.436	.430	.317	.202	.132	.733	.625	.573	.520	.452

Configuration DR1

NPR	Upper flap								Lower flap				
	$p/p_{t,j}$ for $x/h_{t,n}$ of -								$p/p_{t,j}$ for $x/h_{t,n}$ of -				
	3.675	4.140	4.500	5.000	5.500	5.900	6.400	6.900	3.925	4.287	4.440	4.600	4.750
2.013	.747	.379	.235	.437	.564	.649	.605	.504	.735	.622	.571	.518	.451
2.505	.748	.381	.235	.269	.451	.541	.578	.449	.733	.621	.569	.517	.451
3.024	.748	.381	.234	.268	.261	.480	.560	.426	.732	.620	.568	.517	.450
3.415	.748	.381	.234	.268	.259	.321	.548	.460	.732	.620	.568	.517	.450
4.000	.748	.381	.233	.268	.259	.299	.259	.409	.731	.620	.568	.516	.450
5.037	.748	.381	.233	.267	.258	.300	.259	.174	.731	.620	.568	.517	.450
6.061	.748	.381	.232	.267	.258	.300	.259	.174	.730	.621	.569	.517	.451
7.541	.748	.381	.232	.267	.257	.301	.260	.174	.730	.621	.570	.519	.451
8.606	.748	.380	.231	.267	.257	.302	.261	.174	.730	.622	.571	.519	.452
10.065	.748	.380	.231	.266	.257	.303	.262	.175	.731	.624	.573	.520	.452

TABLE V.- Continued

(k) Configurations ER2 and FR2

Configuration ER2

NPR	Upper flap								Lower flap				
	$p/p_{t,j}$ for $x/h_{t,n}$ of -								$p/p_{t,j}$ for $x/h_{t,n}$ of -				
	3.675	4.140	4.500	5.500	6.500	7.600	8.700	10.000	3.925	4.287	4.440	4.600	4.750
1.985	.723	.392	.384	.518	.511	.564	.510	.502	.735	.623	.572	.519	.451
2.488	.724	.392	.383	.343	.400	.512	.371	.435	.733	.622	.569	.518	.451
3.003	.724	.393	.385	.338	.277	.500	.332	.276	.732	.621	.568	.518	.451
3.406	.724	.394	.384	.338	.254	.391	.398	.214	.731	.621	.567	.517	.451
3.973	.725	.394	.383	.338	.145	.191	.421	.232	.731	.621	.567	.517	.451
4.965	.725	.393	.383	.338	.145	.147	.246	.339	.730	.621	.567	.518	.450
5.000	.725	.393	.383	.339	.145	.145	.241	.336	.730	.621	.567	.518	.450
6.009	.725	.393	.383	.339	.145	.088	.098	.237	.730	.622	.568	.518	.451
7.474	.725	.394	.384	.341	.145	.087	.056	.127	.730	.622	.570	.519	.451
8.676	.725	.393	.384	.342	.145	.087	.056	.086	.730	.623	.571	.519	.452
8.657	.725	.393	.384	.342	.145	.087	.056	.086	.730	.623	.571	.519	.452
9.947	.725	.393	.383	.342	.146	.087	.056	.085	.731	.624	.572	.520	.452

Configuration FR2

NPR	Upper flap								Lower flap				
	$p/p_{t,j}$ for $x/h_{t,n}$ of -								$p/p_{t,j}$ for $x/h_{t,n}$ of -				
	3.675	4.140	4.500	5.500	6.500	7.600	8.700	10.000	3.925	4.287	4.440	4.600	4.750
1.989	.745	.400	.283	.581	.509	.547	.556	.526	.735	.624	.574	.521	.455
2.513	.745	.399	.282	.295	.462	.370	.445	.449	.733	.623	.572	.520	.455
3.005	.745	.399	.282	.294	.378	.471	.360	.392	.733	.623	.570	.520	.454
3.412	.746	.399	.282	.294	.151	.332	.424	.300	.732	.623	.570	.522	.454
3.999	.746	.399	.281	.294	.135	.220	.446	.289	.732	.623	.569	.522	.454
5.002	.746	.399	.280	.294	.135	.172	.226	.291	.731	.623	.570	.522	.454
6.111	.746	.399	.280	.294	.135	.067	.154	.225	.731	.623	.571	.522	.455
7.496	.746	.399	.280	.294	.134	.067	.055	.190	.731	.624	.573	.522	.455
8.612	.746	.398	.279	.294	.135	.067	.055	.130	.730	.625	.574	.523	.455
9.982	.746	.398	.279	.294	.135	.067	.055	.047	.732	.626	.575	.523	.456

TABLE V.- Continued

(1) Configurations GR2 and HR2

Configuration GR2

NPR	Upper flap								Lower flap				
	$p/p_{t,j}$ for $x/h_{t,n}$ of -								$p/p_{t,j}$ for $x/h_{t,n}$ of -				
	3.675	4.140	4.500	5.500	6.500	7.600	8.700	10.000	3.925	4.287	4.440	4.600	4.750
2.013	.747	.397	.313	.583	.588	.499	.502	.496	.735	.622	.571	.519	.452
2.518	.748	.399	.313	.367	.525	.391	.389	.366	.734	.621	.569	.519	.452
2.990	.748	.400	.312	.309	.524	.341	.257	.436	.733	.621	.568	.519	.452
3.378	.748	.401	.311	.309	.410	.466	.215	.216	.733	.621	.568	.518	.452
4.012	.748	.401	.311	.309	.199	.309	.383	.172	.732	.621	.567	.519	.452
4.991	.748	.400	.310	.309	.199	.228	.203	.254	.732	.621	.568	.519	.452
6.019	.749	.401	.310	.310	.199	.101	.149	.216	.732	.621	.569	.519	.452
7.512	.749	.401	.310	.310	.199	.101	.058	.109	.731	.622	.570	.520	.453
8.710	.748	.401	.309	.311	.200	.101	.058	.098	.731	.623	.571	.520	.453
8.670	.748	.401	.309	.311	.200	.101	.058	.098	.731	.623	.571	.520	.453
10.062	.749	.401	.309	.311	.200	.102	.058	.085	.733	.624	.573	.521	.454

Configuration HR2

NPR	Upper flap								Lower flap				
	$p/p_{t,j}$ for $x/h_{t,n}$ of -								$p/p_{t,j}$ for $x/h_{t,n}$ of -				
	3.675	4.140	4.500	5.500	6.500	7.600	8.700	10.000	3.925	4.287	4.440	4.600	4.750
1.982	.777	.381	.239	.583	.542	.599	.554	.500	.734	.621	.571	.519	.451
2.518	.778	.382	.238	.248	.444	.511	.448	.384	.732	.620	.568	.518	.451
3.015	.778	.383	.238	.246	.368	.517	.385	.312	.731	.620	.567	.518	.451
3.374	.778	.383	.238	.246	.293	.456	.432	.267	.731	.620	.567	.518	.451
4.059	.779	.383	.237	.246	.233	.298	.384	.289	.731	.620	.566	.518	.451
5.017	.779	.383	.237	.246	.121	.218	.292	.267	.731	.620	.566	.518	.451
6.015	.779	.382	.236	.246	.121	.117	.240	.289	.730	.621	.567	.519	.451
7.452	.779	.382	.236	.246	.121	.096	.086	.229	.730	.621	.568	.519	.452
8.655	.779	.382	.236	.246	.121	.096	.083	.141	.730	.622	.570	.520	.452
10.001	.779	.382	.235	.246	.121	.096	.083	.053	.732	.623	.571	.520	.453

TABLE V.- Continued

(m) Configurations AS3 and BS3

Configuration AS3

NPR	Upper flap								Lower flap				
	$p/p_{t,j}$ for $x/h_{t,n}$ of -								$p/p_{t,j}$ for $x/h_{t,n}$ of -				
	3.675	4.140	4.500	5.000	5.500	5.900	6.400	6.900	3.925	4.287	4.650	5.000	5.400
2.009	.772	.398	.383	.438	.469	.607	.535	.489	.742	.617	.506	.387	.368
2.521	.772	.399	.381	.436	.382	.411	.535	.405	.741	.616	.505	.386	.327
2.988	.771	.400	.382	.435	.381	.400	.388	.390	.742	.615	.504	.386	.332
3.381	.772	.401	.383	.434	.381	.400	.350	.293	.742	.614	.504	.386	.333
4.001	.772	.401	.382	.434	.380	.400	.350	.226	.742	.613	.503	.386	.332
5.047	.772	.401	.381	.433	.380	.400	.351	.220	.743	.613	.504	.387	.329
5.985	.773	.402	.381	.433	.380	.400	.351	.220	.742	.613	.504	.387	.328
7.465	.773	.401	.381	.433	.380	.401	.353	.221	.743	.613	.505	.387	.325
8.624	.773	.401	.381	.433	.380	.402	.353	.221	.744	.615	.506	.388	.322
9.868	.773	.400	.380	.433	.381	.402	.354	.222	.748	.616	.507	.388	.320
9.993	.773	.400	.380	.433	.381	.402	.354	.222	.748	.617	.507	.388	.319

Configuration BS3

NPR	Upper flap								Lower flap				
	$p/p_{t,j}$ for $x/h_{t,n}$ of -								$p/p_{t,j}$ for $x/h_{t,n}$ of -				
	3.675	4.140	4.500	5.000	5.500	5.900	6.400	6.900	3.925	4.287	4.650	5.000	5.400
2.008	.744	.397	.287	.324	.506	.616	.612	.534	.745	.617	.507	.388	.470
2.512	.744	.398	.285	.325	.298	.469	.569	.505	.744	.615	.505	.387	.272
3.029	.744	.399	.285	.326	.298	.282	.493	.518	.744	.614	.505	.386	.272
3.414	.745	.400	.285	.326	.297	.282	.302	.449	.744	.614	.504	.386	.272
4.029	.745	.400	.285	.325	.297	.282	.291	.383	.744	.613	.504	.386	.272
5.009	.745	.400	.285	.325	.297	.282	.291	.264	.744	.613	.504	.386	.271
6.001	.746	.399	.284	.325	.297	.282	.291	.265	.744	.612	.505	.387	.271
7.505	.746	.399	.284	.325	.296	.281	.292	.266	.744	.613	.505	.387	.271
8.612	.746	.398	.283	.325	.296	.282	.293	.267	.744	.613	.506	.388	.271
10.097	.746	.398	.283	.325	.296	.282	.294	.268	.746	.615	.507	.388	.271

TABLE V.- Continued

(n) Configurations CS3 and DS3

Configuration CS3

NPR	Upper flap								Lower flap				
	$p/p_{t,j}$ for $x/h_{t,n}$ of -								$p/p_{t,j}$ for $x/h_{t,n}$ of -				
	3.675	4.140	4.500	5.000	5.500	5.900	6.400	6.900	3.925	4.287	4.650	5.000	5.400
2.028	.763	.377	.311	.447	.607	.551	.498	.487	.746	.617	.502	.384	.465
2.498	.762	.377	.311	.439	.487	.531	.409	.358	.745	.616	.500	.383	.270
2.991	.763	.377	.311	.439	.470	.459	.402	.297	.745	.615	.499	.382	.270
3.377	.763	.377	.311	.439	.469	.406	.429	.275	.746	.615	.498	.382	.270
3.990	.763	.377	.311	.438	.469	.406	.319	.292	.745	.614	.498	.382	.269
5.046	.763	.377	.310	.438	.470	.407	.319	.220	.746	.614	.499	.382	.269
6.026	.763	.377	.310	.438	.470	.407	.320	.217	.746	.614	.499	.382	.269
7.545	.762	.376	.309	.437	.470	.408	.321	.218	.745	.615	.500	.383	.269
8.645	.762	.376	.309	.437	.471	.409	.321	.218	.746	.616	.501	.383	.269
9.960	.762	.375	.308	.437	.471	.410	.322	.219	.747	.617	.502	.384	.269

Configuration DS3

NPR	Upper flap								Lower flap				
	$p/p_{t,j}$ for $x/h_{t,n}$ of -								$p/p_{t,j}$ for $x/h_{t,n}$ of -				
	3.675	4.140	4.500	5.000	5.500	5.900	6.400	6.900	3.925	4.287	4.650	5.000	5.400
2.026	.749	.381	.235	.392	.478	.607	.611	.511	.743	.614	.503	.384	.466
2.500	.749	.382	.234	.269	.435	.513	.578	.460	.743	.613	.501	.383	.267
3.024	.749	.382	.235	.269	.261	.494	.568	.428	.743	.613	.500	.383	.268
3.431	.749	.382	.234	.269	.260	.421	.577	.452	.743	.613	.499	.383	.267
3.974	.749	.382	.234	.269	.260	.346	.366	.502	.743	.613	.499	.383	.267
5.041	.749	.382	.234	.268	.259	.346	.365	.277	.743	.613	.499	.383	.268
6.013	.749	.382	.233	.268	.259	.346	.366	.277	.743	.613	.500	.384	.268
7.524	.749	.382	.232	.267	.259	.346	.367	.277	.742	.615	.501	.384	.268
8.637	.749	.382	.232	.267	.258	.347	.368	.278	.743	.616	.502	.385	.268
10.047	.749	.381	.231	.267	.258	.347	.369	.279	.747	.618	.503	.385	.268

TABLE V.- Continued

(o) Configurations ES2 and FS2

Configuration ES2

NPR	Upper flap, $p/p_{t,j}$ for $x/h_{t,n}$ of -								Lower flap, $p/p_{t,j}$ for $x/h_{t,n}$ of -				
	3.675	4.140	4.500	5.500	6.500	7.600	8.700	10.000	3.925	4.287	4.650	5.000	5.400
1.999	.724	.391	.385	.369	.519	.561	.507	.498	.745	.618	.502	.386	.401
2.542	.724	.391	.384	.368	.361	.470	.405	.392	.744	.616	.500	.385	.329
2.998	.724	.392	.385	.368	.273	.495	.349	.246	.743	.616	.499	.385	.335
3.457	.725	.392	.385	.368	.260	.258	.478	.204	.743	.615	.498	.384	.334
3.981	.725	.392	.384	.367	.260	.177	.372	.298	.743	.615	.498	.384	.331
4.985	.725	.392	.384	.367	.260	.132	.128	.301	.743	.615	.498	.384	.331
6.017	.725	.392	.384	.368	.260	.132	.083	.189	.743	.614	.499	.384	.327
7.528	.725	.392	.383	.368	.261	.132	.072	.114	.743	.615	.500	.385	.323
8.497	.725	.392	.384	.370	.262	.132	.072	.101	.743	.615	.501	.385	.320
8.634	.726	.391	.384	.369	.262	.132	.072	.099	.743	.615	.501	.385	.321
10.026	.725	.391	.383	.370	.262	.133	.072	.062	.745	.616	.502	.385	.318

Configuration FS2

NPR	Upper flap, $p/p_{t,j}$ for $x/h_{t,n}$ of -								Lower flap, $p/p_{t,j}$ for $x/h_{t,n}$ of -				
	3.675	4.140	4.500	5.500	6.500	7.600	8.700	10.000	3.925	4.287	4.650	5.000	5.400
1.991	.745	.398	.282	.489	.514	.546	.556	.524	.745	.619	.506	.388	.478
2.496	.745	.398	.282	.301	.507	.382	.448	.448	.744	.618	.504	.387	.269
3.003	.746	.399	.281	.301	.369	.481	.373	.398	.743	.617	.503	.387	.269
3.417	.746	.399	.281	.301	.204	.288	.433	.294	.743	.617	.502	.386	.269
3.990	.746	.399	.281	.301	.204	.208	.432	.335	.743	.617	.502	.386	.268
4.985	.746	.399	.280	.301	.204	.156	.164	.427	.743	.617	.502	.386	.268
5.986	.746	.399	.280	.301	.204	.109	.122	.281	.743	.617	.503	.387	.268
7.467	.746	.398	.279	.301	.204	.109	.076	.100	.743	.617	.504	.387	.268
8.599	.746	.398	.279	.301	.204	.109	.076	.085	.744	.618	.505	.388	.268
10.034	.746	.397	.279	.301	.204	.109	.076	.059	.746	.619	.506	.388	.268

TABLE V.- Continued

(p) Configurations GS2 and HS2

Configuration GS2

NPR	Upper flap								Lower flap				
	$p/p_{t,j}$ for $x/h_{t,n}$ of -								$p/p_{t,j}$ for $x/h_{t,n}$ of -				
	3.675	4.140	4.500	5.500	6.500	7.600	8.700	10.000	3.925	4.287	4.650	5.000	5.400
1.991	.747	.398	.312	.544	.599	.507	.507	.501	.745	.617	.503	.384	.478
2.516	.747	.399	.312	.321	.553	.399	.385	.367	.743	.616	.501	.384	.270
3.004	.747	.400	.312	.321	.525	.352	.250	.447	.743	.615	.500	.383	.270
3.372	.747	.401	.311	.321	.416	.462	.226	.226	.743	.615	.499	.383	.270
3.994	.748	.400	.311	.321	.310	.292	.271	.199	.743	.615	.499	.383	.269
5.041	.748	.400	.310	.321	.310	.208	.217	.147	.743	.615	.499	.383	.269
6.039	.748	.401	.309	.321	.310	.150	.125	.142	.743	.615	.499	.383	.268
7.556	.748	.401	.309	.321	.310	.150	.096	.079	.743	.615	.501	.384	.268
7.497	.748	.401	.309	.322	.310	.150	.097	.080	.743	.615	.501	.384	.268
8.608	.748	.400	.309	.322	.310	.150	.074	.062	.743	.616	.502	.384	.268
10.123	.748	.400	.308	.322	.312	.150	.074	.052	.745	.617	.503	.384	.268

Configuration HS2

NPR	Upper flap								Lower flap				
	$p/p_{t,j}$ for $x/h_{t,n}$ of -								$p/p_{t,j}$ for $x/h_{t,n}$ of -				
	3.675	4.140	4.500	5.500	6.500	7.600	8.700	10.000	3.925	4.287	4.650	5.000	5.400
2.002	.777	.382	.239	.456	.550	.593	.549	.496	.743	.614	.503	.385	.474
2.546	.778	.383	.238	.252	.478	.510	.440	.382	.742	.613	.501	.384	.269
3.031	.778	.383	.238	.251	.369	.498	.413	.292	.742	.613	.500	.384	.269
3.403	.778	.383	.238	.251	.317	.491	.369	.268	.742	.613	.499	.383	.269
3.992	.779	.383	.237	.251	.172	.414	.445	.198	.742	.613	.498	.383	.268
6.025	.780	.382	.236	.250	.172	.154	.238	.393	.743	.614	.499	.384	.267
7.570	.780	.382	.236	.250	.171	.154	.112	.174	.743	.614	.500	.384	.267
8.631	.780	.382	.235	.249	.173	.154	.112	.137	.743	.615	.501	.384	.267
10.115	.780	.382	.235	.249	.173	.154	.113	.065	.746	.616	.503	.385	.267

TABLE V.- Continued

(q) Configurations IT5 and JT5

Configuration IT5

NPR	Upper flap $p/p_{t,j}$ for $x/h_{t,n}$ of -								Lower flap $p/p_{t,j}$ for $x/h_{t,n}$ of -				
	3.675	4.140	4.500	5.000	5.800	6.600	7.500	8.400	3.925	4.170	4.430	4.690	4.950
1.993	.738	.356	.310	.422	.603	.515	.507	.487	.705	.544	.497	.414	.350
2.516	.739	.356	.310	.311	.560	.427	.362	.452	.703	.546	.493	.413	.332
3.071	.738	.357	.310	.311	.334	.489	.327	.223	.703	.546	.492	.413	.331
3.393	.738	.357	.310	.310	.334	.415	.312	.260	.702	.545	.491	.413	.331
4.012	.738	.357	.309	.310	.333	.219	.286	.187	.702	.544	.491	.413	.331
5.013	.738	.359	.309	.310	.332	.219	.177	.184	.702	.544	.491	.412	.330
5.980	.737	.359	.308	.309	.332	.219	.112	.127	.702	.544	.491	.413	.330
7.566	.738	.359	.308	.309	.332	.220	.112	.063	.701	.545	.493	.413	.331
8.620	.737	.359	.307	.309	.333	.221	.112	.063	.701	.545	.494	.413	.331
10.038	.736	.357	.307	.309	.333	.221	.112	.063	.702	.546	.495	.413	.331

Configuration JT5

NPR	Upper flap $p/p_{t,j}$ for $x/h_{t,n}$ of -								Lower flap $p/p_{t,j}$ for $x/h_{t,n}$ of -				
	3.675	4.140	4.500	5.000	5.800	6.600	7.500	8.400	3.925	4.170	4.430	4.690	4.950
1.984	.756	.352	.205	.328	.522	.588	.589	.528	.705	.544	.495	.413	.353
2.518	.757	.356	.205	.204	.362	.464	.527	.452	.703	.546	.492	.412	.331
2.990	.756	.358	.205	.203	.323	.370	.491	.404	.702	.547	.491	.412	.331
3.384	.756	.359	.205	.203	.201	.325	.414	.440	.702	.546	.490	.411	.331
4.000	.756	.360	.204	.203	.175	.290	.342	.356	.702	.545	.489	.411	.330
5.015	.757	.360	.204	.202	.175	.146	.283	.344	.701	.545	.489	.411	.330
5.994	.757	.361	.203	.202	.175	.146	.140	.106	.701	.545	.490	.411	.330
7.502	.757	.361	.203	.201	.174	.145	.140	.106	.701	.545	.491	.411	.330
8.573	.757	.361	.204	.201	.174	.145	.140	.106	.701	.546	.492	.412	.330
9.977	.757	.361	.203	.201	.174	.145	.141	.106	.702	.547	.493	.412	.331

TABLE V.- Continued

(r) Configurations KT5 and LT5

Configuration KT5

NPR	Upper flap								Lower flap				
	$p/p_{t,j}$ for $x/h_{t,n}$ of -								$p/p_{t,j}$ for $x/h_{t,n}$ of -				
	3.675	4.140	4.500	5.000	5.800	6.600	7.500	8.400	3.925	4.170	4.430	4.690	4.950
2.013	.746	.351	.289	.290	.558	.532	.550	.528	.704	.544	.497	.415	.345
2.526	.747	.353	.288	.289	.398	.471	.474	.431	.702	.547	.494	.414	.337
3.007	.747	.354	.288	.289	.240	.398	.498	.331	.701	.546	.492	.414	.337
3.406	.746	.355	.287	.289	.239	.173	.453	.428	.701	.546	.491	.413	.336
3.971	.747	.356	.287	.288	.239	.168	.272	.454	.701	.545	.491	.413	.335
4.984	.747	.358	.285	.288	.238	.168	.110	.231	.700	.545	.491	.413	.335
5.996	.746	.359	.284	.288	.238	.167	.110	.084	.700	.545	.491	.414	.334
7.498	.746	.360	.285	.288	.237	.167	.110	.084	.700	.545	.493	.414	.335
8.596	.746	.360	.286	.288	.237	.167	.111	.084	.700	.546	.494	.414	.335
9.989	.746	.358	.286	.288	.237	.167	.111	.084	.701	.547	.495	.415	.336

Configuration LT5

NPR	Upper flap								Lower flap				
	$p/p_{t,j}$ for $x/h_{t,n}$ of -								$p/p_{t,j}$ for $x/h_{t,n}$ of -				
	3.675	4.140	4.500	5.000	5.800	6.600	7.500	8.400	3.925	4.170	4.430	4.690	4.950
1.993	.709	.353	.221	.397	.535	.611	.539	.503	.706	.544	.496	.417	.347
2.543	.710	.353	.220	.221	.405	.548	.458	.367	.704	.546	.493	.416	.335
3.001	.710	.354	.220	.221	.364	.468	.472	.294	.703	.546	.492	.415	.335
3.401	.710	.354	.220	.221	.328	.425	.391	.306	.703	.546	.491	.415	.335
4.010	.710	.355	.219	.220	.194	.304	.493	.272	.702	.545	.491	.415	.334
4.989	.710	.354	.219	.220	.194	.255	.292	.388	.702	.544	.491	.415	.334
5.978	.710	.355	.219	.220	.194	.255	.152	.230	.701	.544	.491	.415	.334
7.483	.710	.355	.218	.220	.193	.256	.152	.090	.701	.545	.493	.416	.334
8.598	.710	.355	.218	.220	.193	.256	.152	.090	.701	.545	.494	.416	.335
10.018	.710	.355	.218	.220	.193	.257	.153	.090	.702	.546	.495	.416	.335

TABLE V.- *Continued*

(s) Configurations MT6 and NT2

Configuration MT6

NPR	Upper flap, $p/p_{t,j}$ for $x/h_{t,n}$ of -								Lower flap, $p/p_{t,j}$ for $x/h_{t,n}$ of -				
	3.675	4.140	4.300	4.500	4.800	5.100	5.500	6.000	3.925	4.170	4.430	4.690	4.950
1.998	.763	.360	.253	.246	.413	.444	.559	.565	.706	.545	.498	.417	.345
2.490	.763	.360	.254	.246	.252	.295	.504	.538	.704	.548	.495	.416	.334
3.014	.764	.361	.254	.246	.252	.276	.360	.497	.704	.548	.493	.415	.334
3.388	.764	.361	.253	.246	.251	.275	.360	.328	.703	.548	.492	.415	.333
4.005	.764	.361	.254	.245	.250	.275	.360	.328	.703	.547	.492	.415	.333
4.995	.765	.361	.253	.245	.250	.274	.360	.328	.703	.546	.492	.415	.333
6.004	.765	.361	.254	.245	.249	.274	.360	.328	.703	.546	.493	.415	.333
7.505	.765	.361	.254	.245	.249	.274	.360	.329	.702	.547	.494	.415	.333
8.572	.765	.361	.254	.245	.249	.274	.360	.330	.702	.548	.495	.416	.333
10.012	.765	.361	.253	.245	.248	.273	.361	.331	.704	.549	.496	.416	.334

Configuration NT2

NPR	Upper flap, $p/p_{t,j}$ for $x/h_{t,n}$ of -								Lower flap, $p/p_{t,j}$ for $x/h_{t,n}$ of -				
	3.675	4.140	4.500	5.500	6.800	8.100	9.400	10.900	3.925	4.170	4.430	4.690	4.950
1.992	.763	.355	.254	.474	.524	.570	.526	.494	.706	.546	.496	.415	.358
2.526	.764	.357	.254	.232	.421	.497	.429	.387	.704	.548	.493	.414	.333
3.008	.764	.359	.254	.231	.416	.428	.369	.301	.703	.547	.492	.413	.333
3.413	.764	.359	.254	.231	.299	.481	.274	.273	.703	.546	.491	.413	.333
4.012	.764	.359	.254	.231	.146	.378	.366	.184	.703	.546	.490	.413	.332
5.011	.764	.359	.253	.230	.139	.226	.338	.211	.702	.545	.490	.414	.332
6.099	.765	.359	.253	.230	.138	.102	.244	.266	.702	.545	.491	.412	.332
7.493	.765	.359	.252	.230	.138	.091	.145	.226	.701	.545	.492	.413	.333
8.652	.765	.359	.252	.230	.138	.091	.064	.181	.701	.545	.493	.413	.333
10.041	.764	.359	.252	.230	.138	.091	.064	.082	.703	.546	.494	.413	.333

TABLE V.- Continued

(t) Configurations OU7 and OV4

Configuration OU7

NPR	Upper flap								Lower flap				
	$p/p_{t,j}$ for $x/h_{t,n}$ of -								$p/p_{t,j}$ for $x/h_{t,n}$ of -				
	3.675	4.140	4.500	5.000	5.800	6.600	7.500	8.400	3.925	4.170	4.270	4.370	4.470
1.988	.762	.365	.252	.416	.586	.602	.551	.503	.713	.516	.516	.505	.464
2.530	.762	.367	.251	.250	.402	.544	.476	.377	.711	.517	.515	.505	.462
3.040	.763	.368	.251	.249	.324	.385	.463	.363	.711	.519	.513	.504	.461
3.458	.763	.368	.251	.249	.182	.316	.394	.325	.711	.519	.512	.504	.461
3.391	.762	.368	.251	.249	.183	.323	.402	.379	.711	.519	.512	.504	.461
4.001	.763	.368	.250	.249	.181	.278	.320	.316	.711	.518	.511	.504	.461
5.008	.763	.368	.250	.248	.181	.131	.240	.276	.711	.517	.511	.505	.461
5.968	.763	.368	.249	.248	.181	.131	.104	.148	.711	.516	.511	.505	.461
7.481	.763	.368	.249	.247	.181	.131	.104	.068	.711	.516	.512	.506	.462
8.635	.764	.368	.249	.247	.181	.131	.104	.068	.712	.517	.513	.506	.462
10.042	.763	.367	.248	.247	.181	.131	.104	.068	.713	.518	.514	.507	.462

Configuration OV4

NPR	Upper flap								Lower flap				
	$p/p_{t,j}$ for $x/h_{t,n}$ of -								$p/p_{t,j}$ for $x/h_{t,n}$ of -				
	3.675	4.140	4.500	5.000	5.800	6.600	7.500	8.400	3.925	4.170	4.600	5.030	5.450
2.012	.762	.363	.250	.250	.497	.608	.555	.500	.716	.489	.454	.327	.483
2.502	.762	.364	.249	.252	.386	.495	.506	.383	.715	.487	.451	.327	.330
3.000	.762	.365	.249	.251	.214	.397	.453	.383	.715	.487	.449	.326	.230
3.424	.762	.365	.249	.250	.213	.362	.481	.309	.715	.488	.449	.326	.230
3.989	.763	.364	.248	.250	.212	.211	.448	.418	.714	.488	.448	.326	.230
5.018	.763	.364	.248	.249	.212	.210	.204	.297	.714	.487	.448	.326	.229
6.060	.763	.363	.247	.249	.211	.210	.205	.201	.714	.485	.448	.326	.229
7.500	.763	.363	.247	.249	.211	.210	.205	.117	.714	.484	.448	.326	.229
8.603	.763	.363	.246	.249	.211	.210	.206	.117	.715	.484	.449	.327	.229
10.008	.763	.362	.246	.249	.210	.211	.207	.117	.717	.485	.450	.327	.230

TABLE V.- Continued

(u) Configurations OW5 and OX7

Configuration OW5

NPR	Upper flap								Lower flap				
	$p/p_{t,j}$ for $x/h_{t,n}$ of -								$p/p_{t,j}$ for $x/h_{t,n}$ of -				
	3.675	4.140	4.500	5.000	5.800	6.600	7.500	8.400	3.925	4.170	4.430	4.690	4.950
1.972	.762	.365	.249	.361	.475	.578	.565	.518	.712	.376	.312	.292	.460
2.540	.763	.366	.248	.214	.347	.372	.446	.432	.709	.375	.309	.290	.254
3.008	.763	.367	.248	.214	.298	.308	.381	.385	.708	.374	.307	.291	.254
3.385	.763	.367	.247	.214	.263	.278	.325	.357	.708	.373	.306	.291	.253
4.031	.764	.367	.247	.214	.182	.235	.268	.306	.707	.373	.306	.290	.253
4.996	.764	.367	.246	.214	.120	.114	.257	.334	.707	.372	.305	.289	.252
5.993	.764	.367	.246	.214	.120	.113	.141	.099	.706	.372	.304	.289	.252
7.491	.764	.367	.246	.214	.120	.112	.140	.099	.706	.372	.303	.289	.252
8.593	.764	.367	.246	.214	.120	.112	.140	.099	.706	.372	.303	.289	.252
10.023	.764	.366	.245	.214	.120	.111	.140	.099	.707	.372	.303	.289	.252

Configuration OX7

NPR	Upper flap								Lower flap				
	$p/p_{t,j}$ for $x/h_{t,n}$ of -								$p/p_{t,j}$ for $x/h_{t,n}$ of -				
	3.675	4.140	4.500	5.000	5.800	6.600	7.500	8.400	3.925	4.348	4.600	4.850	5.100
1.982	.780	.419	.334	.408	.543	.601	.550	.506	.753	.648	.556	.457	.372
2.566	.782	.420	.333	.408	.434	.563	.455	.376	.751	.648	.554	.456	.372
2.489	.781	.420	.333	.407	.473	.554	.473	.376	.751	.648	.554	.457	.372
3.044	.781	.420	.333	.407	.312	.356	.500	.284	.750	.648	.553	.456	.371
3.414	.781	.420	.332	.407	.312	.306	.516	.337	.750	.648	.552	.456	.371
4.036	.781	.420	.331	.407	.312	.211	.270	.453	.751	.649	.552	.456	.371
5.002	.781	.420	.331	.407	.311	.205	.202	.180	.751	.649	.552	.457	.371
6.007	.782	.420	.330	.407	.310	.205	.136	.126	.750	.650	.552	.457	.371
7.501	.782	.420	.330	.407	.309	.206	.137	.080	.750	.651	.553	.458	.371
8.673	.782	.419	.330	.406	.311	.205	.137	.079	.750	.653	.555	.458	.372
9.978	.782	.419	.329	.406	.311	.211	.137	.079	.754	.654	.556	.457	.372

TABLE V.- Concluded

(v) Configuration OT5

NPR	Upper flap								Lower flap				
	$p/p_{t,j}$ for $x/h_{t,n}$ of -								$p/p_{t,j}$ for $x/h_{t,n}$ of -				
	3.675	4.140	4.500	5.000	5.800	6.600	7.500	8.400	3.925	4.170	4.430	4.690	4.950
1.966	.763	.366	.254	.265	.592	.608	.557	.511	.708	.545	.499	.419	.356
2.510	.763	.367	.252	.258	.405	.555	.474	.384	.705	.547	.496	.417	.337
3.007	.763	.367	.252	.258	.290	.432	.432	.364	.704	.548	.494	.417	.337
3.408	.763	.367	.251	.257	.214	.369	.478	.318	.704	.547	.494	.416	.336
4.008	.763	.367	.251	.256	.213	.201	.427	.405	.703	.546	.493	.416	.336
5.029	.763	.367	.250	.255	.212	.200	.148	.318	.703	.546	.493	.416	.335
6.060	.763	.367	.249	.255	.212	.200	.148	.090	.703	.546	.493	.416	.335
7.544	.763	.366	.248	.254	.211	.200	.148	.090	.702	.547	.494	.416	.335
7.489	.763	.366	.248	.254	.211	.200	.148	.090	.702	.546	.494	.416	.335
8.652	.763	.365	.248	.254	.211	.199	.148	.090	.702	.547	.495	.416	.335
10.085	.764	.365	.248	.254	.210	.199	.149	.089	.704	.548	.496	.417	.336

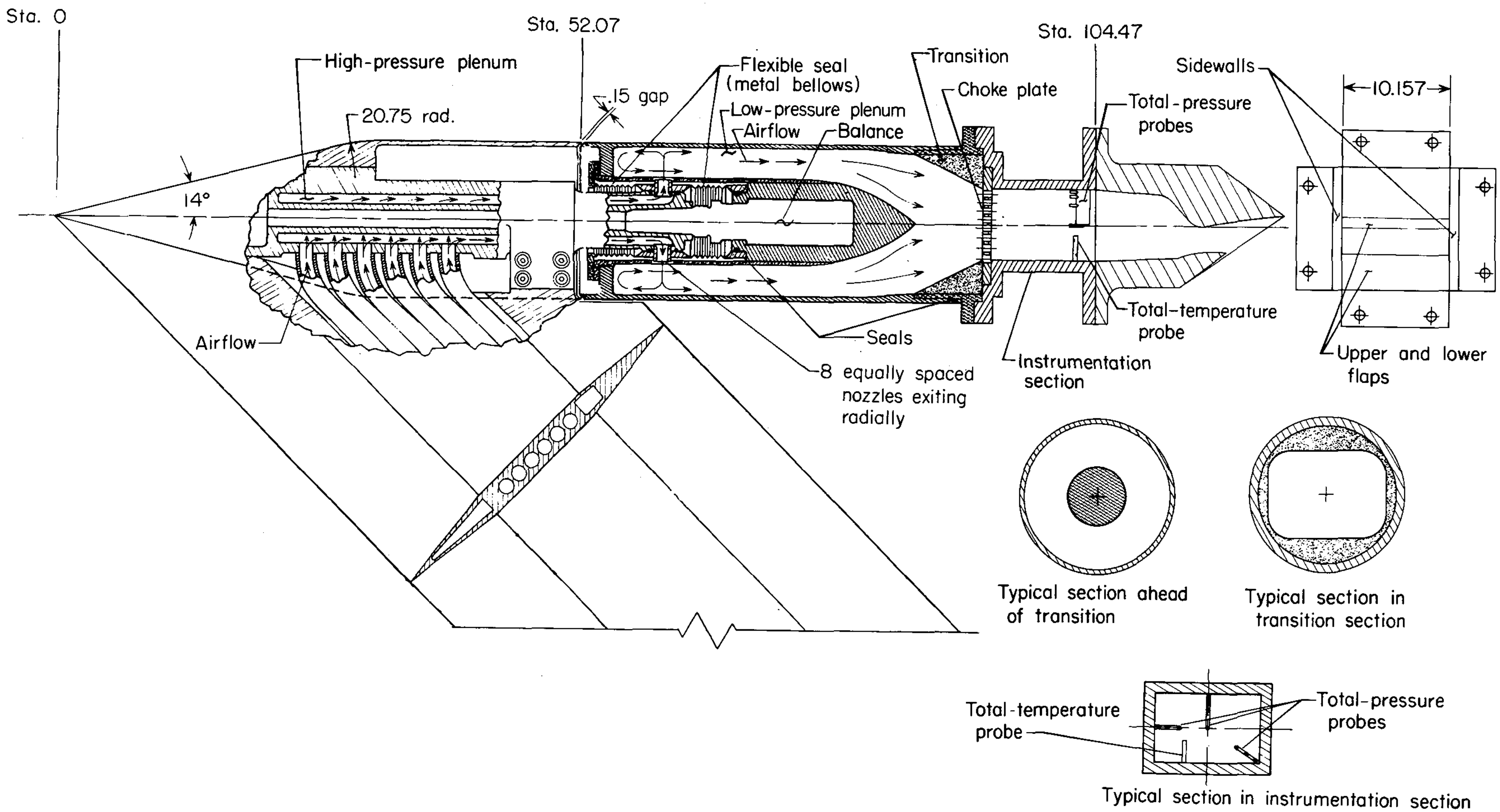

(a) Air-powered nacelle test apparatus.

Figure 1. Air-powered nacelle model with typical nozzle configuration installed. All dimensions are in centimeters unless otherwise noted.

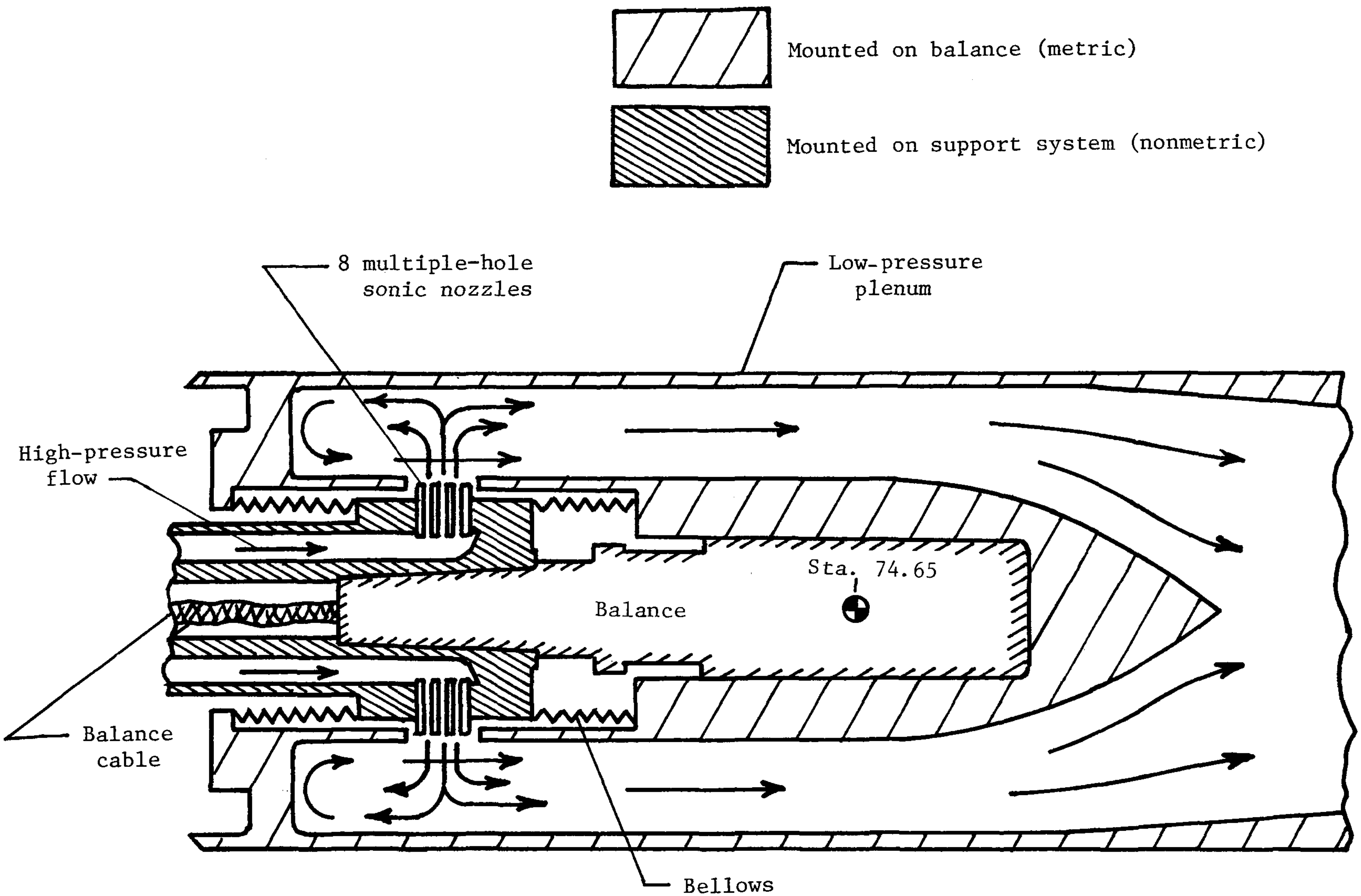

(b) Schematic cross section of flow transfer system.

Figure 1. Concluded.

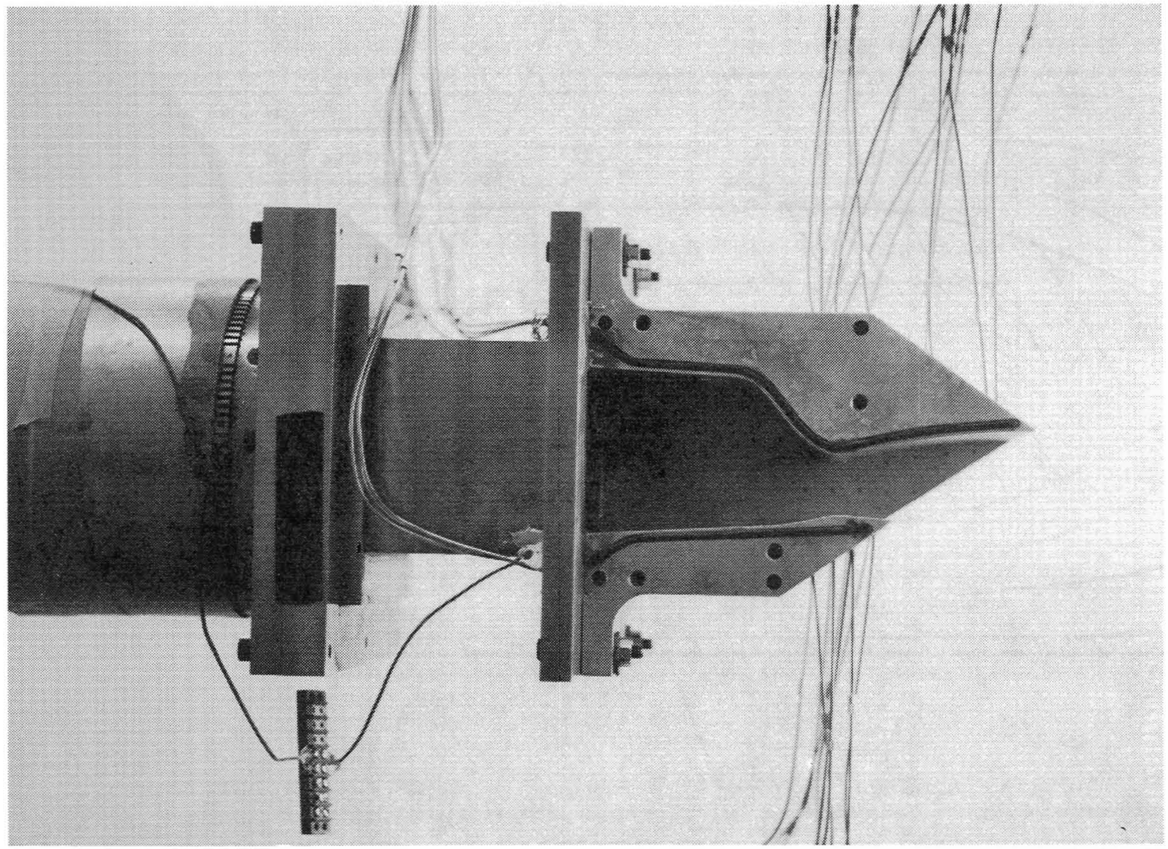

L-82-116

Figure 2. Single-expansion-ramp nozzle mounted on air-powered nacelle model. (Nozzle sidewall removed for clarity.)

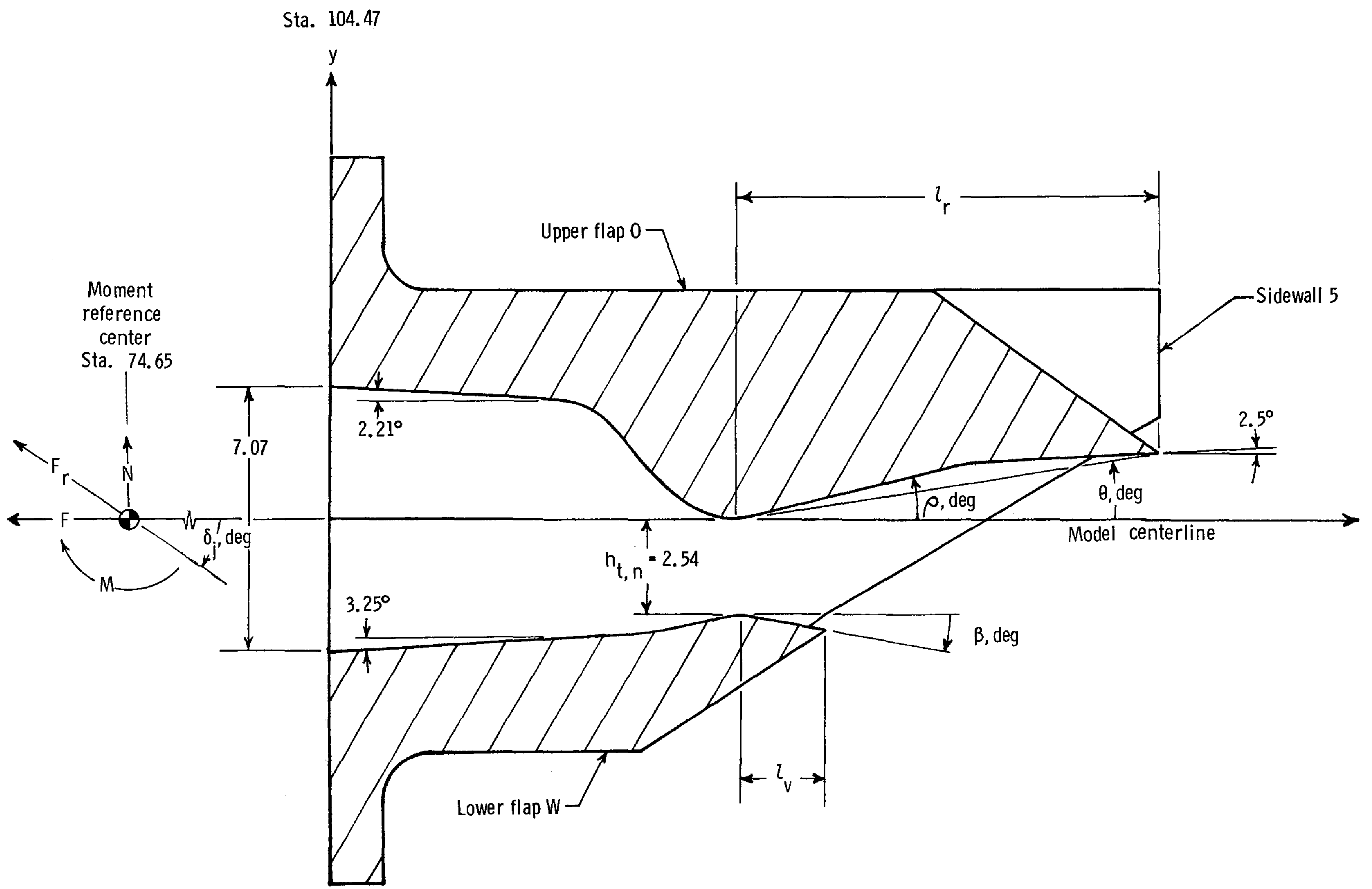

Figure 3. Typical nozzle configuration indicating coordinate axes and five geometric parameters varied for upper and lower flaps (configuration OW5 shown). All dimensions are in centimeters unless otherwise indicated.

Sidewall	$x_1/h_{t,n}$	$y_1/h_{t,n}$	$x_2/h_{t,n}$	$y_2/h_{t,n}$	$x_3/h_{t,n}$	$y_3/h_{t,n}$	$x_4/h_{t,n}$	$y_4/h_{t,n}$
1	6.670	2.374	6.670	0.424	4.850	-1.055	2.963	-2.375
2	10.260	↓	10.260	1.267	4.745	-1.064	3.217	↓
3	7.020	↓	7.020	.589	5.395	-1.138	4.230	↓
4	10.260	↓	10.260	1.267	5.395	-1.138	3.217	↓
5	8.640	↓	8.640	1.054	5.070	-1.000	3.217	↓
6	6.140	↓	6.140	.305	5.070	↓	3.942	↓
7	8.640	↓	8.640	.696	4.570	↓	3.217	↓

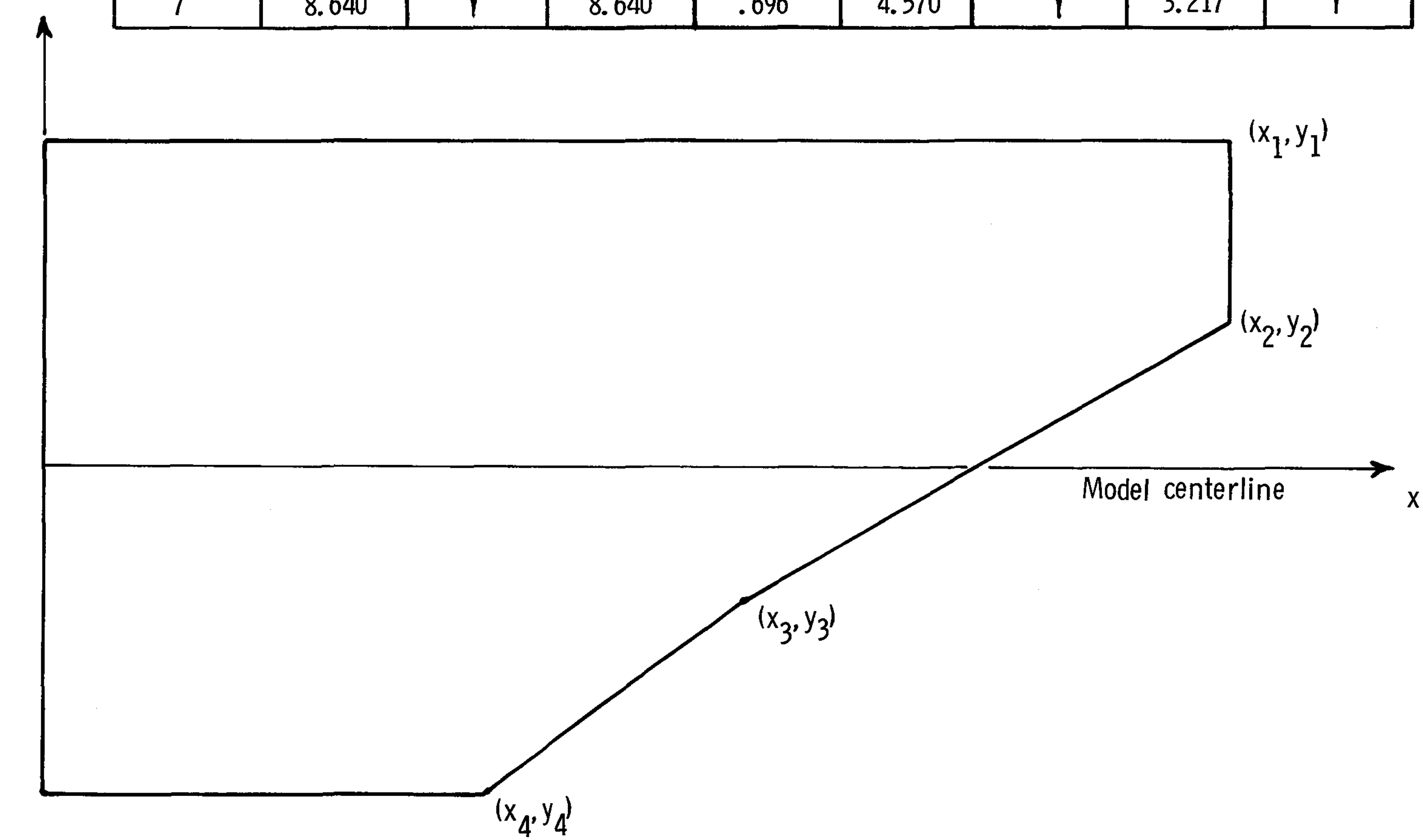

Figure 4. Planform of nozzle sidewall indicating coordinate axes and coordinates for downstream edge of sidewalls.

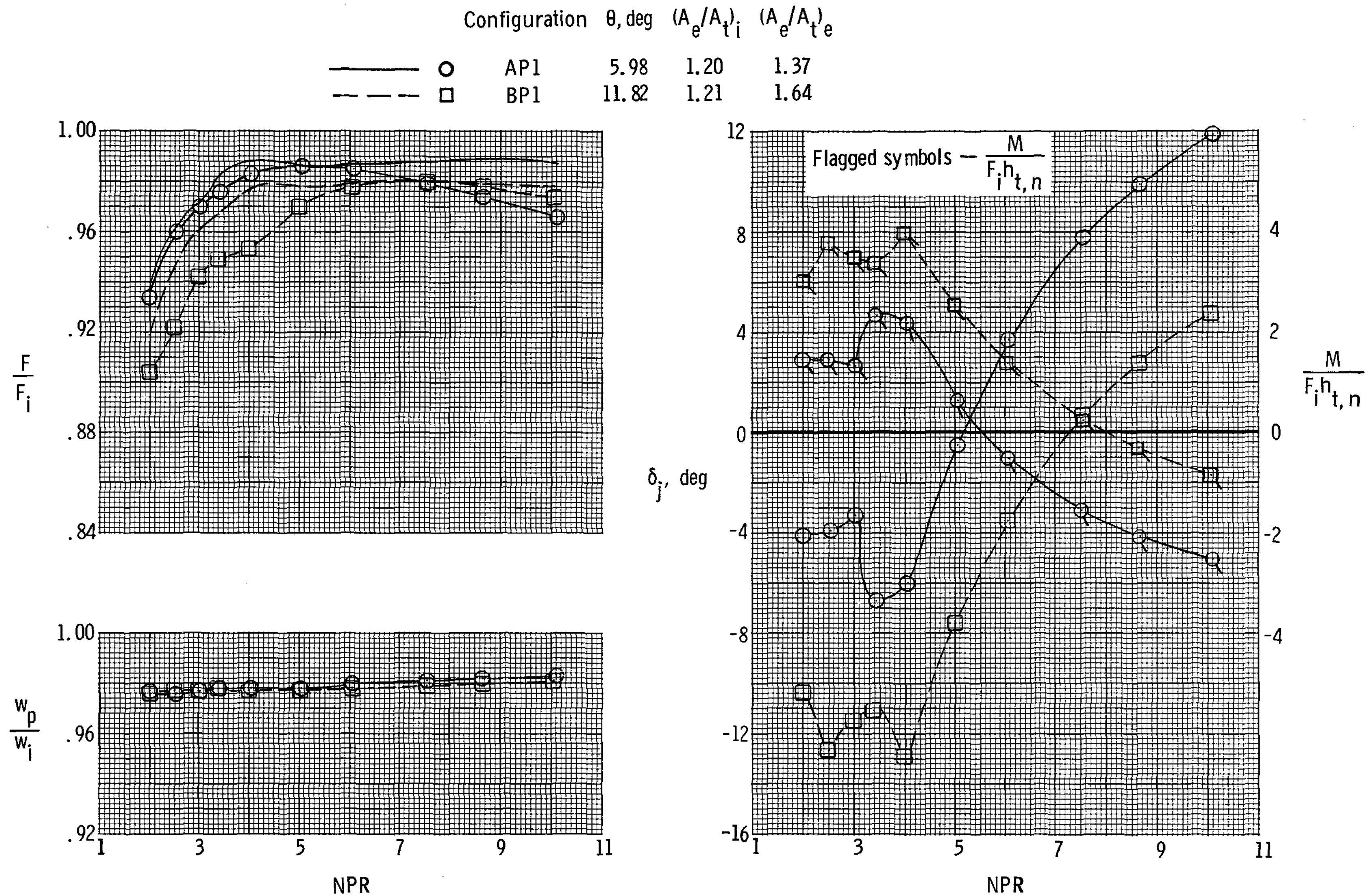

(a) Configurations AP1 and BP1.

Figure 5. Variation of nozzle thrust ratio, discharge coefficient, and thrust vector angle with nozzle pressure ratio for single-expansion-ramp nozzles. Lines without symbols indicate resultant thrust ratio F_r/F_i.

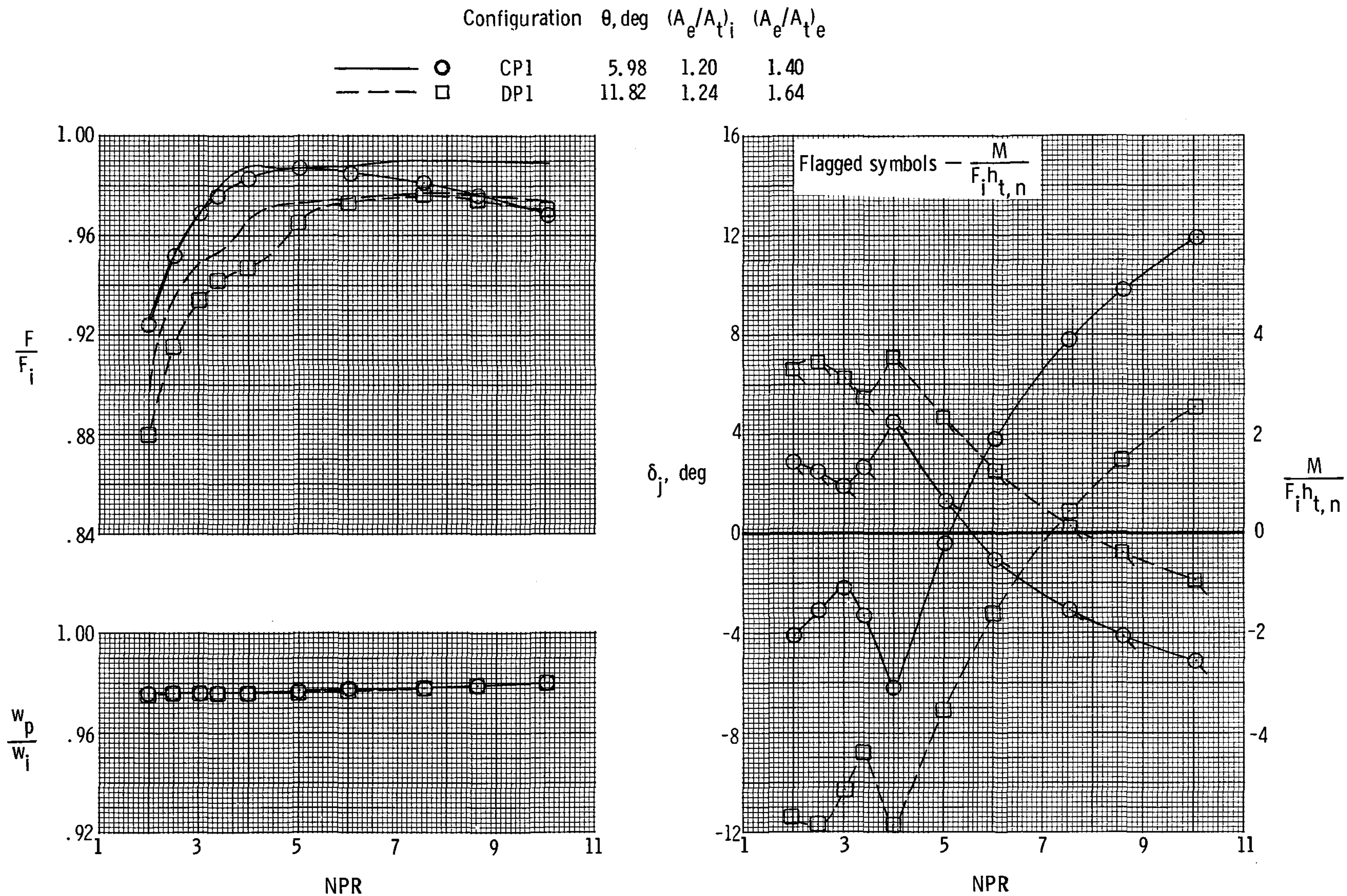

(b) Configurations CP1 and DP1.

Figure 5. Continued.

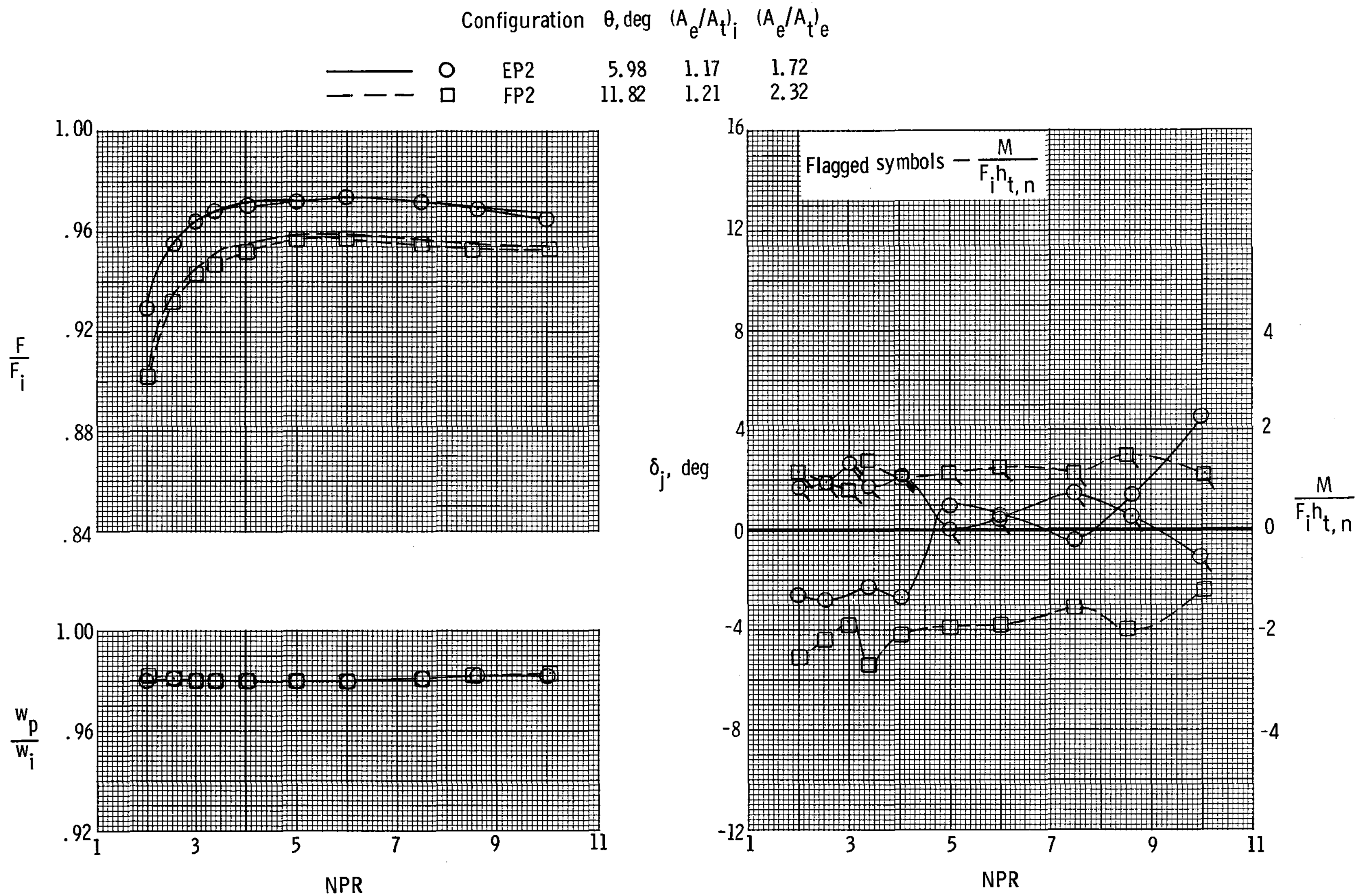

(c) Configurations EP2 and FP2.

Figure 5. Continued.

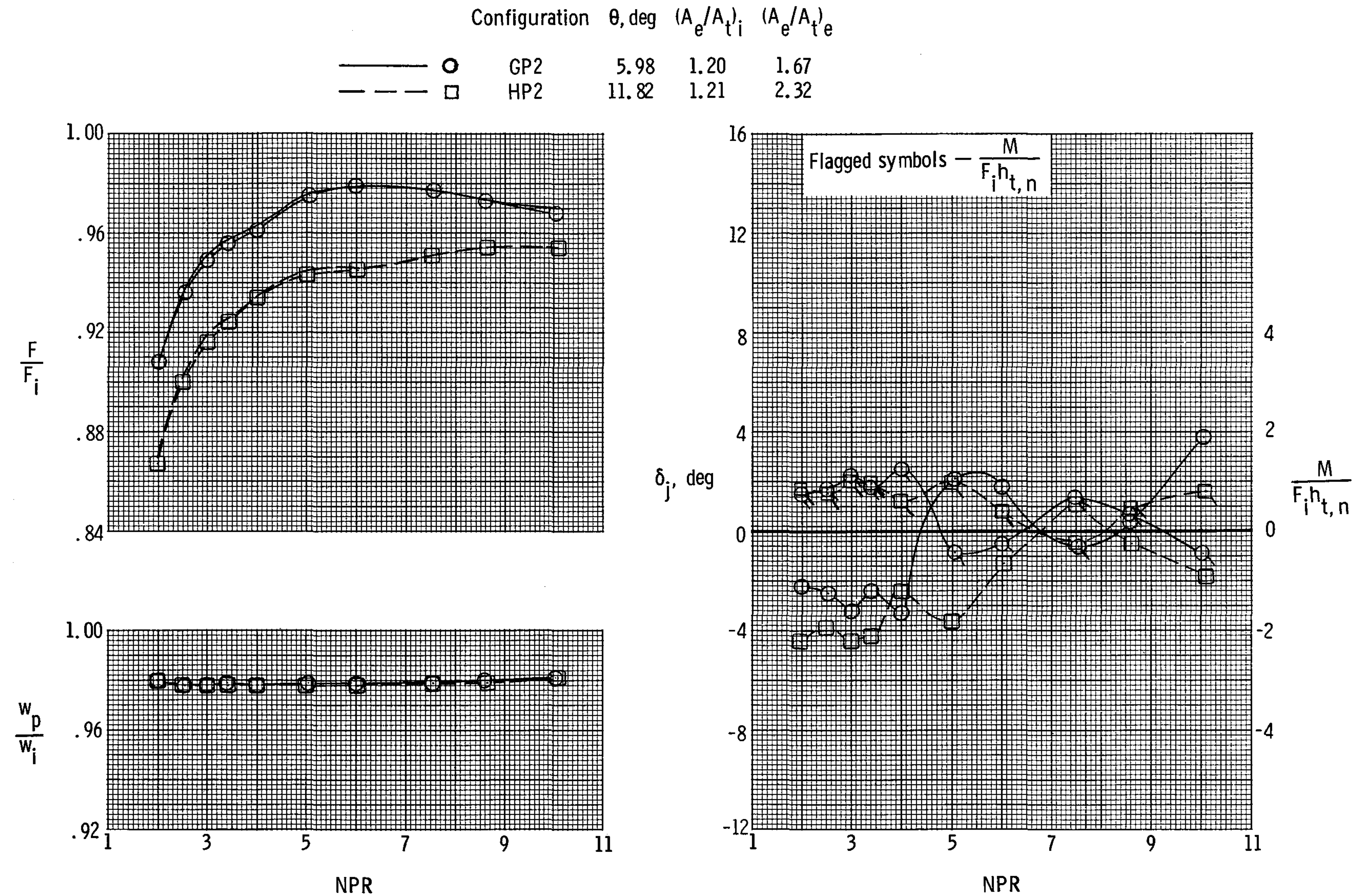

(d) Configurations GP2 and HP2.

Figure 5. Continued.

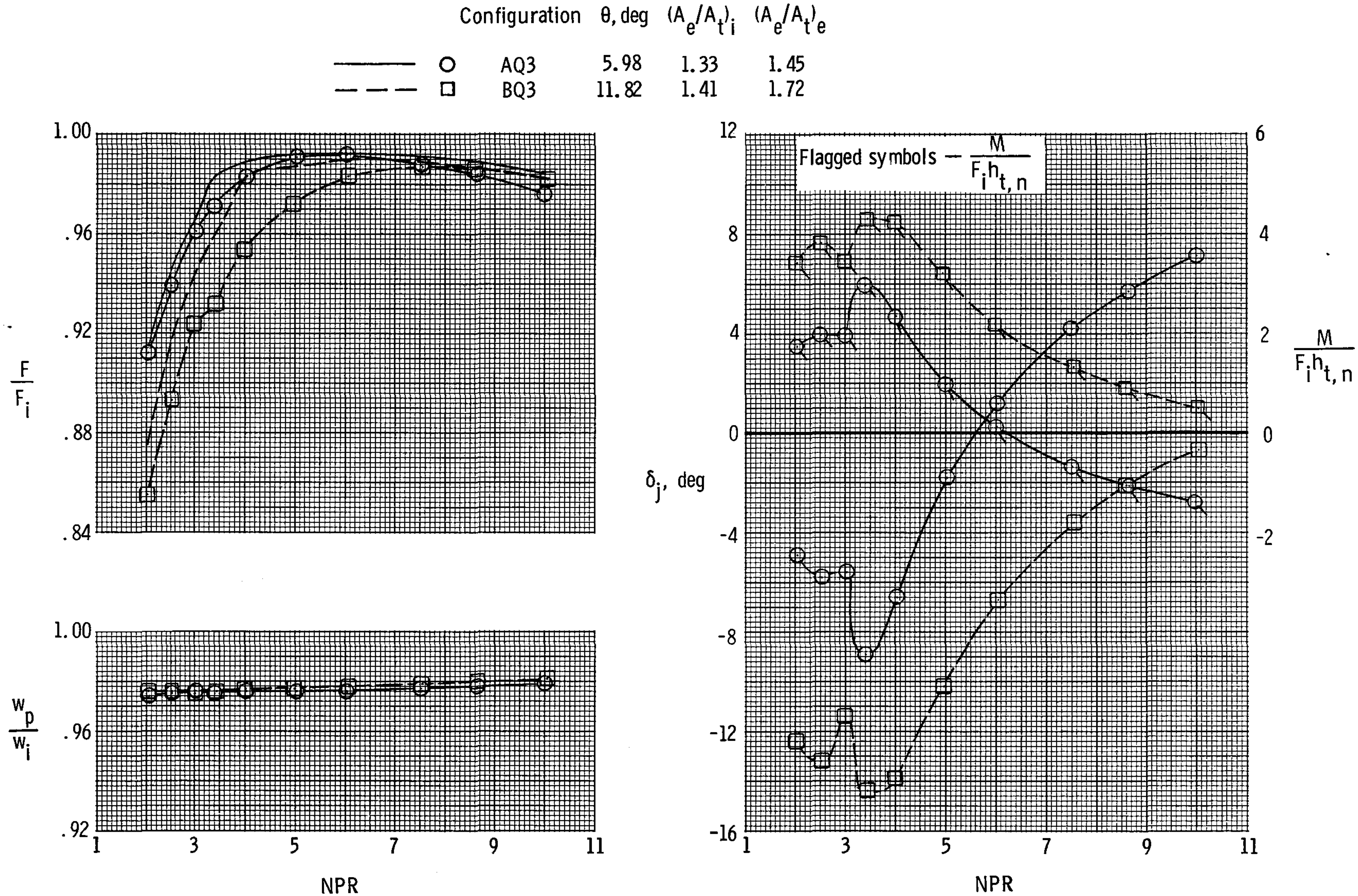

(e) Configurations AQ3 and BQ3.

Figure 5. Continued.

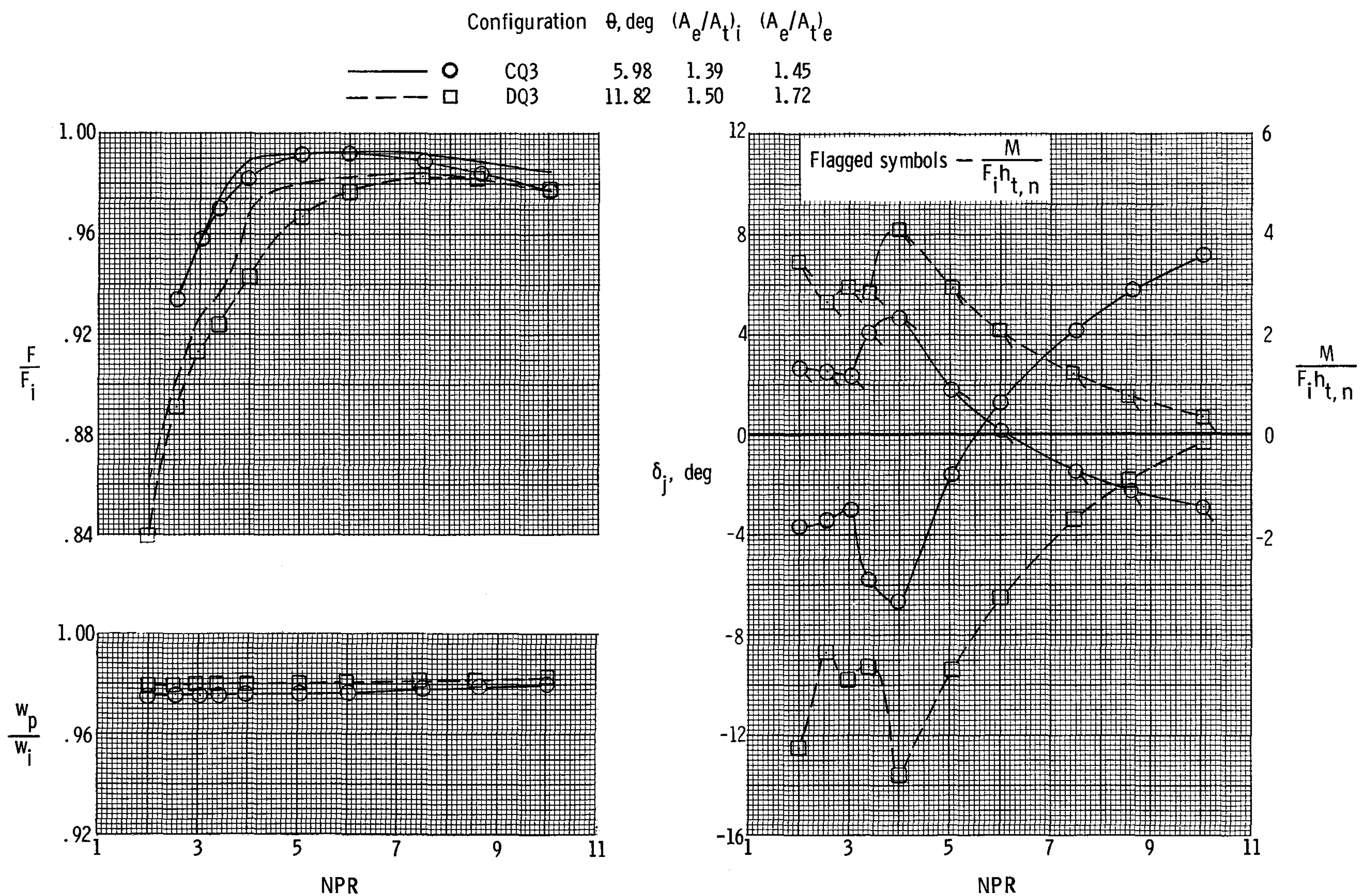

(f) Configurations CQ3 and DQ3.

Figure 5. Continued.

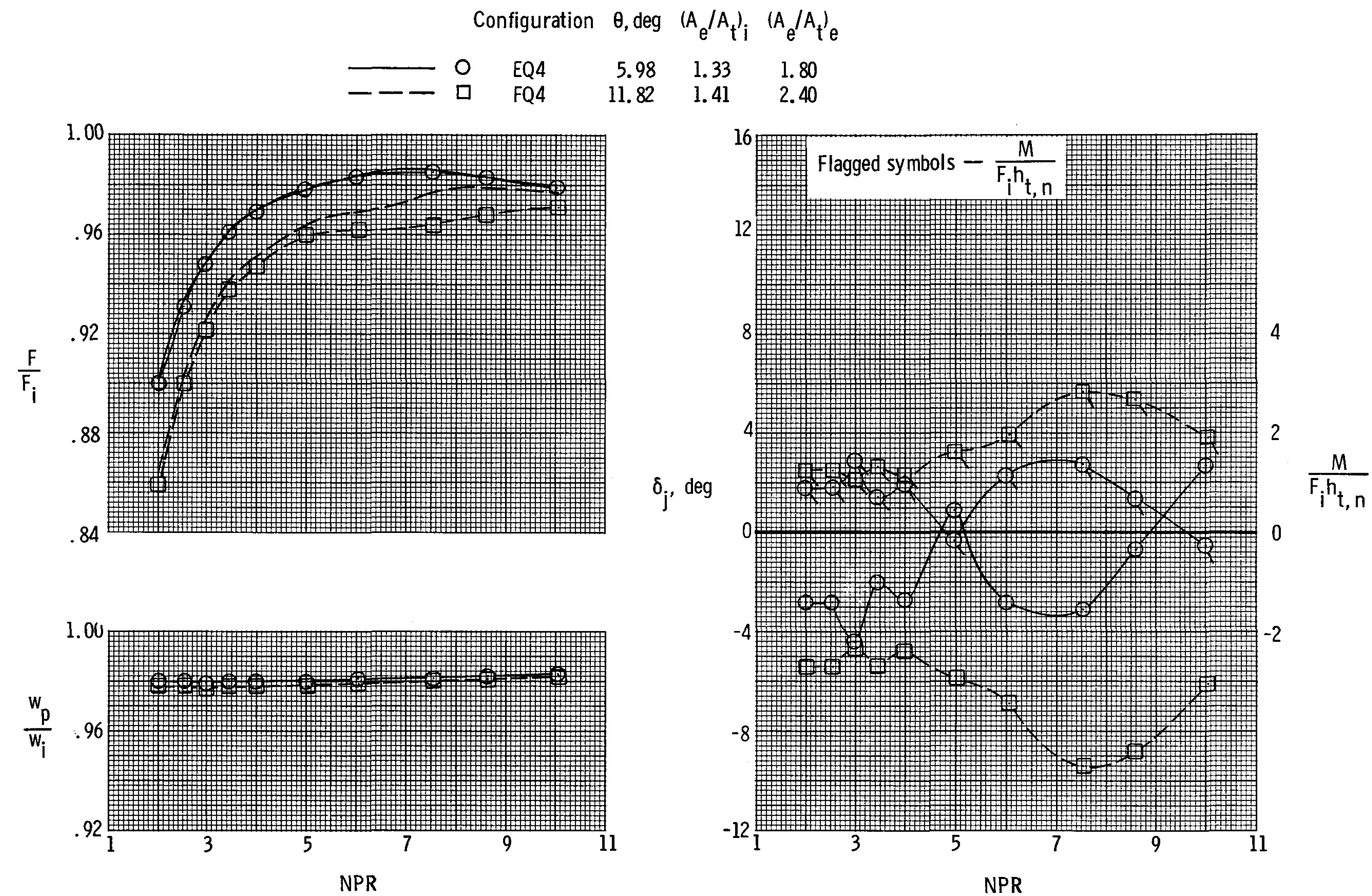

(g) Configurations EQ4 and FQ4.

Figure 5. Continued.

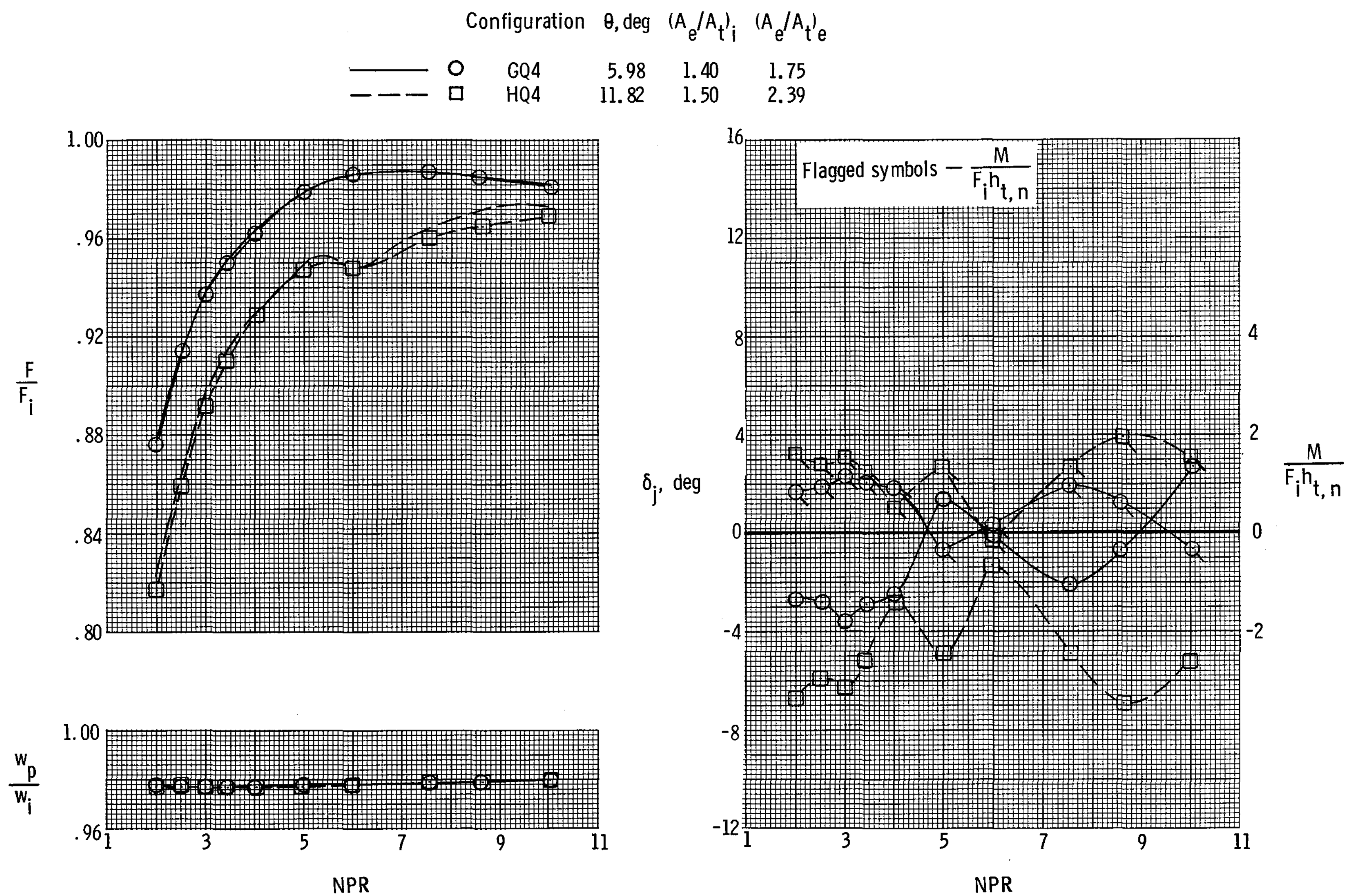

(h) Configurations GQ4 and HQ4.

Figure 5. Continued.

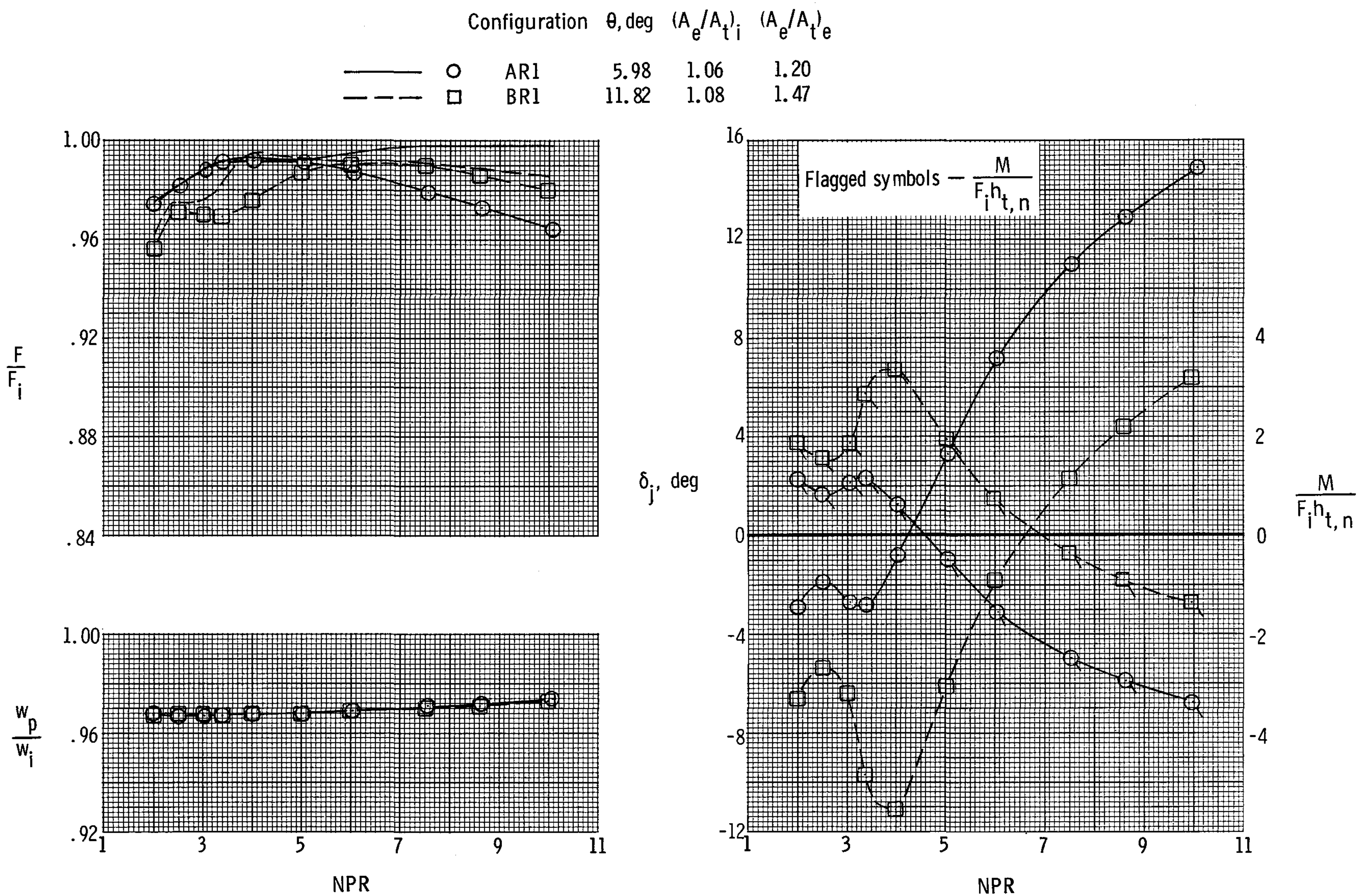

(i) Configurations AR1 and BR1.

Figure 5. Continued.

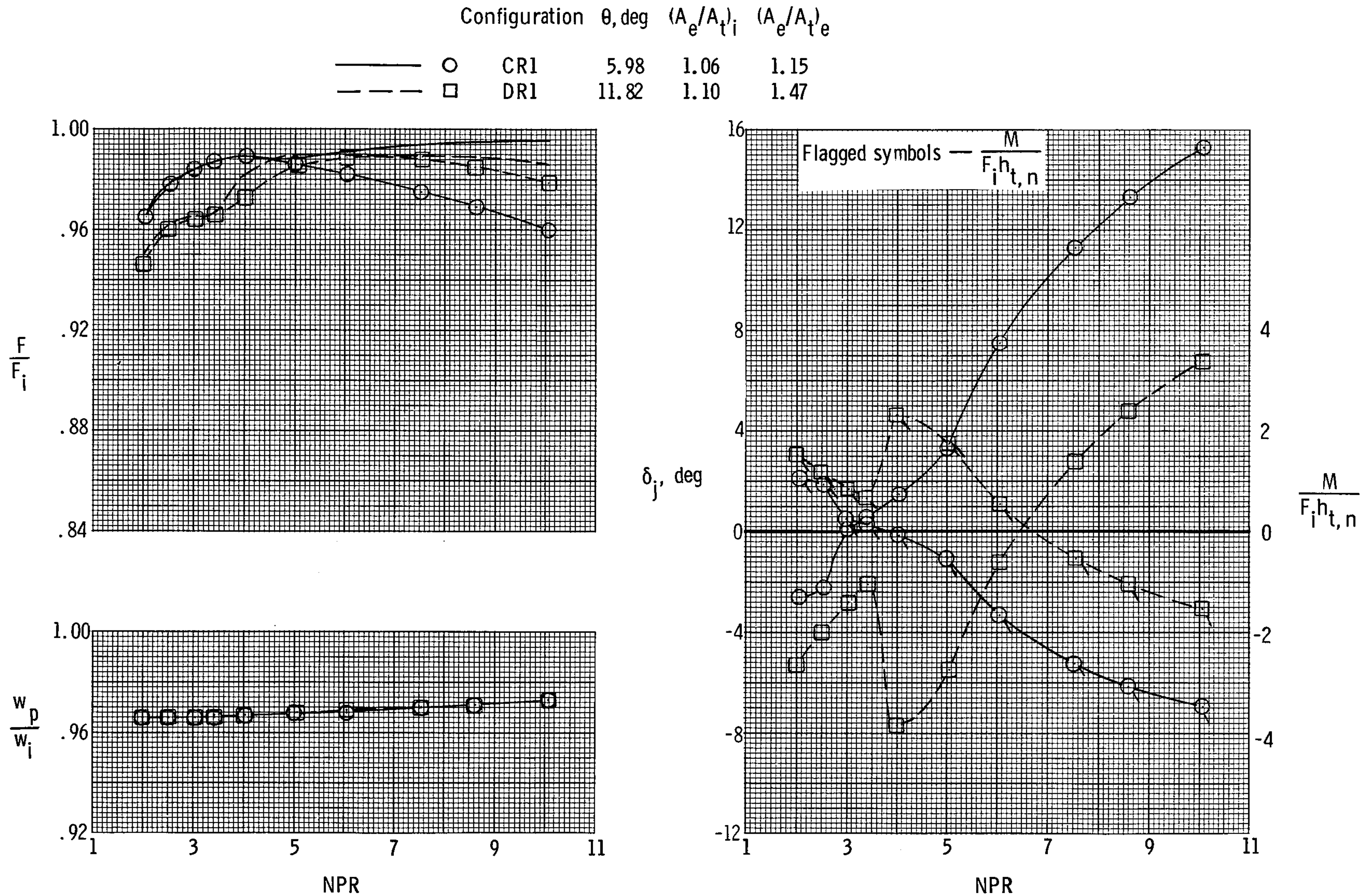

(j) Configurations CR1 and DR1.

Figure 5. Continued.

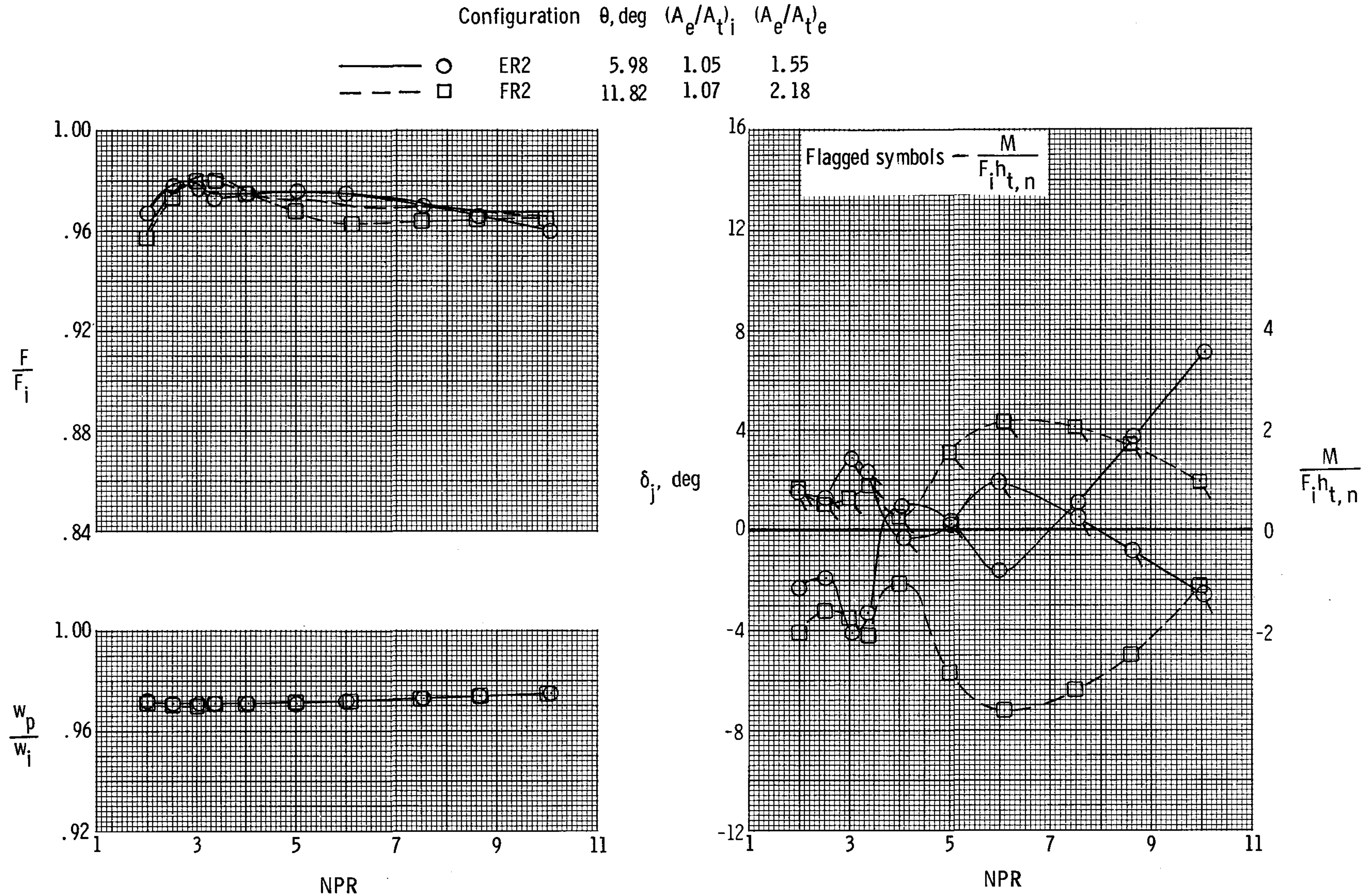

(k) Configurations ER2 and FR2.

Figure 5. Continued.

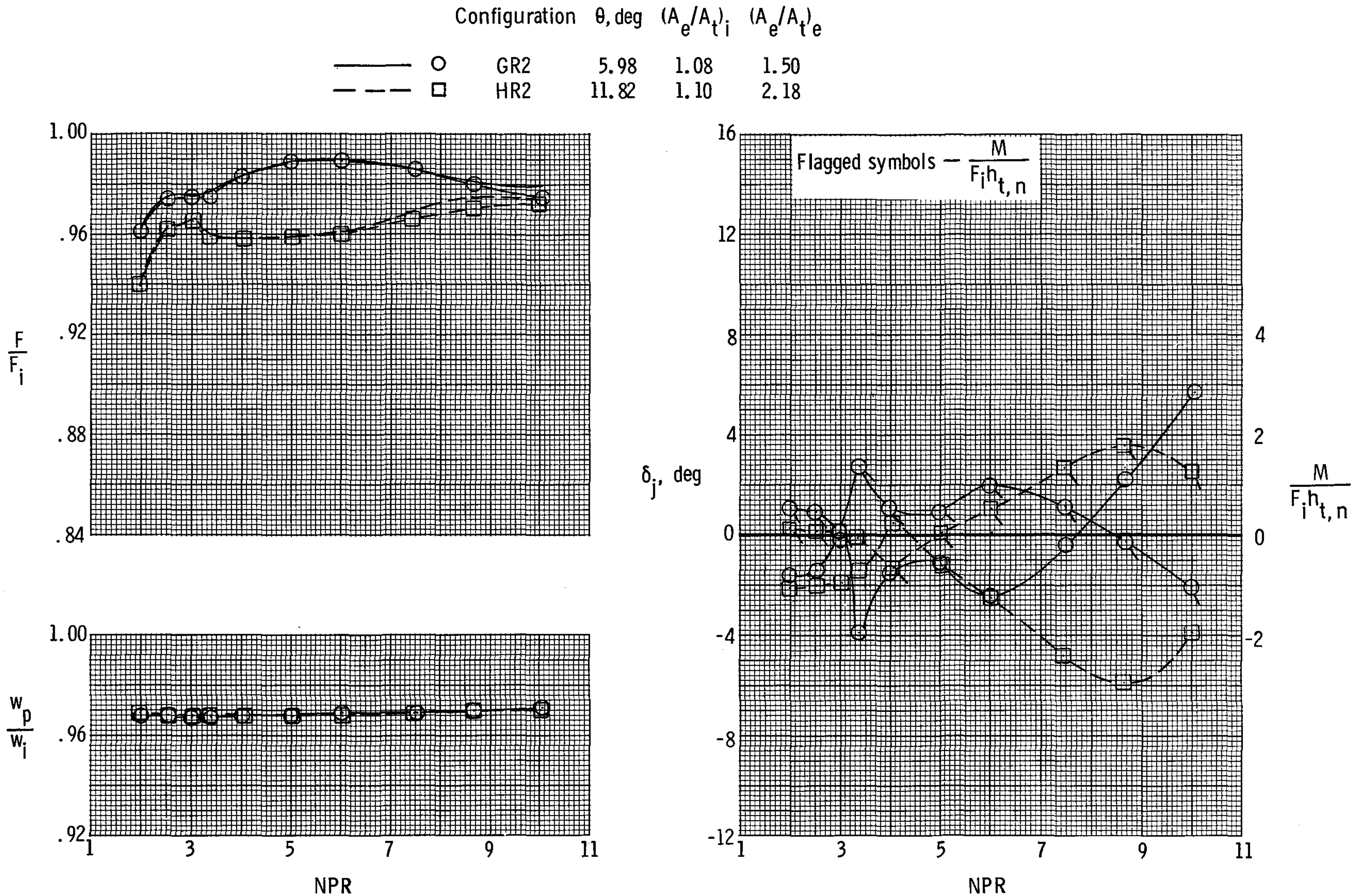

(l) Configurations GR2 and HR2.

Figure 5. Continued.

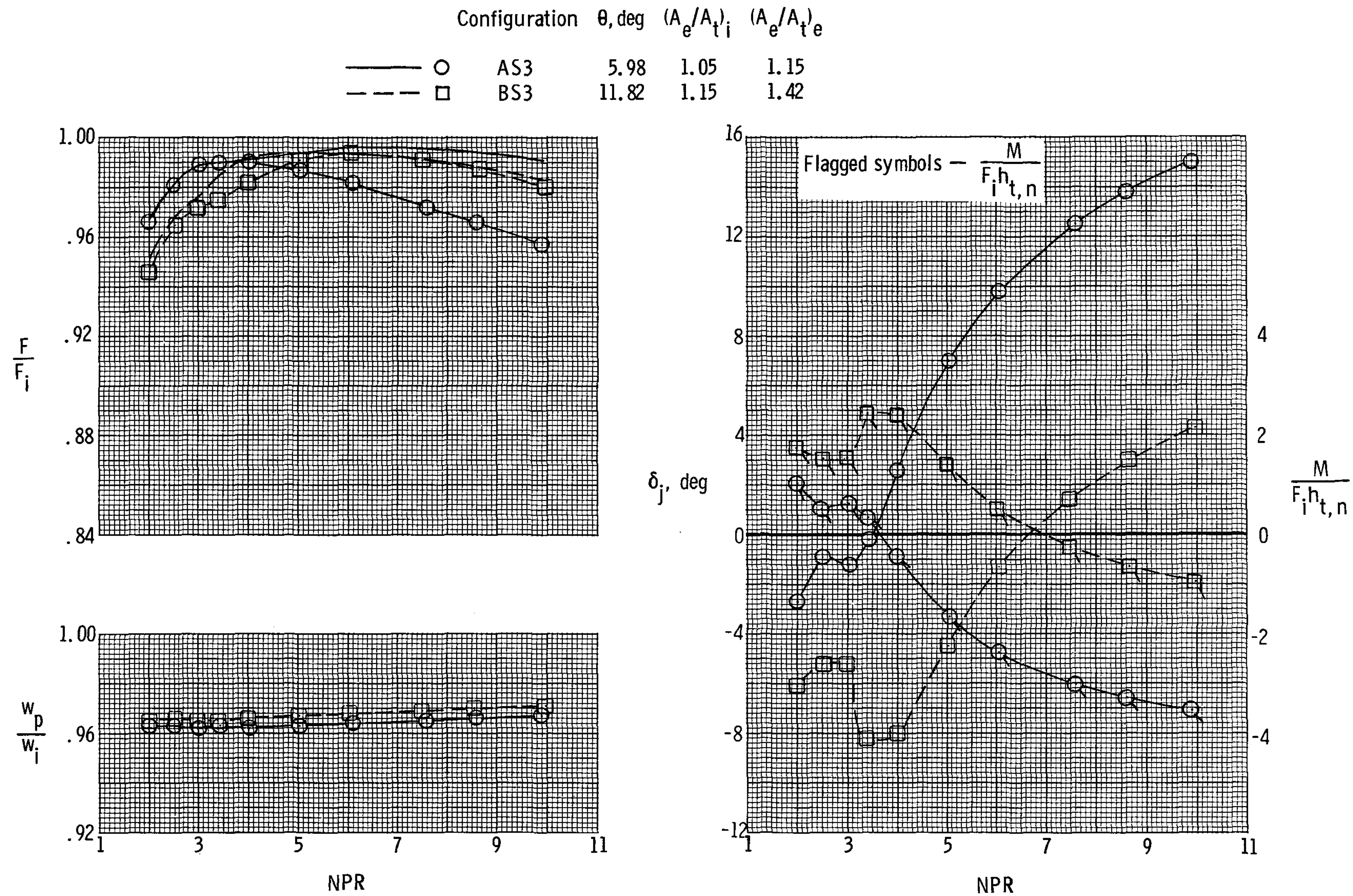

(m) Configurations AS3 and BS3.

Figure 5. Continued.

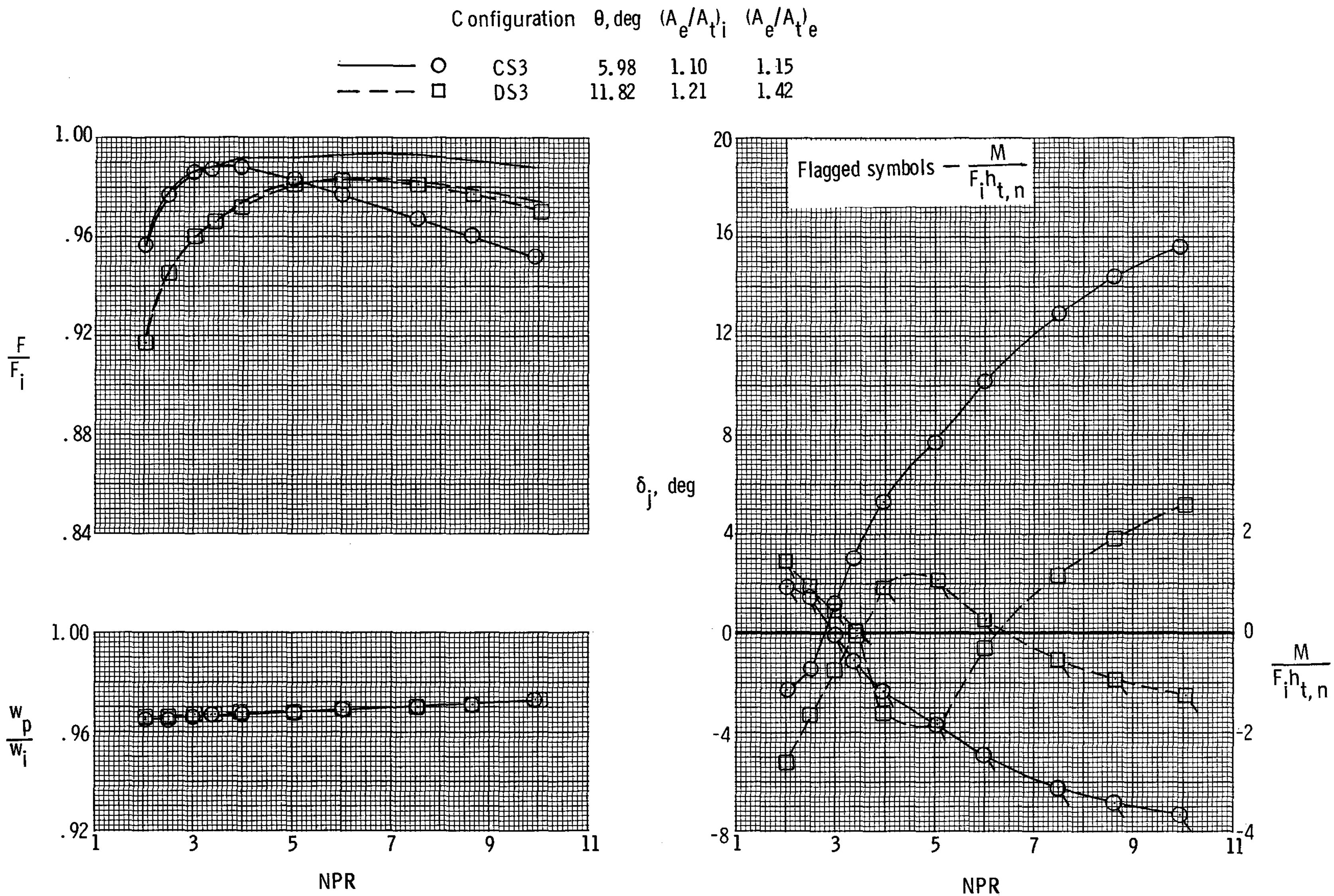

(n) Configurations CS3 and DS3.

Figure 5. Continued.

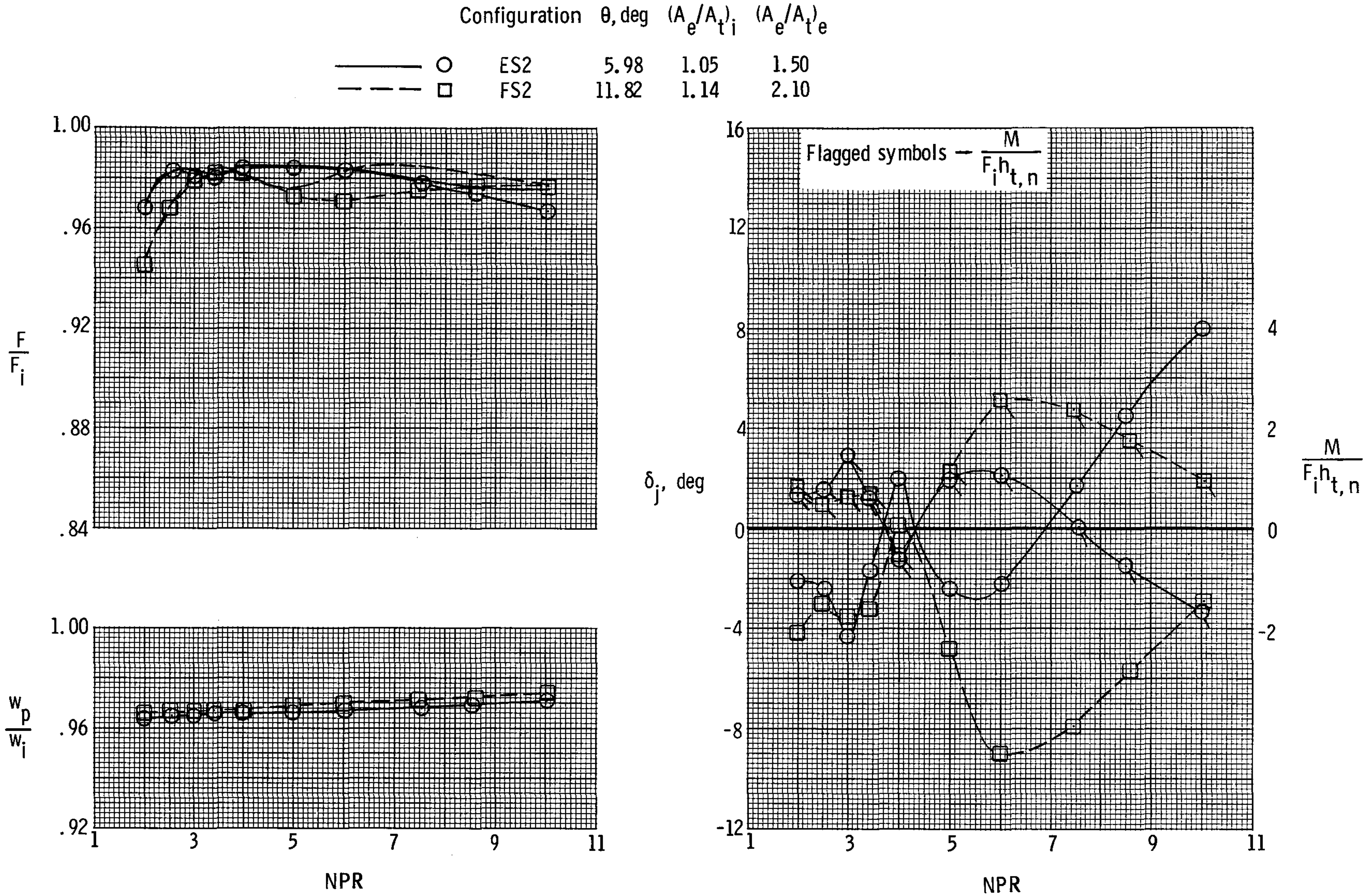

(o) Configurations ES2 and FS2.

Figure 5. Continued.

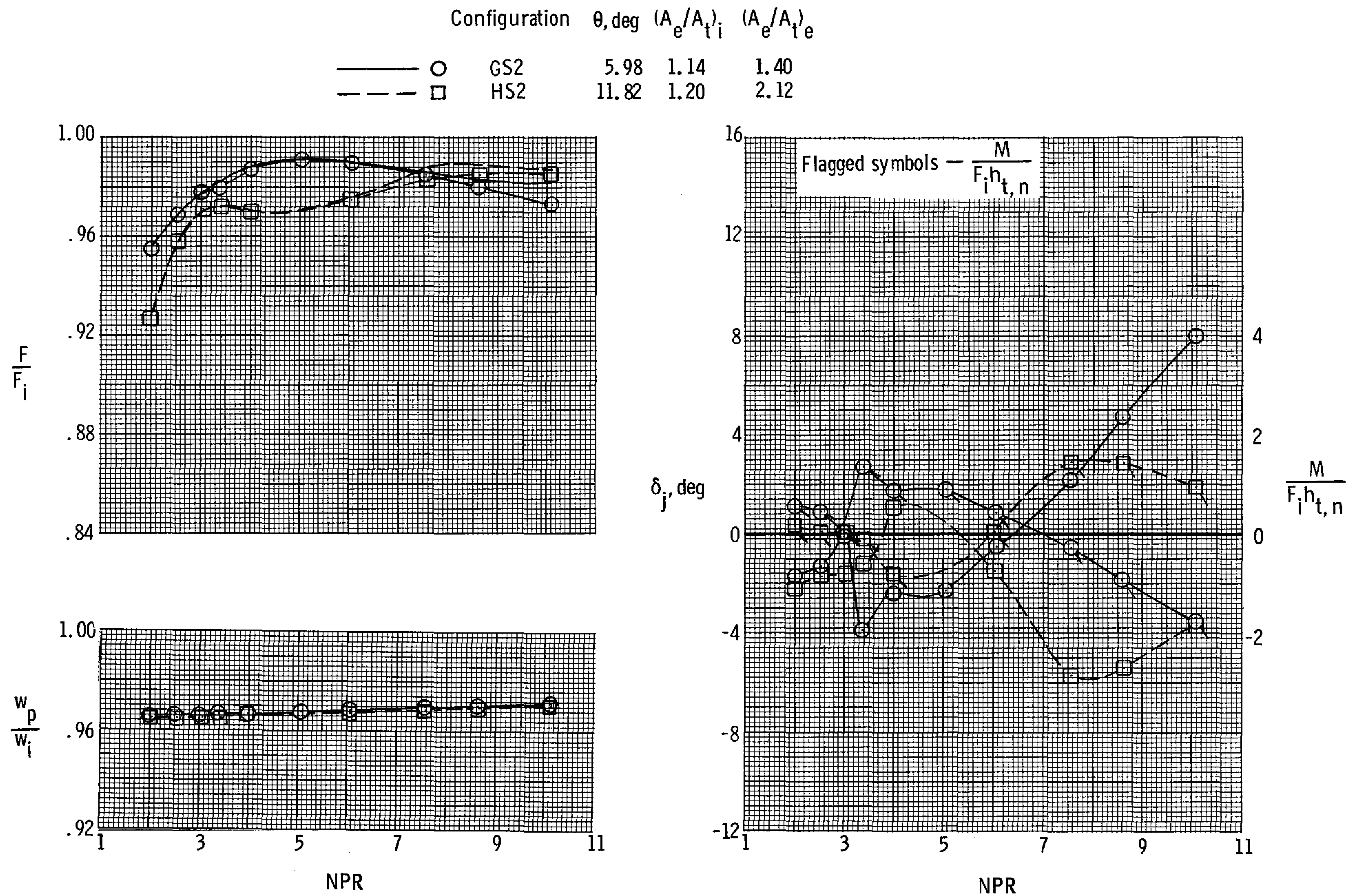

(p) Configurations GS2 and HS2.

Figure 5. Continued.

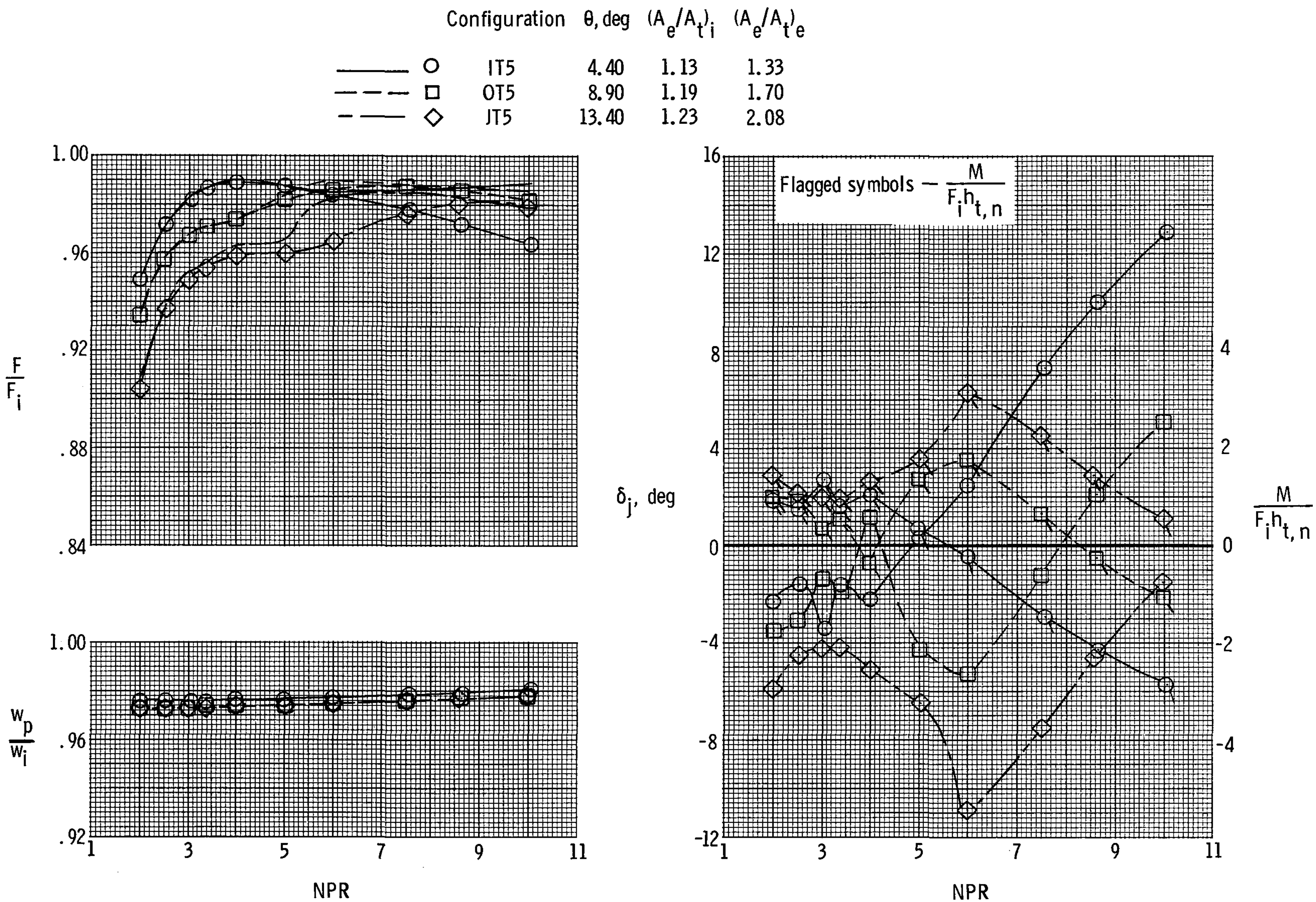

(q) Configurations IT5, OT5, and JT5.

Figure 5. Continued.

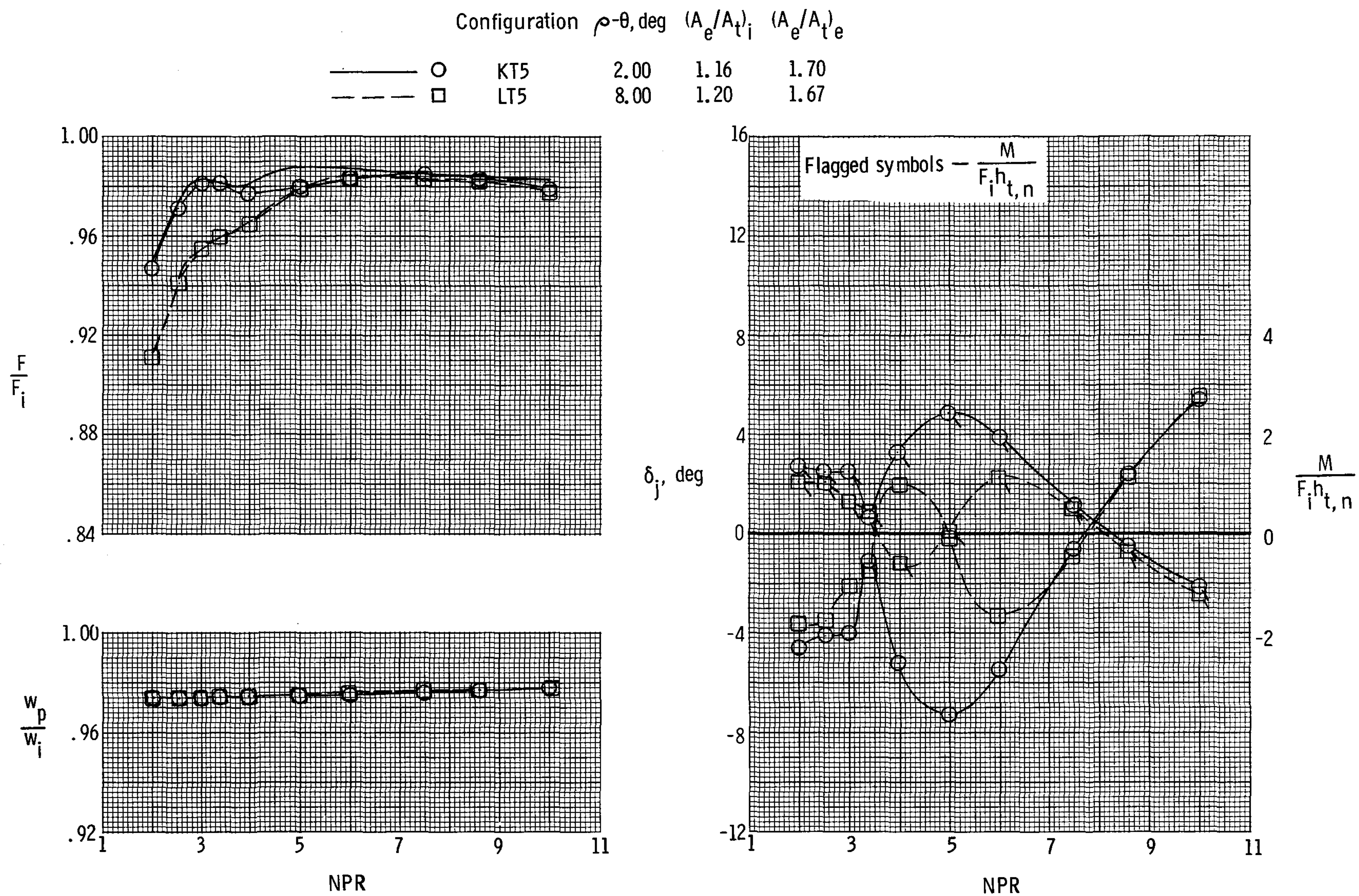

(r) Configurations KT5 and LT5.

Figure 5. Continued.

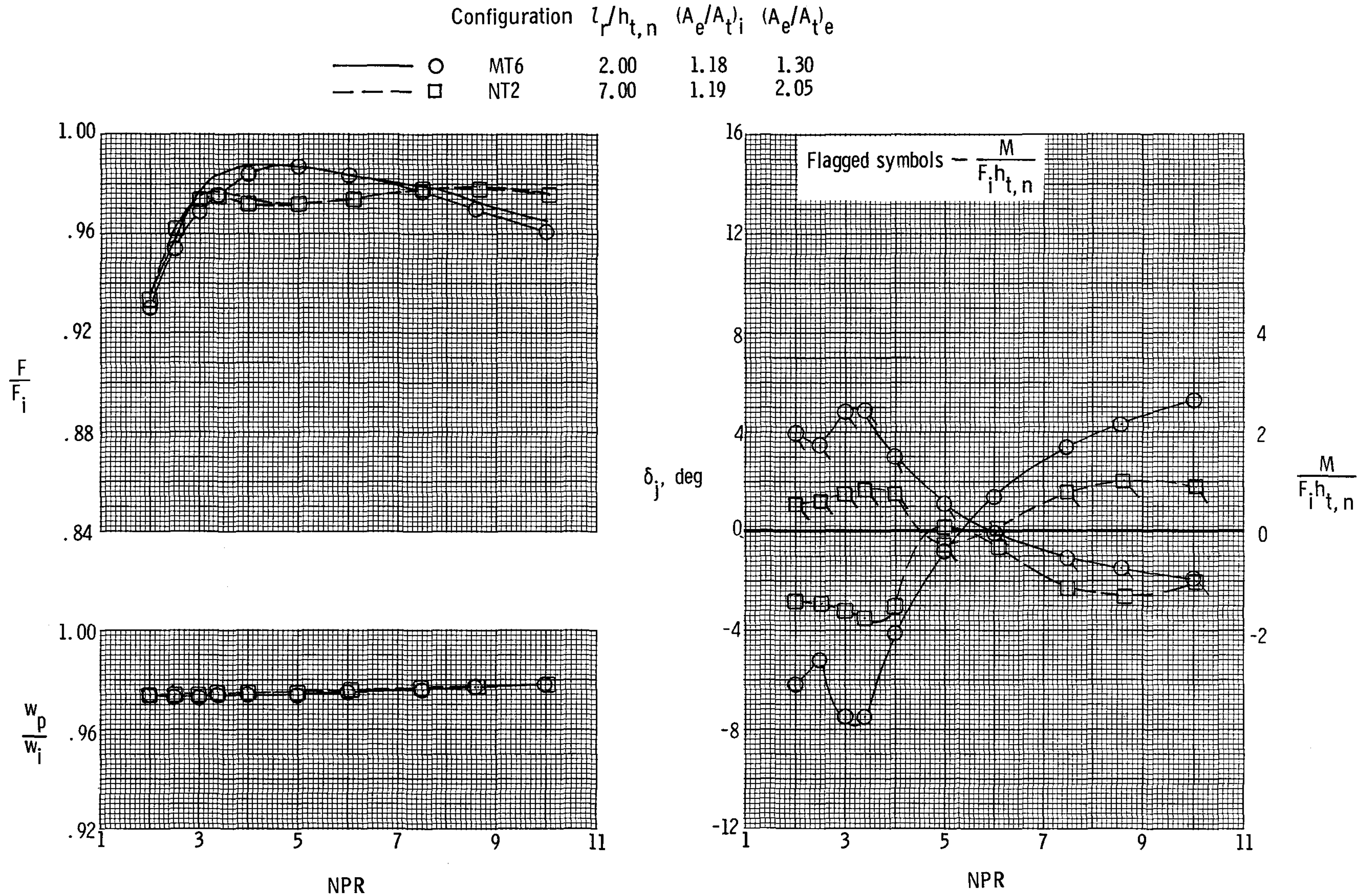

(s) Configurations MT6 and NT2.

Figure 5. Continued.

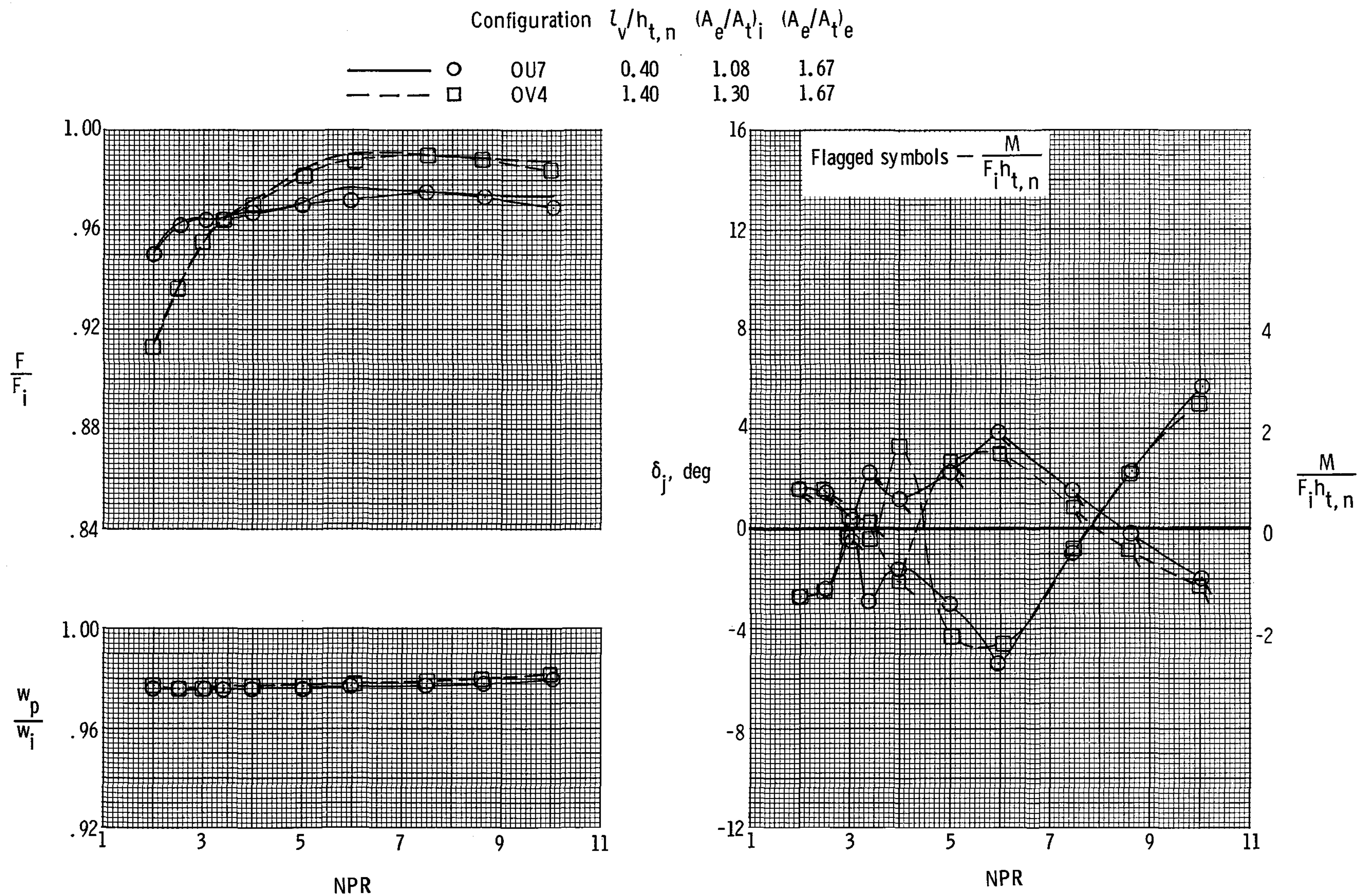

(t) Configurations OU7 and OV4.

Figure 5. Continued.

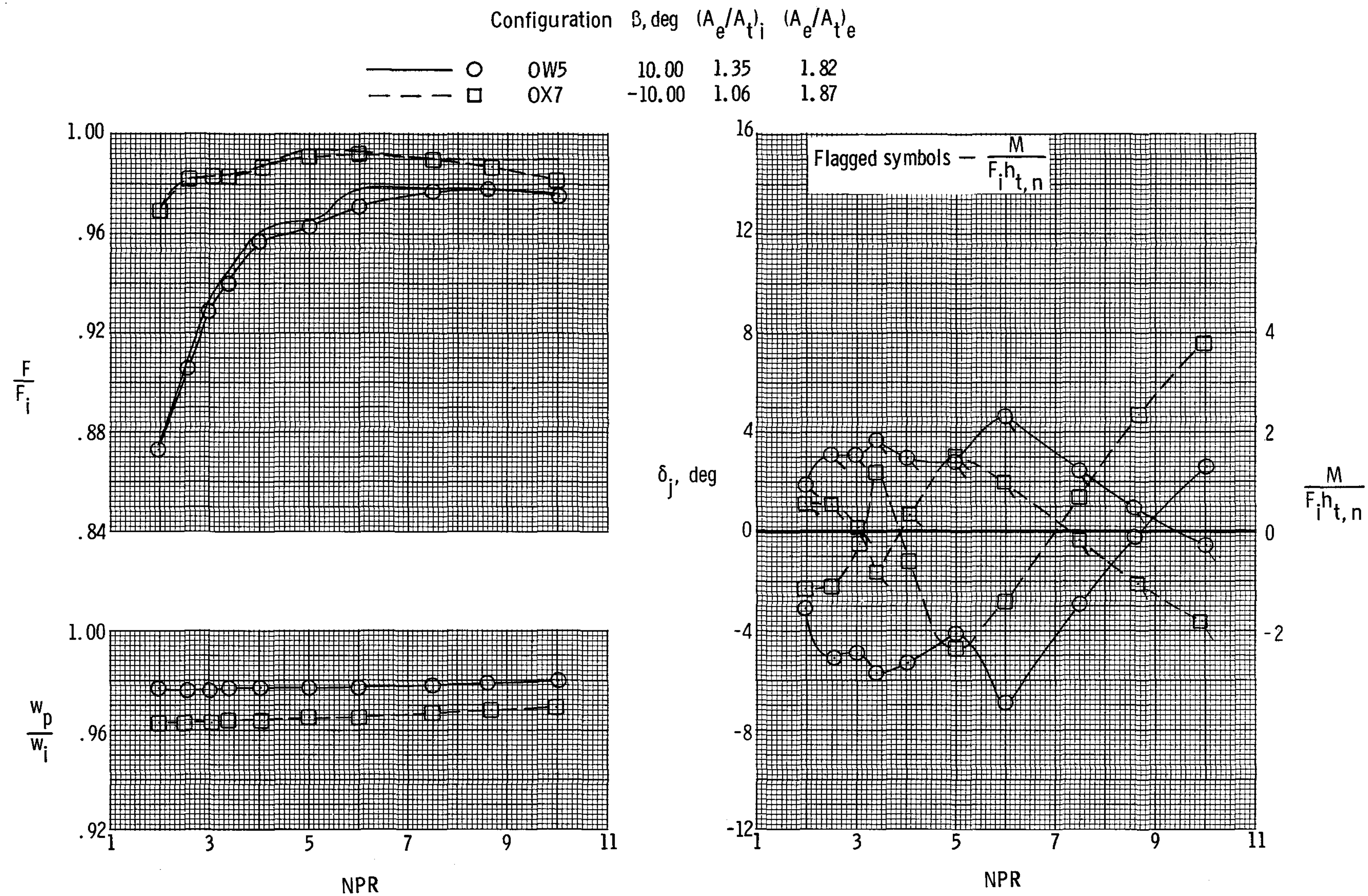

(u) Configurations OW5 and OX7.

Figure 5. Concluded.

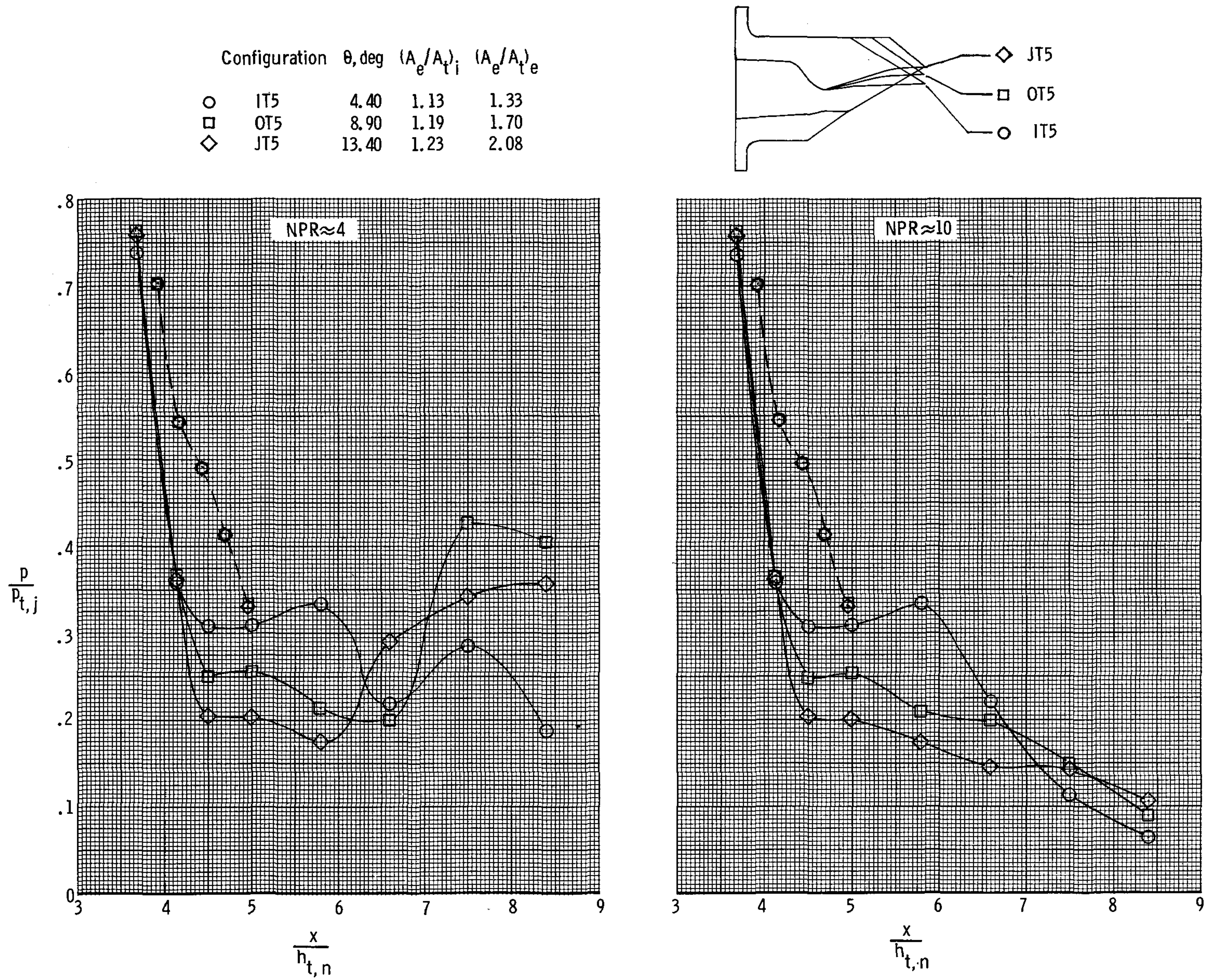

Figure 6. Effect of ramp chordal angle on nozzle internal static-pressure distributions at two nozzle pressure ratios. Dashed lines indicate lower flap static pressures.

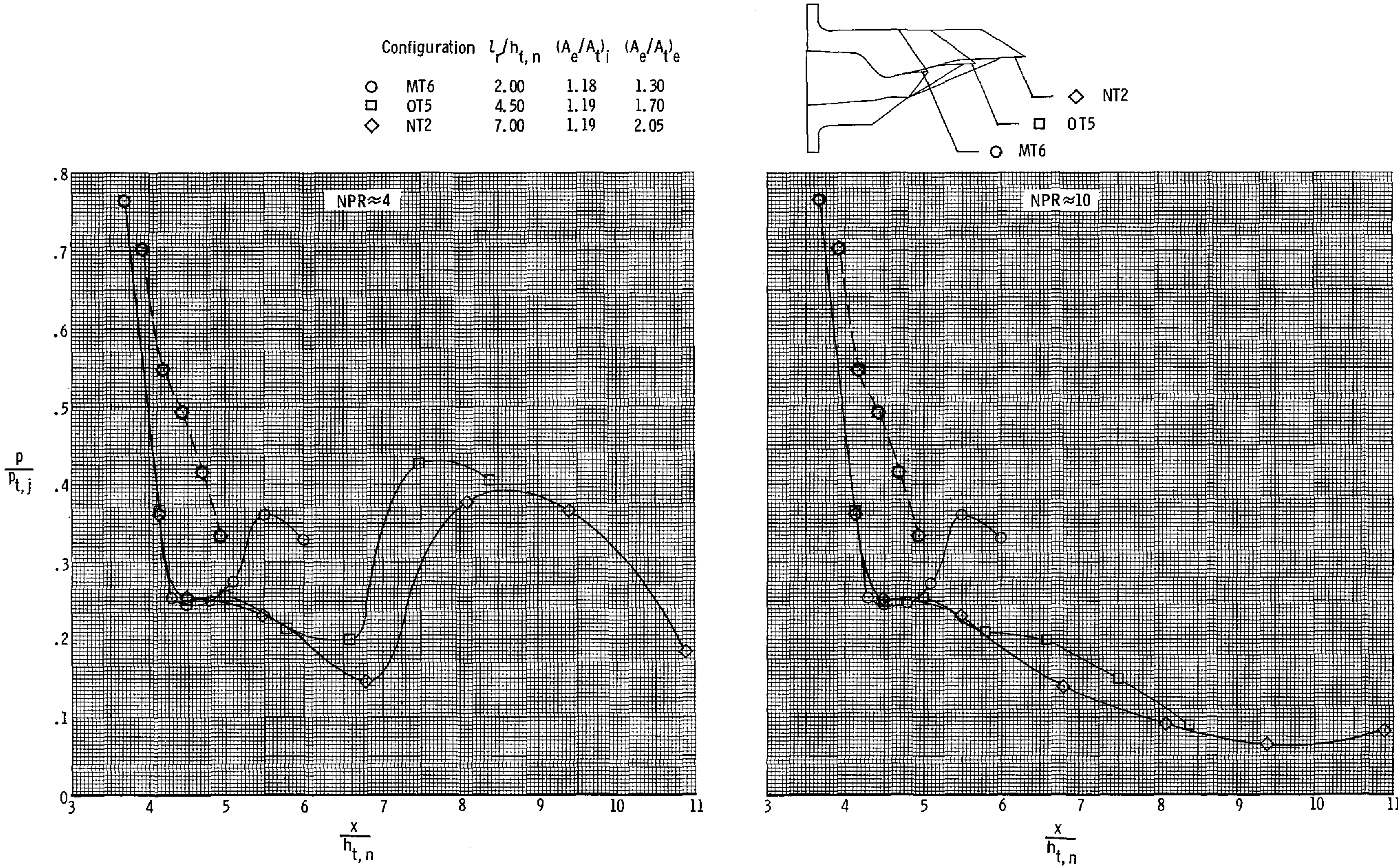

Figure 7. Effect of expansion-ramp length on nozzle internal static-pressure distributions at two nozzle pressure ratios. Dashed lines indicate lower flap static pressures.

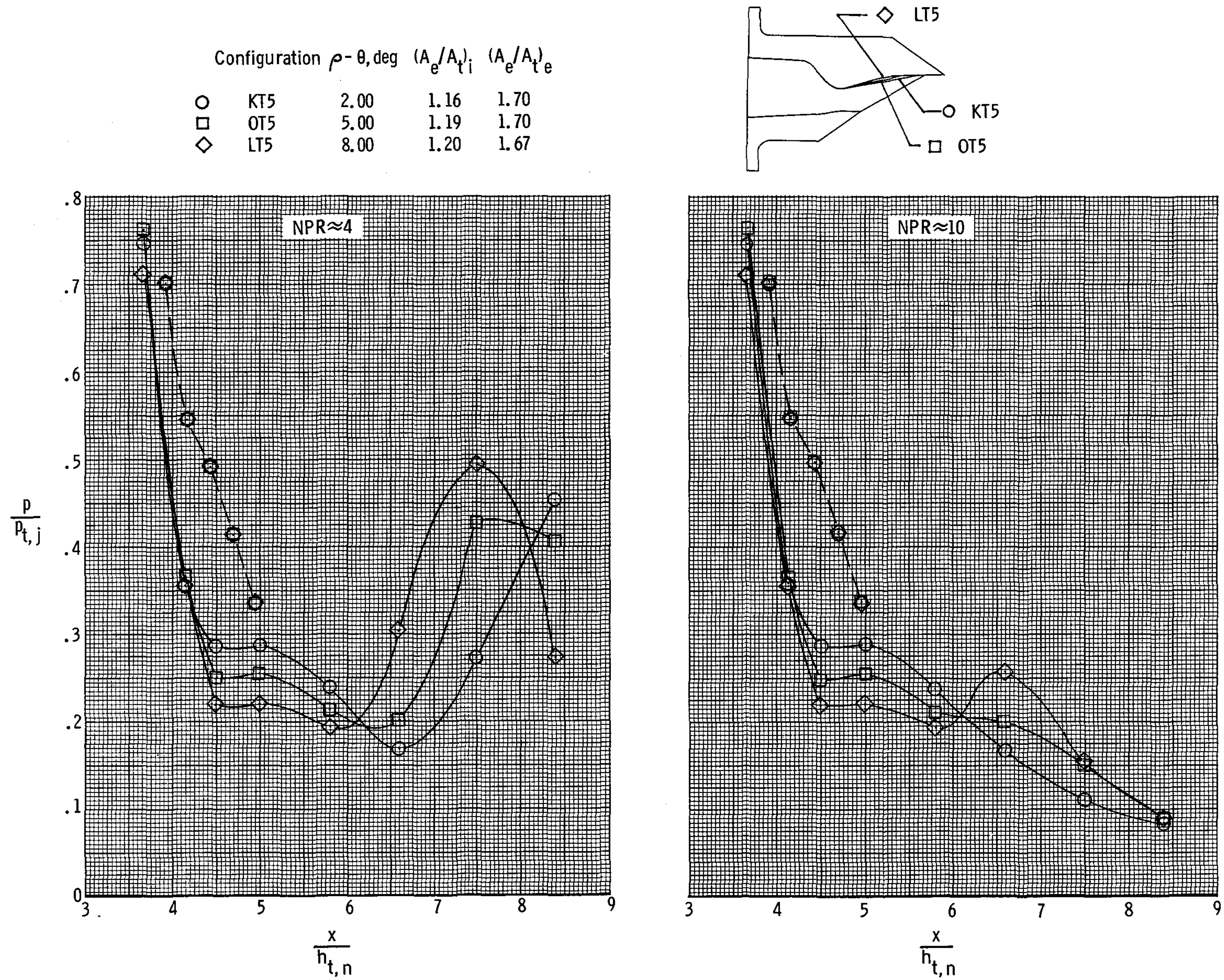

Figure 8. Effect of initial ramp angle on nozzle internal static-pressure distributions at two nozzle pressure ratios. Dashed lines indicate lower flap static pressures.

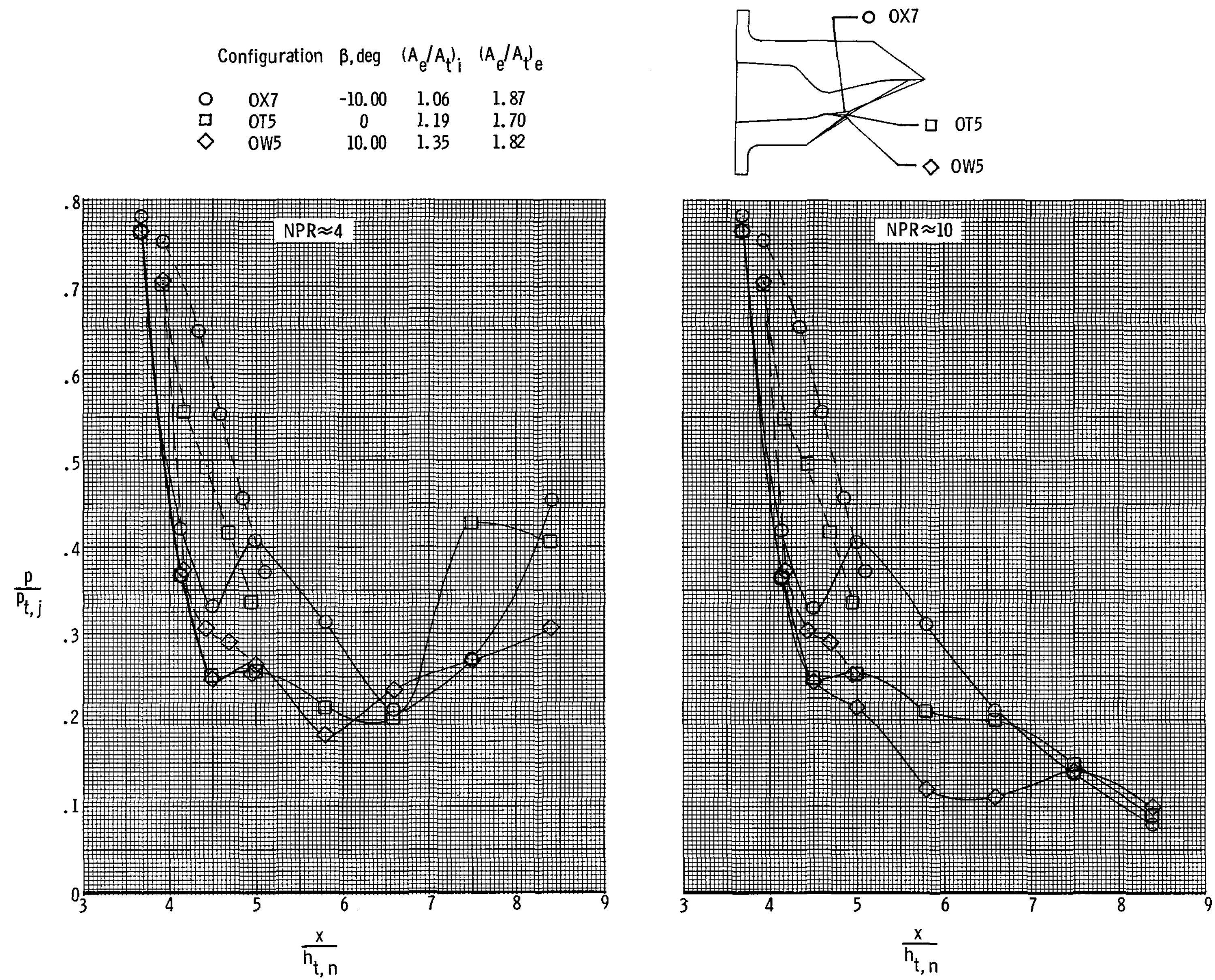

Figure 9. Effect of lower flap angle on nozzle internal static-pressure distributions at two nozzle pressure ratios. Dashed lines indicate lower flap static pressures.

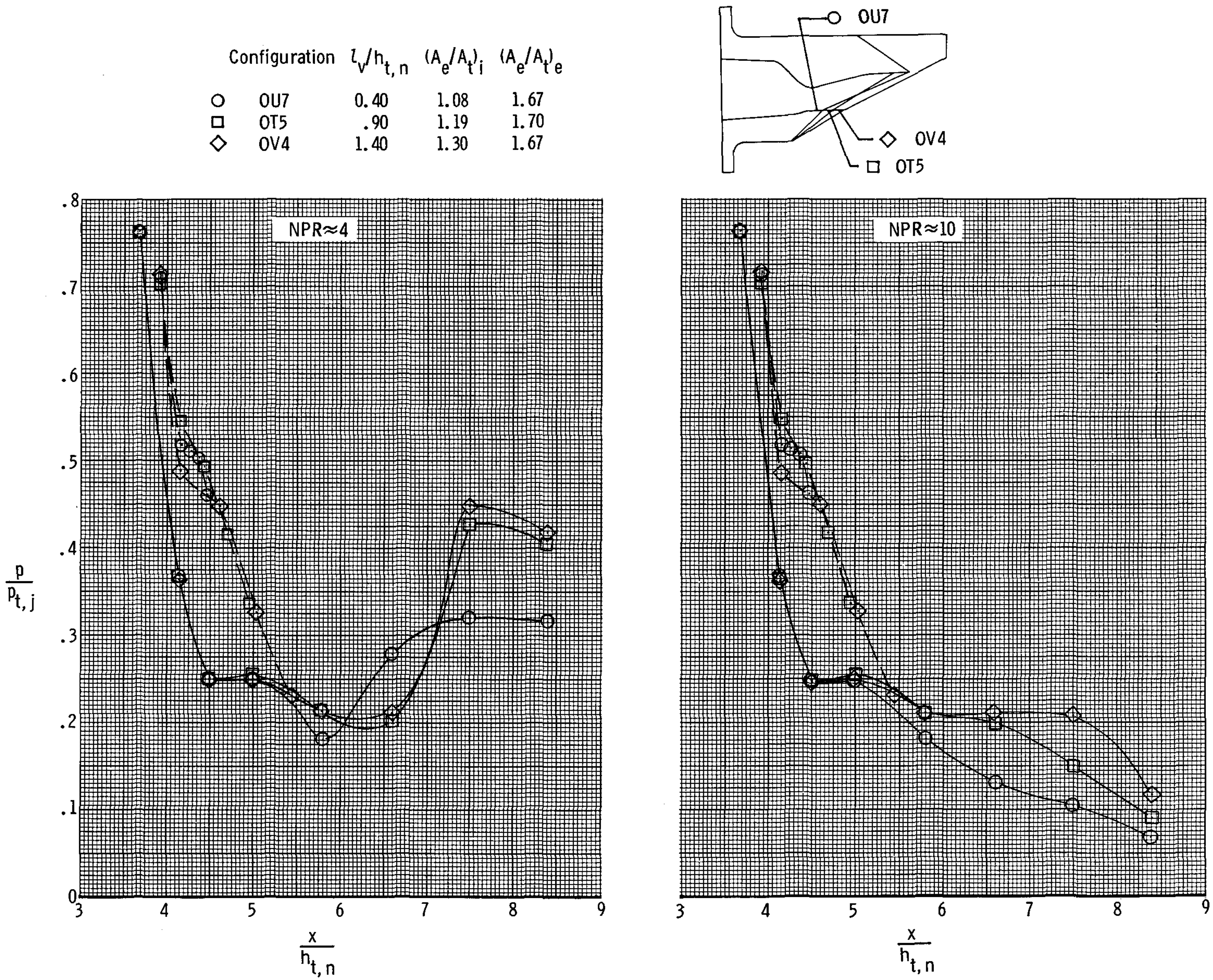

Figure 10. Effect of lower flap length on nozzle internal static-pressure distributions at two nozzle pressure ratios. Dashed lines indicate lower flap static pressures.

	Configuration	θ, deg	ρ-θ, deg	$l_r/h_{t,n}$	$l_v/h_{t,n}$	β, deg	$(A_e/A_t)_i$	$(A_e/A_t)_e$
○	BP1	11.82	3.05	2.88	0.575	6.49	1.21	1.64
□	DP1	↓	6.95	↓			1.24	↓
◇	EP1	5.98	3.05	6.12			1.17	1.72
△	GP2	↓	6.95	↓	↓	↓	1.20	1.67
◺	KT5	8.90	2.00	4.50	.900	0	1.16	1.70
◻	OT5		5.00				1.19	↓
◠	LT5	↓	8.00	↓	↓	↓	1.20	1.67

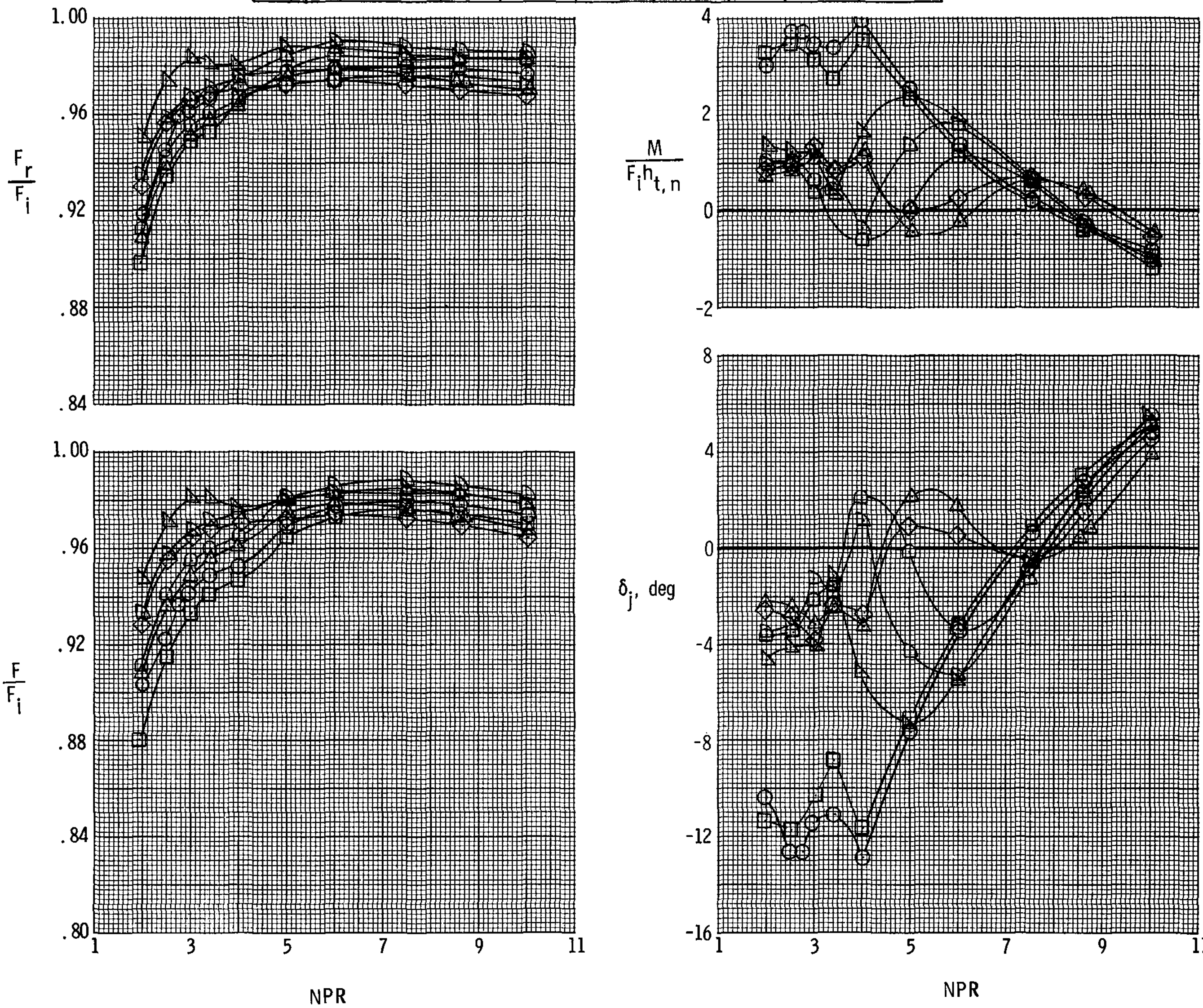

(a) $(A_e/A_t)_i \approx 1.20$ and $(A_e/A_t)_e \approx 1.68$.

Figure 11. Internal performance comparisons of nozzles having approximately the same combinations of internal and external expansion ratios.

	Configuration	θ, deg	φ-θ, deg	$l_r/h_{t,n}$	$l_v/h_{t,n}$	β, deg	$(A_e/A_t)_i$	$(A_e/A_t)_e$
○	BR1	11.82	3.05	2.88	0.575	-6.49	1.08	1.47
□	DR1	↓	6.95	↓			1.10	↓
◇	ER2	5.98	3.05	6.12			1.05	1.55
△	GR2		6.95		↓		1.08	1.50
◺	ES2	↓	3.05	↓	1.225	↓	1.05	↓

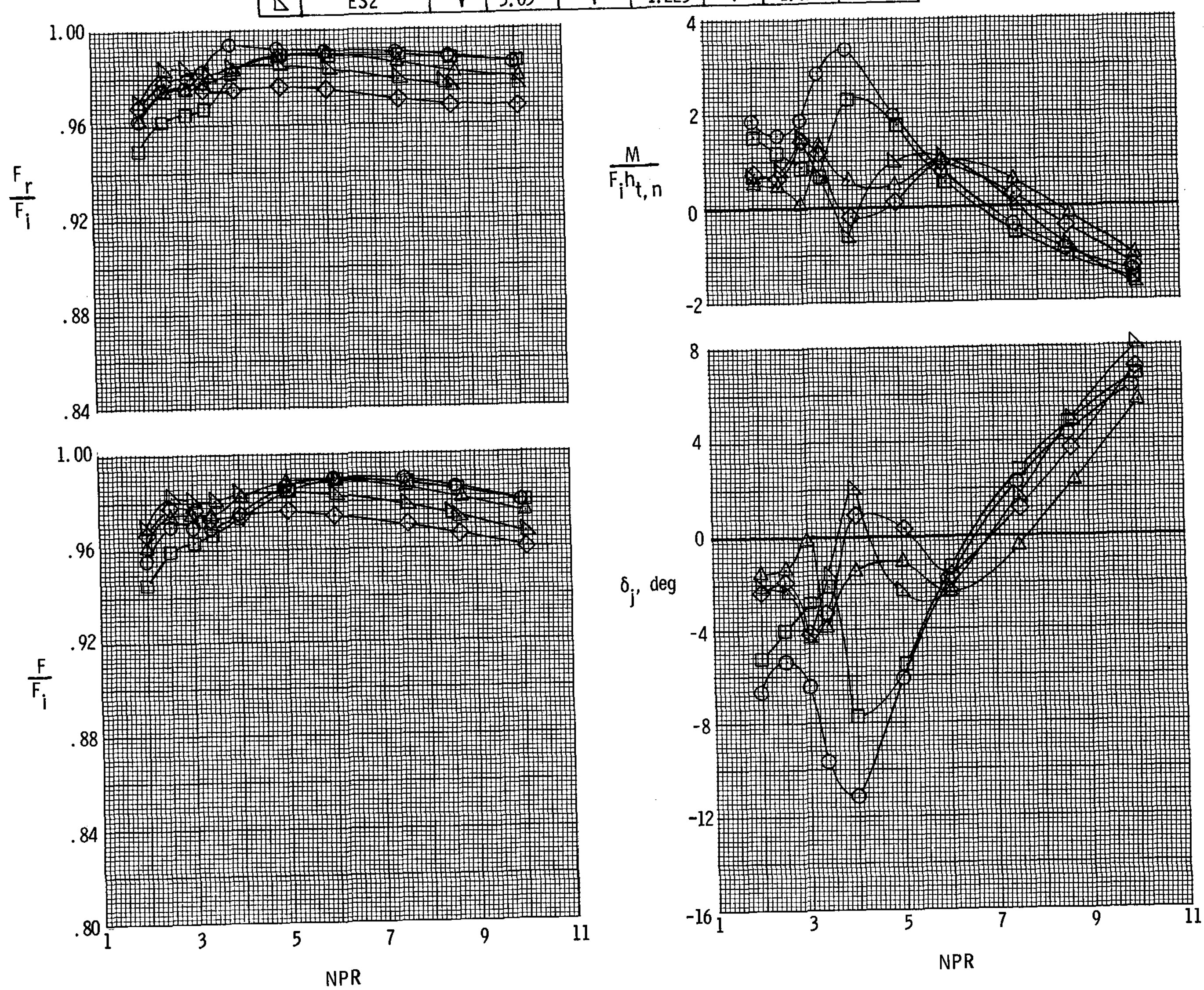

(b) $(A_e/A_t)_i \approx 1.08$ and $(A_e/A_t)_e \approx 1.51$.

Figure 11. Concluded.

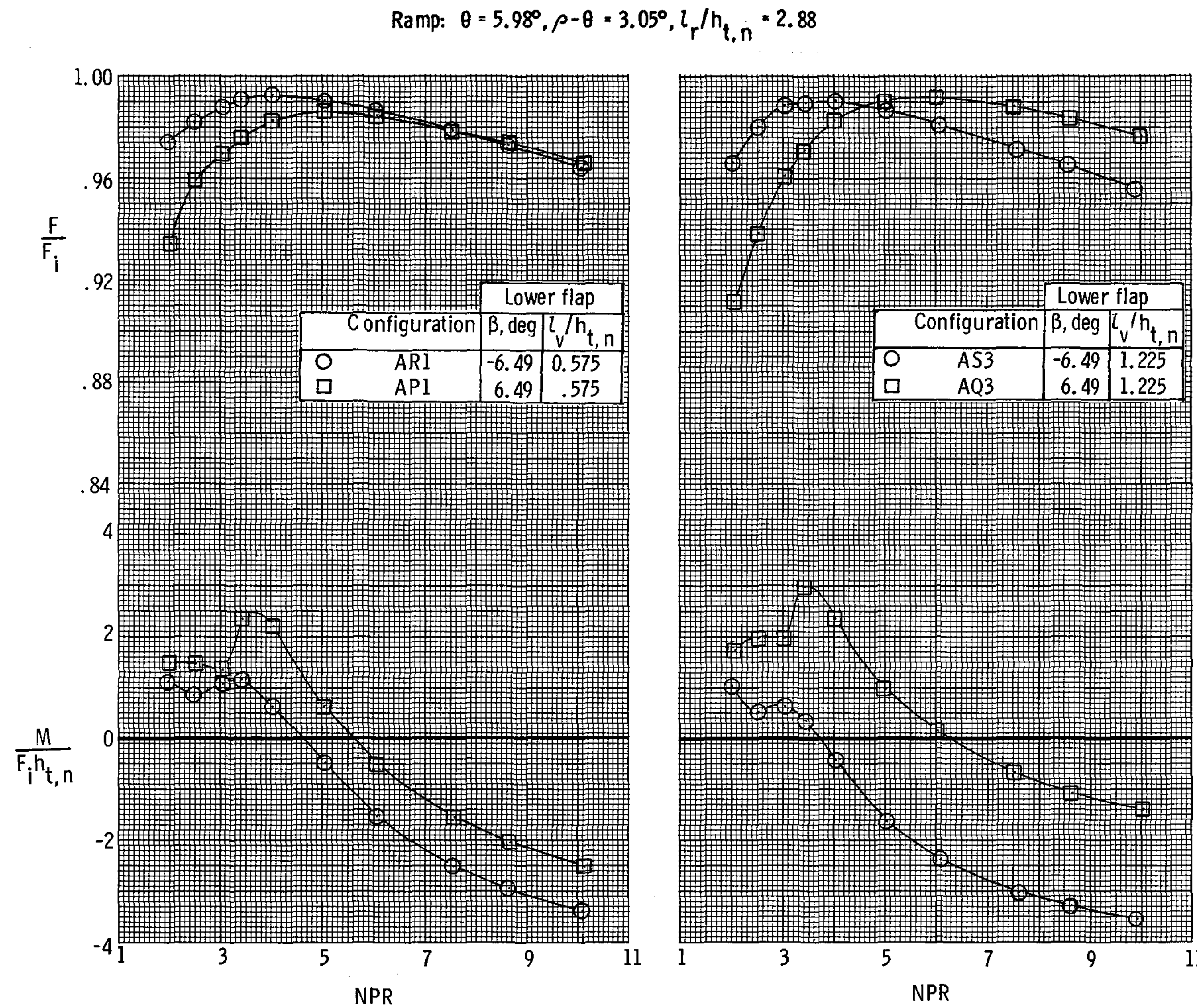

(a) Configurations with upper flap A.

Figure 12. Effect of lower flap deflection on variation of nozzle-thrust and pitching-moment ratios with pressure ratio.

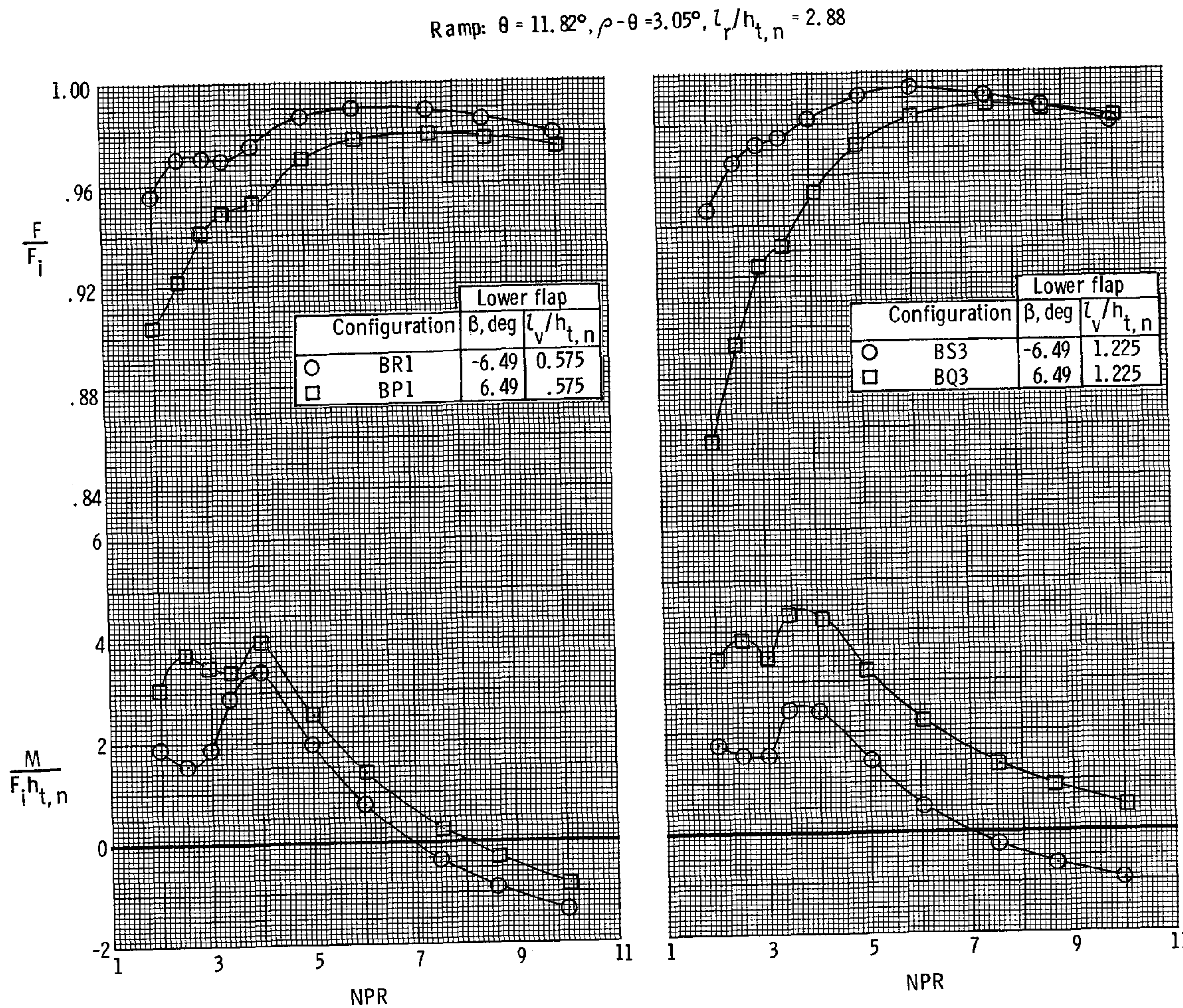

(b) Configurations with upper flap B.

Figure 12. Continued.

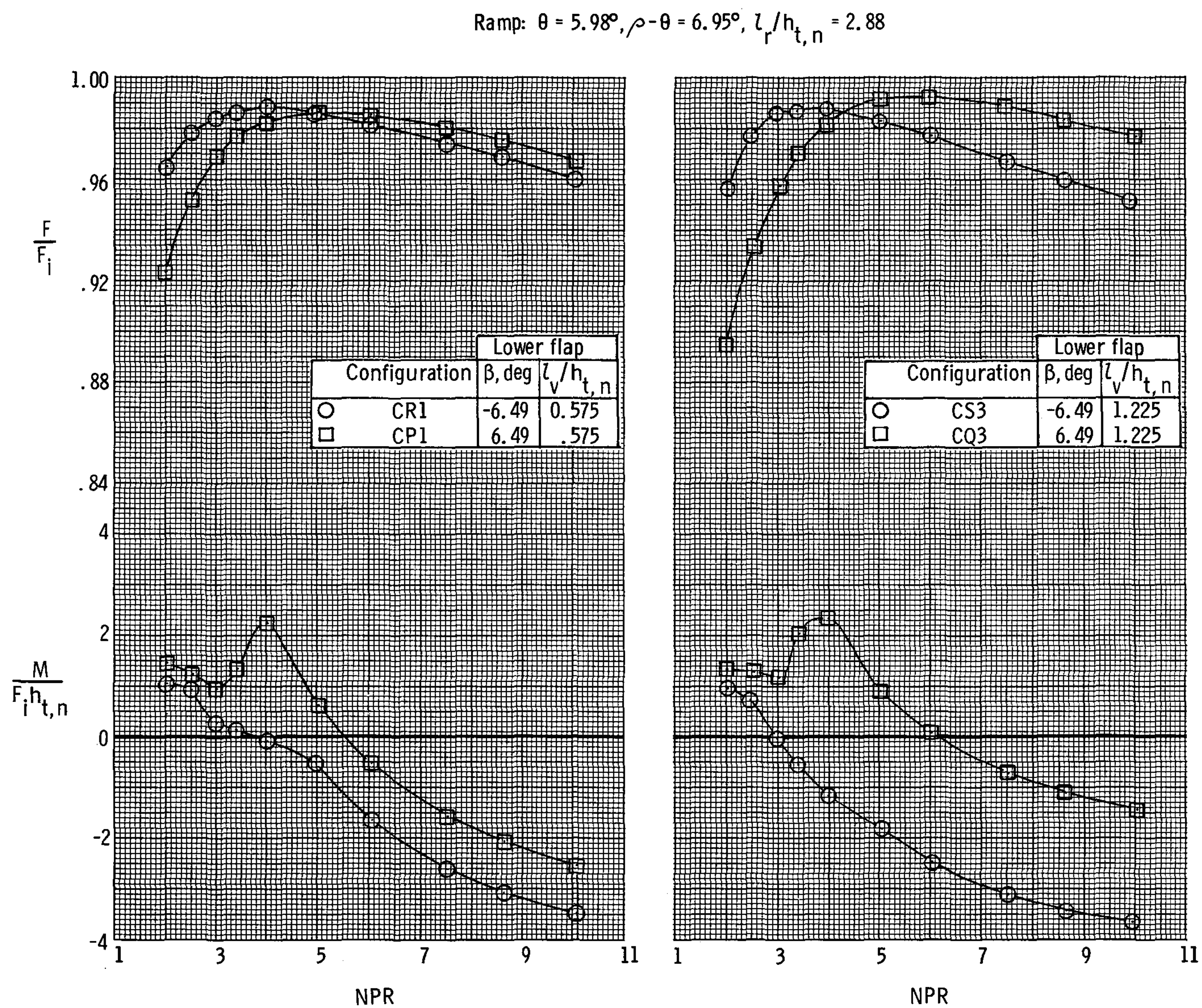

(c) Configurations with upper flap C.

Figure 12. Continued.

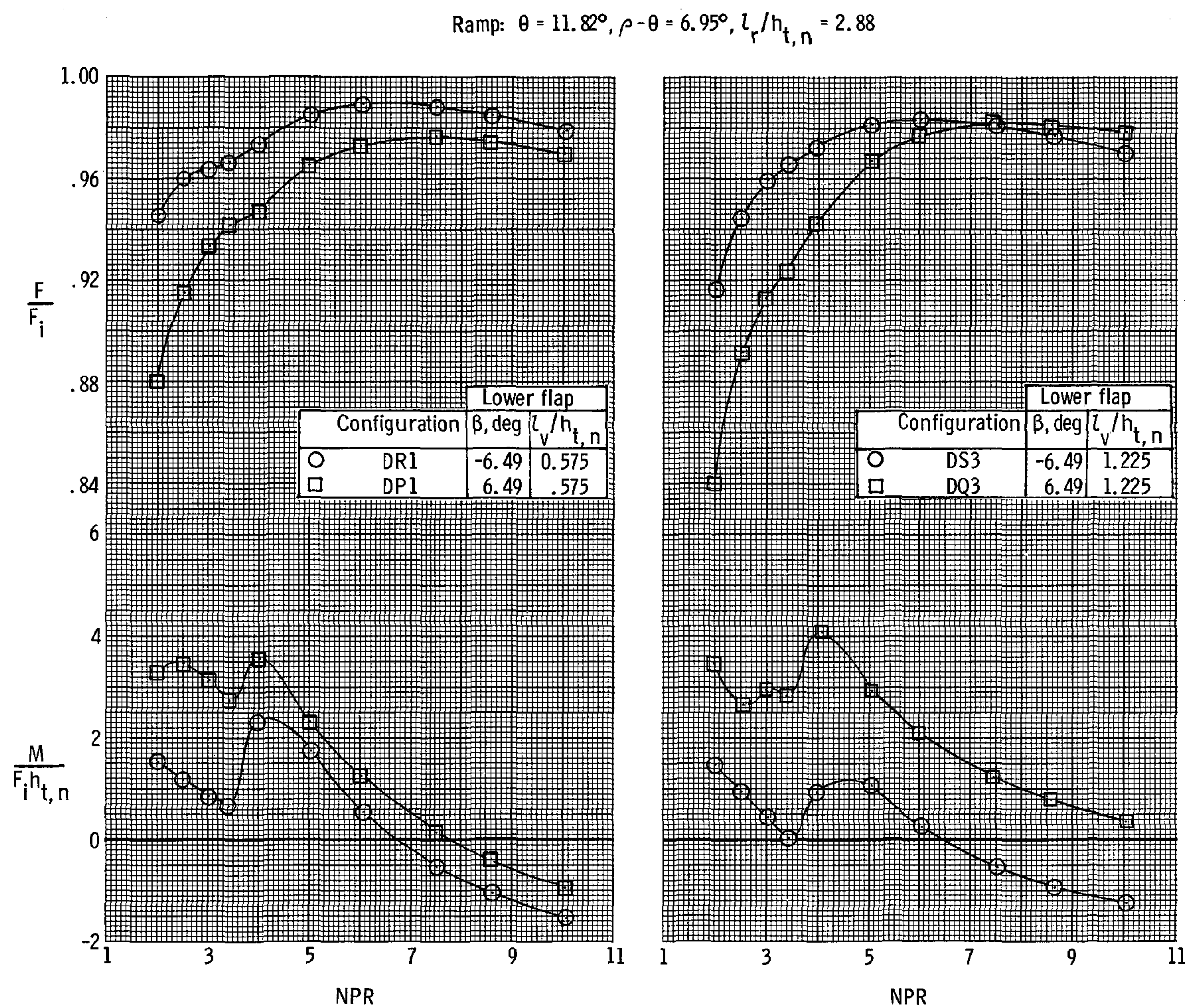

(d) Configurations with upper flap D.

Figure 12. Continued.

Ramp: $\theta = 5.98°, \rho - \theta = 3.05°, l_r/h_{t,n} = 6.12$

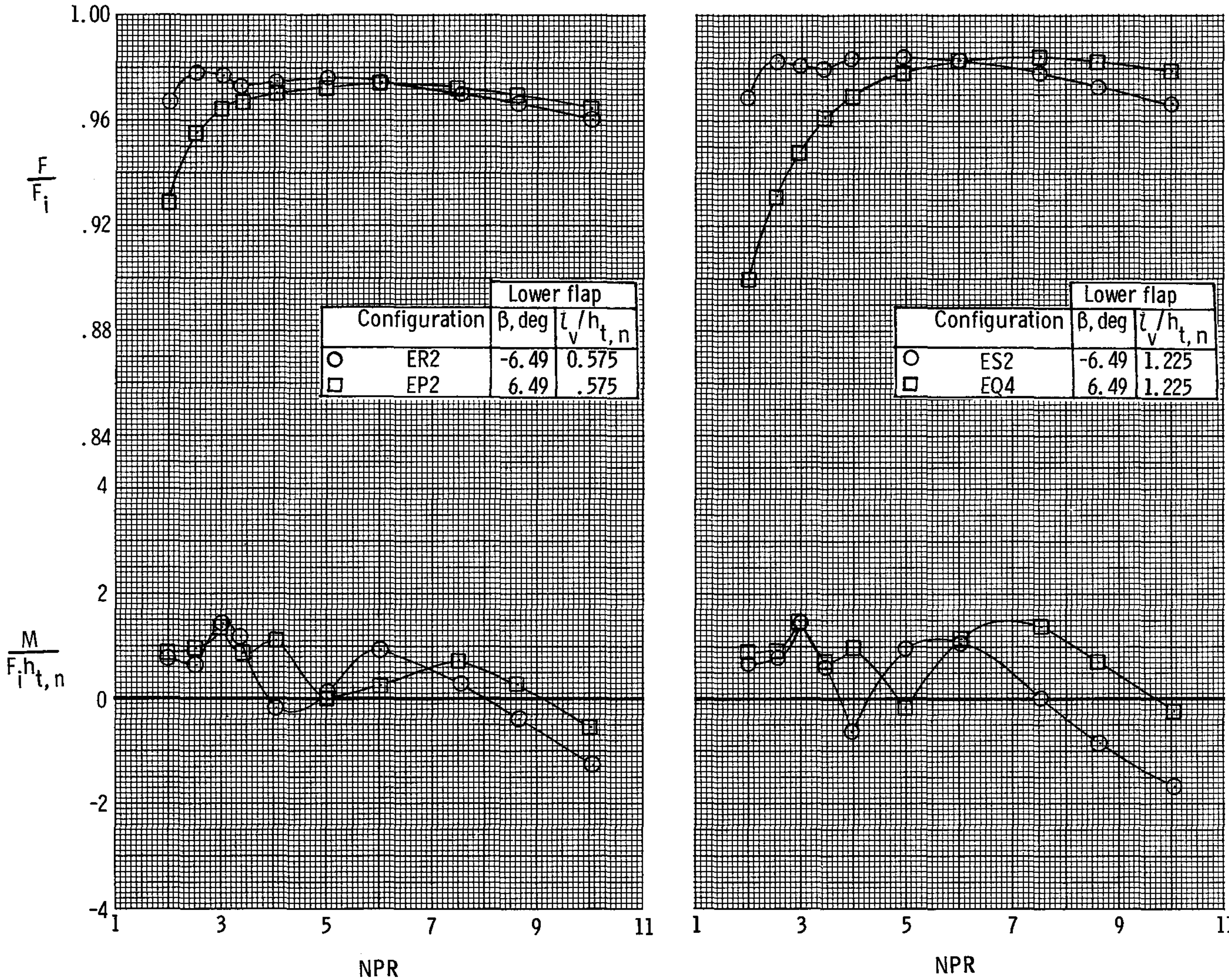

(e) Configurations with upper flap E.

Figure 12. Continued.

Ramp: θ = 11.82°, ρ - θ = 3.05°, $l_r/h_{t,n}$ = 6.12

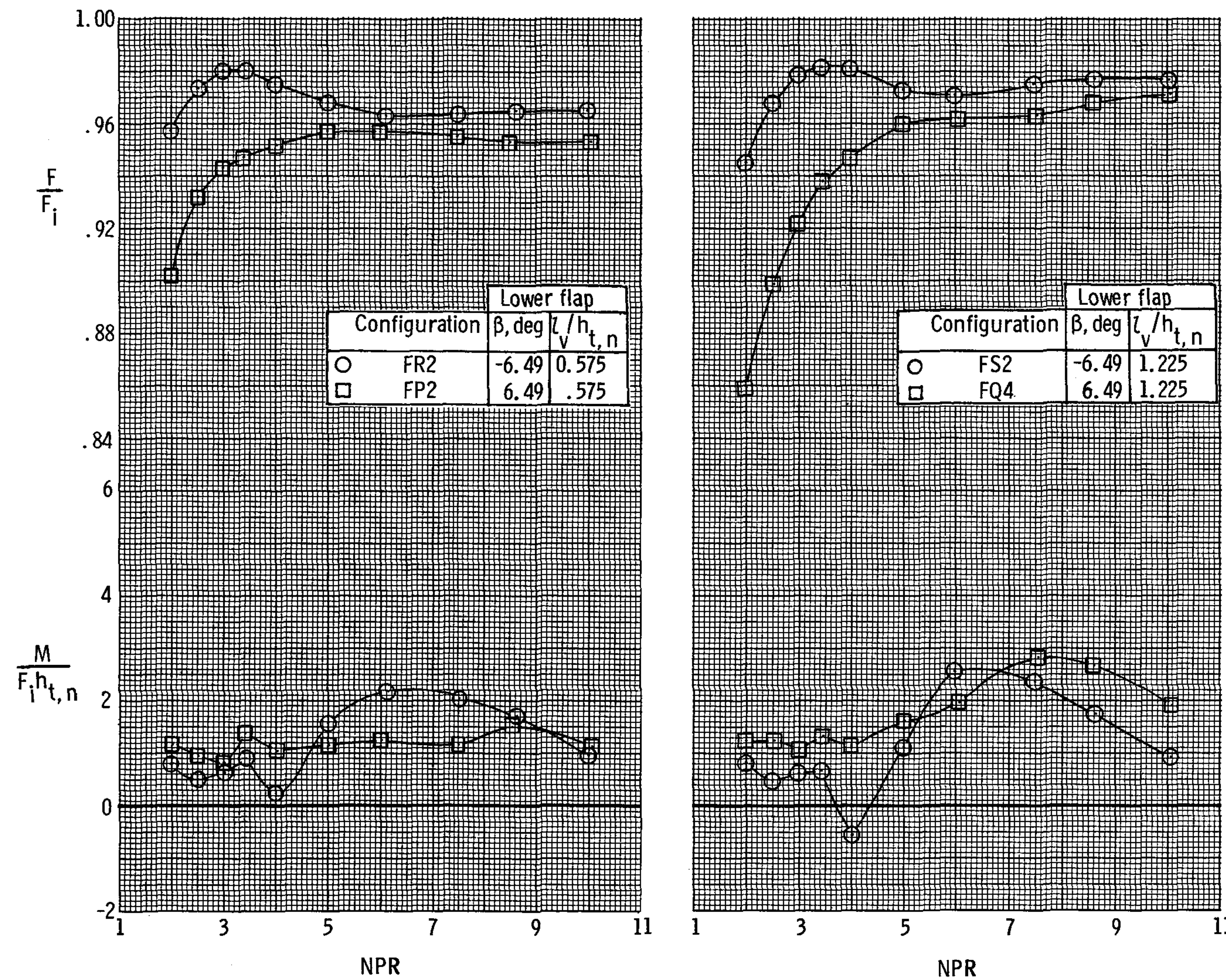

(f) Configurations with upper flap F.

Figure 12. Continued.

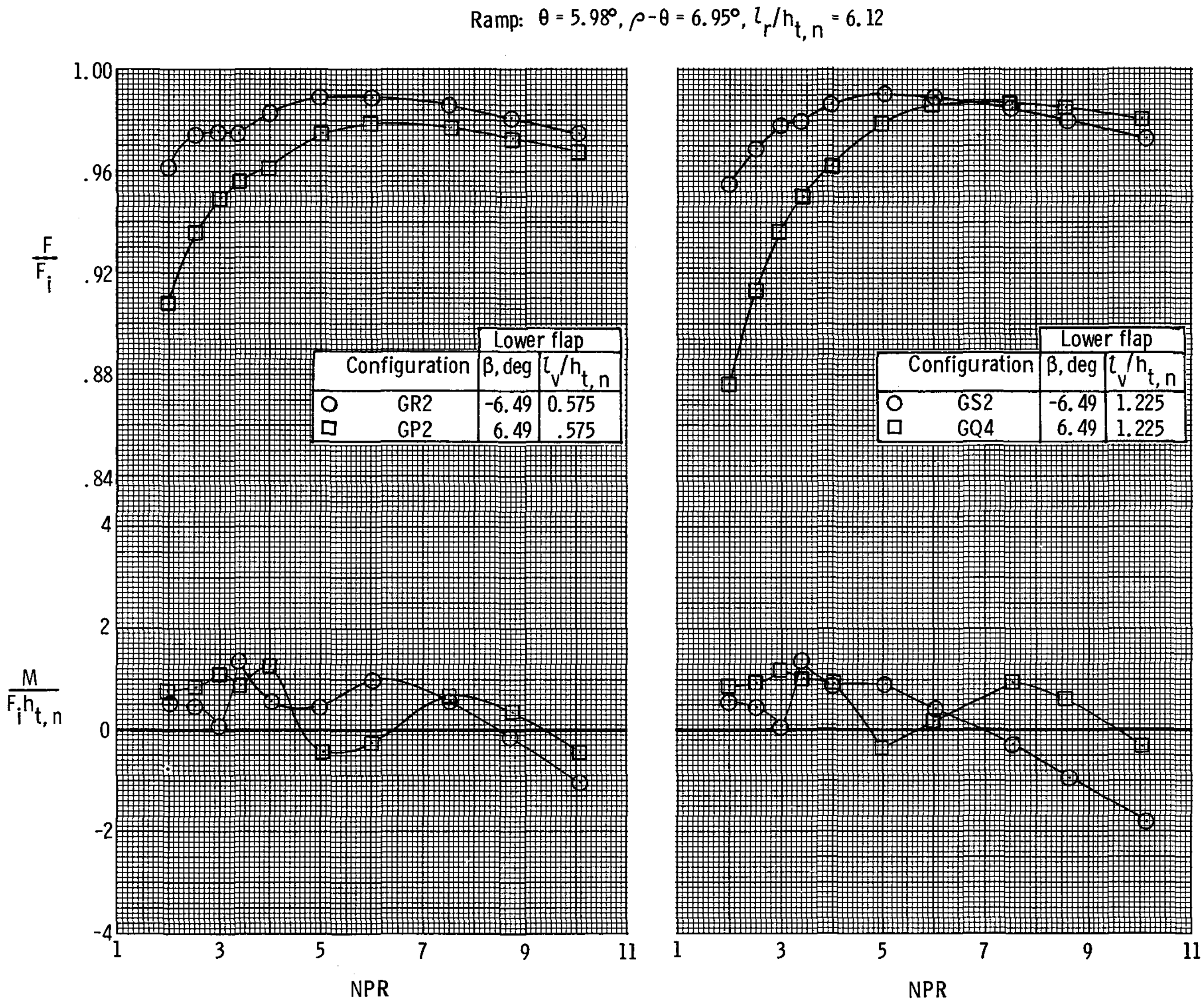

(g) Configurations with upper flap G.

Figure 12. Continued.

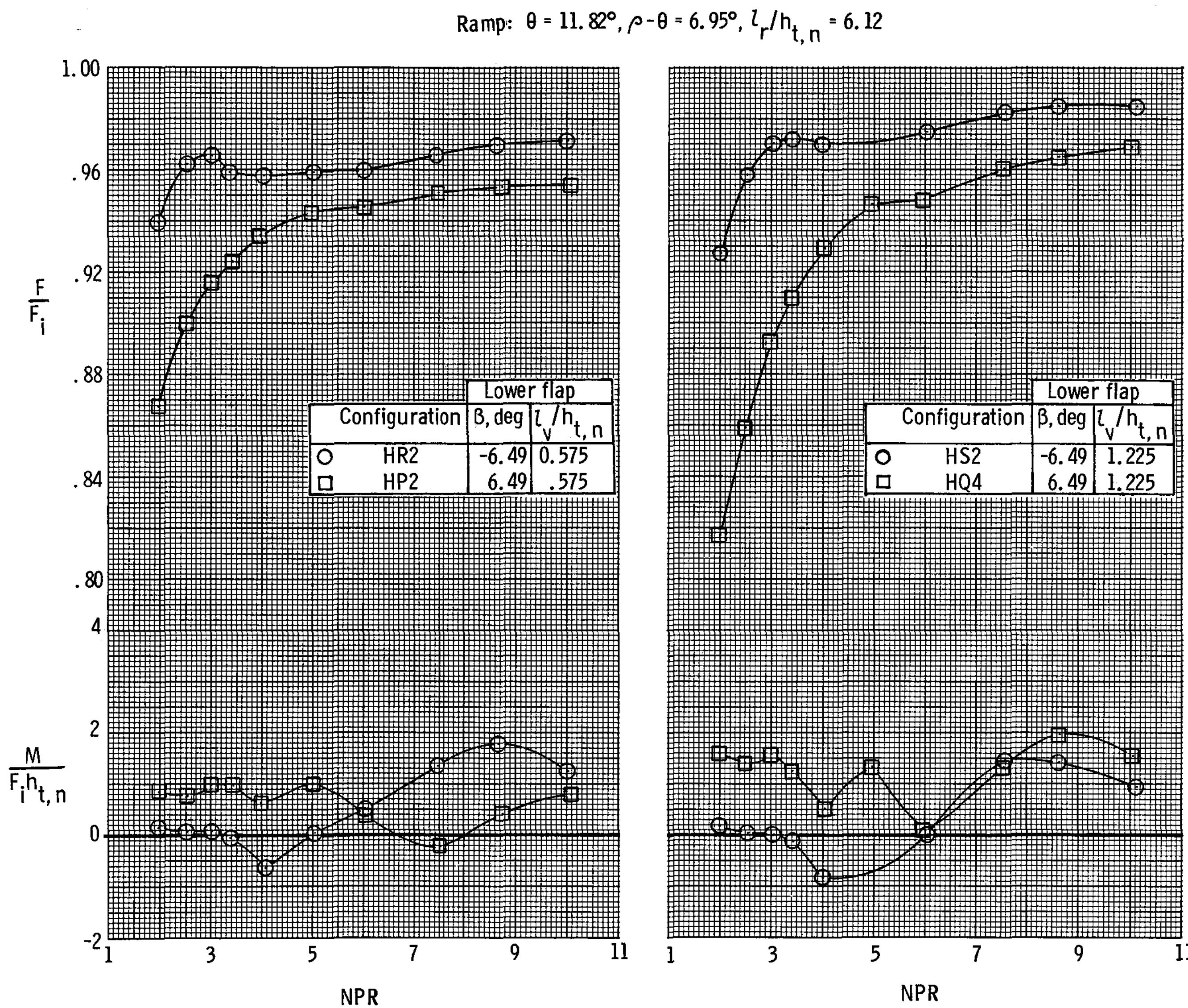

(h) Configurations with upper flap H.

Figure 12. Continued.

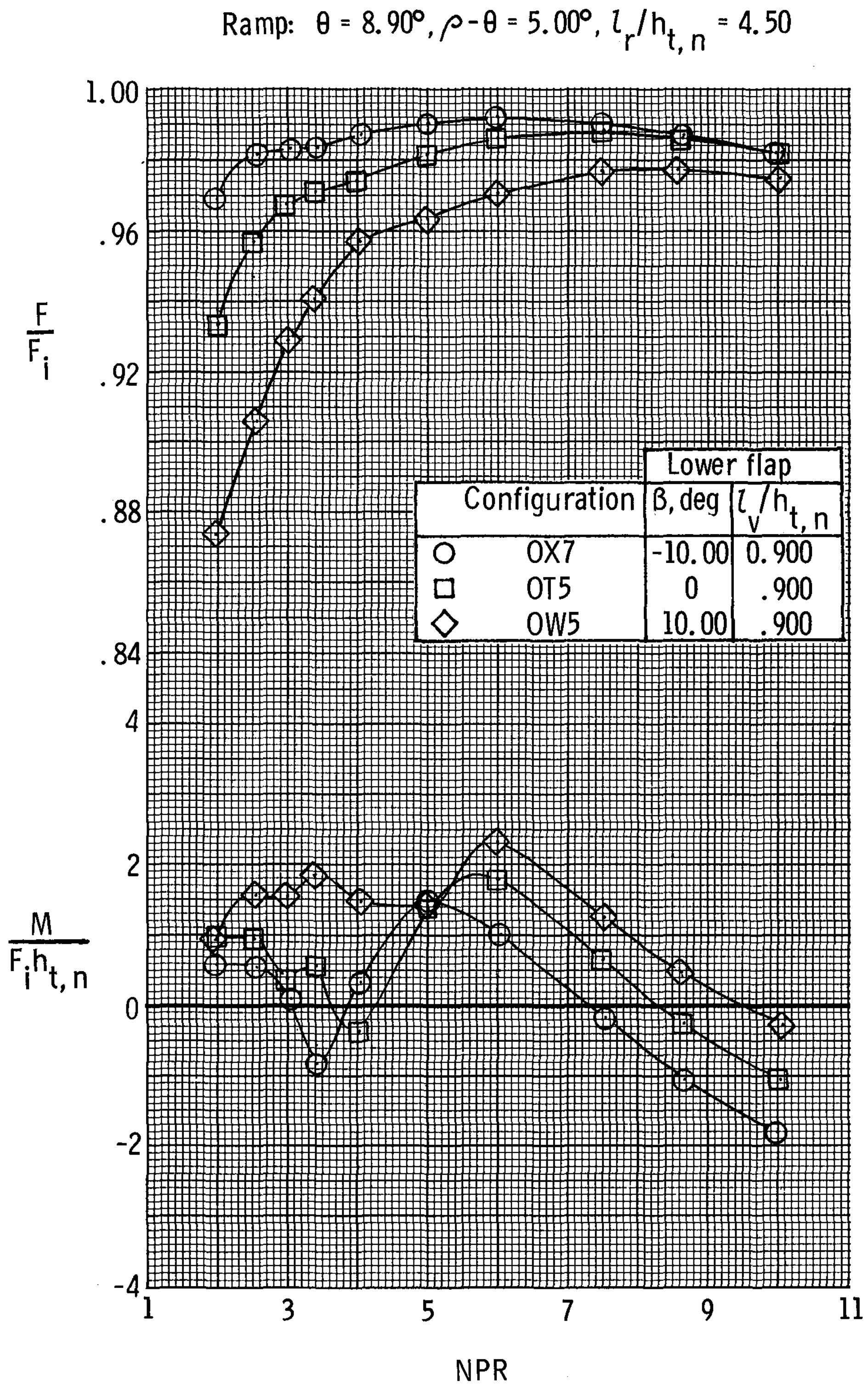

(i) Configurations with upper flap O.

Figure 12. Concluded.

$$\Delta\left(\frac{w_p}{w_i}\right) = \left(\frac{w_p}{w_i}\right)_\beta - \left(\frac{w_p}{w_i}\right)_{\beta = 0^\circ}$$

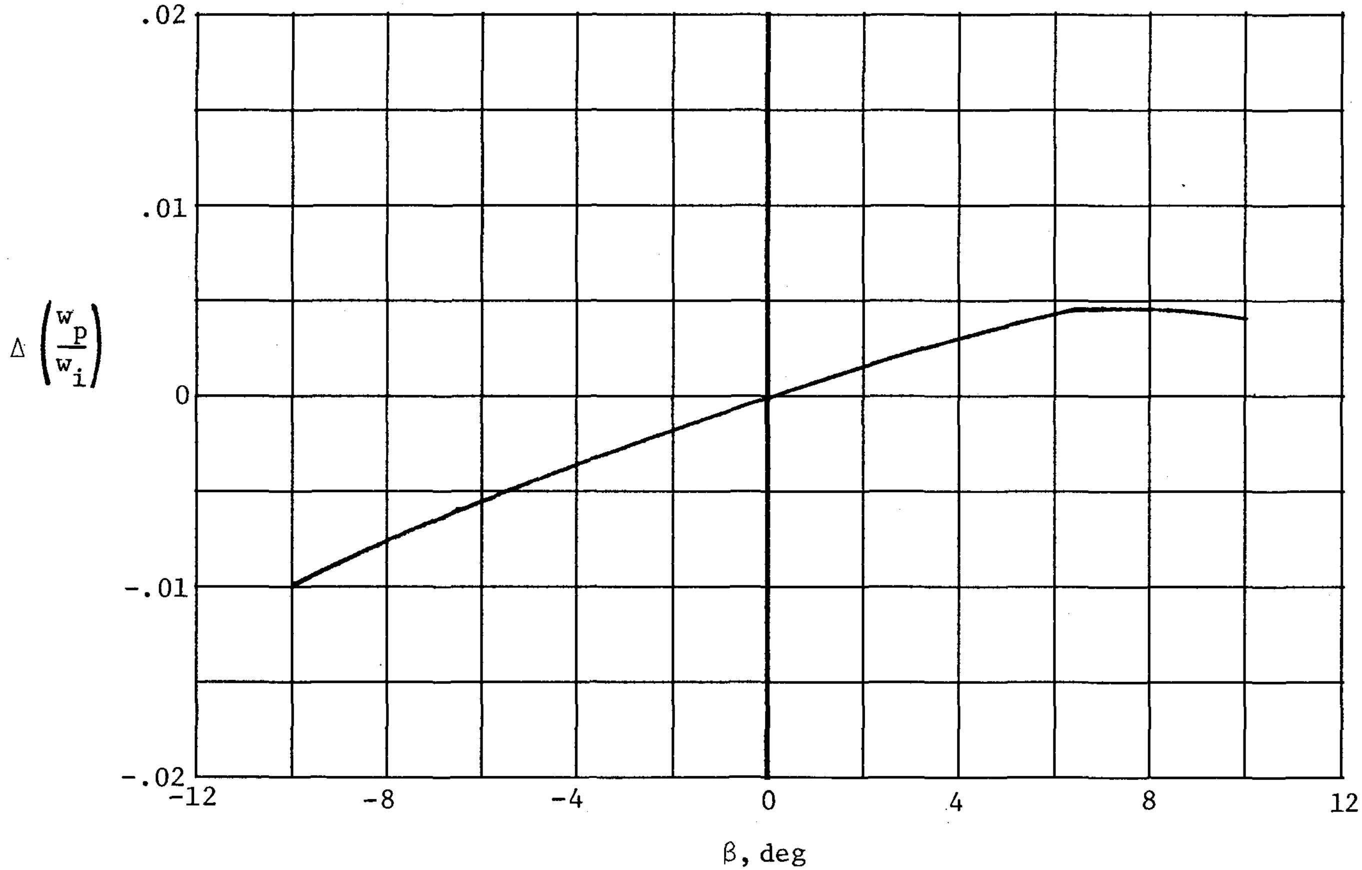

Figure 13. Effect of lower flap deflection on nozzle discharge coefficient (NPR = 5).

1. Report No.	2. Government Accession No.	3. Recipient's Catalog No.
NASA TM-86270		

4. Title and Subtitle
STATIC INTERNAL PERFORMANCE OF SINGLE-EXPANSION-RAMP NOZZLES WITH VARIOUS COMBINATIONS OF INTERNAL GEOMETRIC PARAMETERS

5. Report Date
December 1984

6. Performing Organization Code
505-40-90-01

7. Author(s)
Richard J. Re and Laurence D. Leavitt

8. Performing Organization Report No.
L-15814

9. Performing Organization Name and Address
NASA Langley Research Center
Hampton, VA 23665

10. Work Unit No.

11. Contract or Grant No.

12. Sponsoring Agency Name and Address
National Aeronautics and Space Administration
Washington, DC 20546

13. Type of Report and Period Covered
Technical Memorandum

14. Sponsoring Agency Code

15. Supplementary Notes

16. Abstract
The effects of five geometric design parameters on the internal performance of single-expansion-ramp nozzles were investigated at nozzle pressure ratios up to 10 in the static-test facility of the Langley 16-Foot Transonic Tunnel. The geometric variables on the expansion-ramp surface of the upper flap consisted of ramp chordal angle, ramp length, and initial ramp angle. On the lower flap, the geometric variables consisted of flap angle and flap length. Both internal performance and static-pressure distributions on the centerlines of the upper and lower flaps were obtained for all 43 nozzle configurations tested.

17. Key Words (Suggested by Authors(s))
Nonaxisymmetric nozzles
Two-dimensional nozzles
Single-expansion-ramp nozzles
Internal performance

18. Distribution Statement
Unclassified—Unlimited

Subject Category 02

19. Security Classif.(of this report)	20. Security Classif.(of this page)	21. No. of Pages	22. Price
Unclassified	Unclassified	79	A05

For sale by the National Technical Information Service, Springfield, Virginia 22161

NASA-Langley, 1984

National Aeronautics and
Space Administration

Washington, D.C.
20546

Official Business
Penalty for Private Use, $300

THIRD-CLASS BULK RATE

Postage and Fees Paid
National Aeronautics and
Space Administration
NASA-451

U.S.MAIL

NASA

POSTMASTER: If Undeliverable (Section 158 Postal Manual) Do Not Return